N^* Spectroscopy from Lattice QCD

In celebration of Tony Williams' career on his 60th Birthday

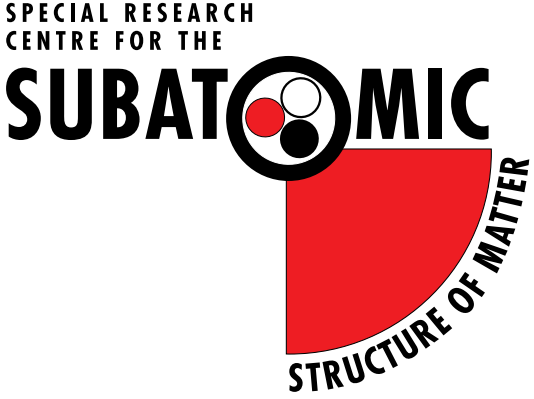

THE UNIVERSITY of ADELAIDE

Co-Authorships at UofA

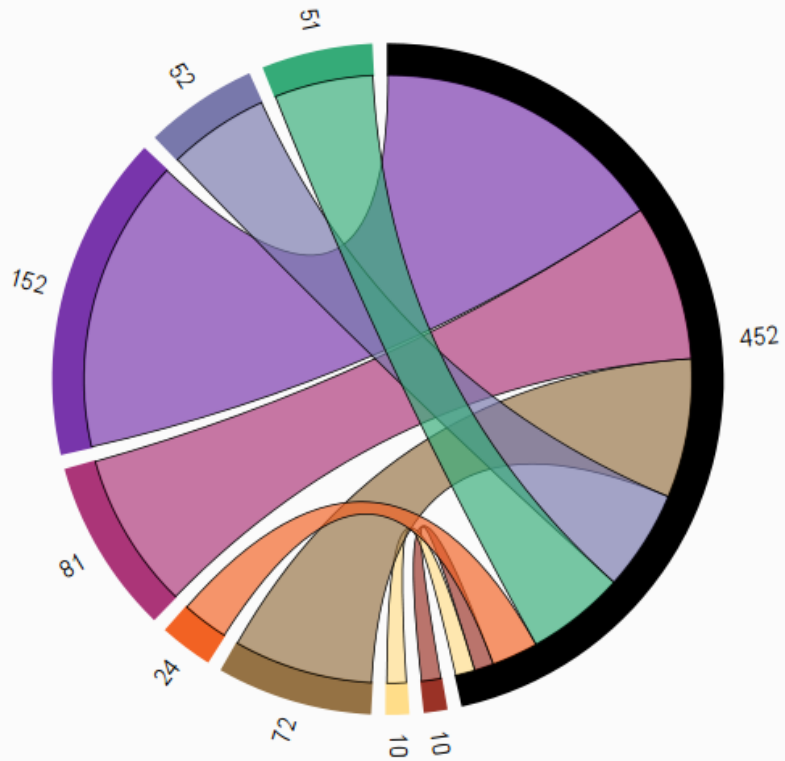

- Sundance Bilson-Thompson (10)
- Jonathan Hall (10)
- Waseem Kamleh (72)
- Selim Mahbub (24)
- Anthony Thomas (81)
- Anthony Williams (152)
- Ross Young (52)
- James Zanotti (51)

Positive Parity Nucleon Spectrum: χQCD (U. Kentucky) Collaboration

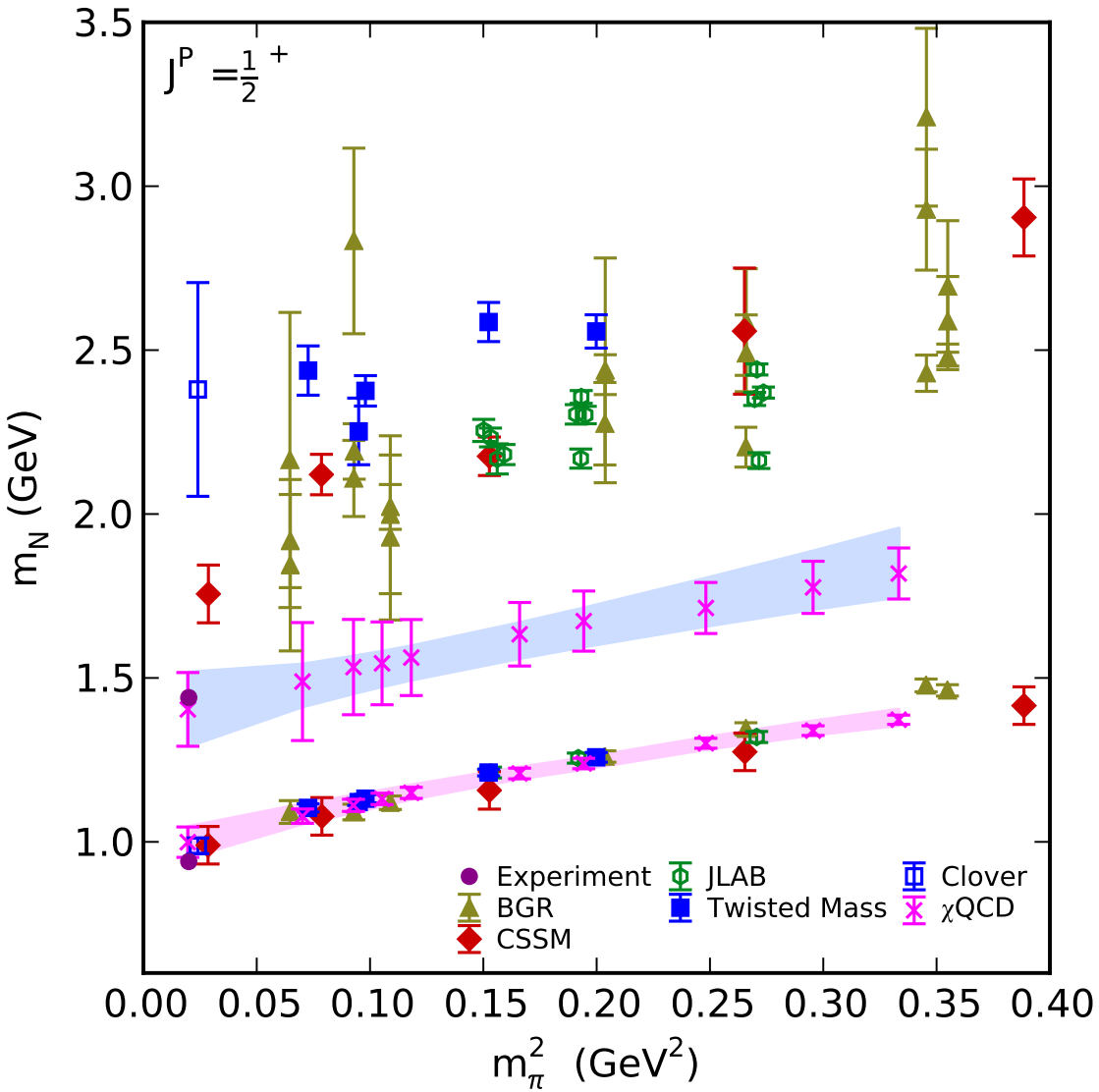

Positive Parity Spectrum: Cyprus (Twisted Mass) Collaboration: Feb. '13

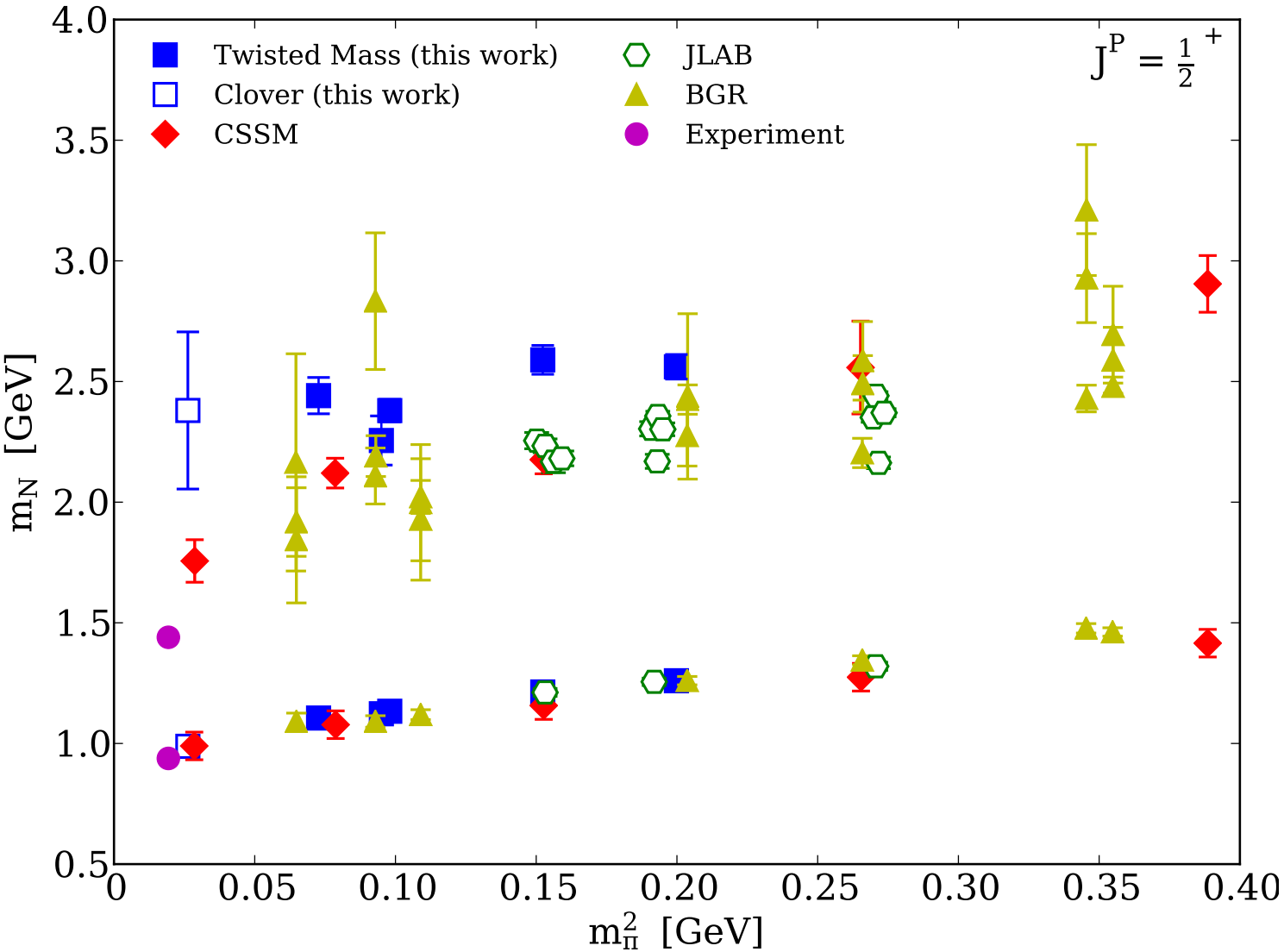

Positive Parity Spectrum: Cyprus (Twisted Mass) Collaboration: Jan. '14

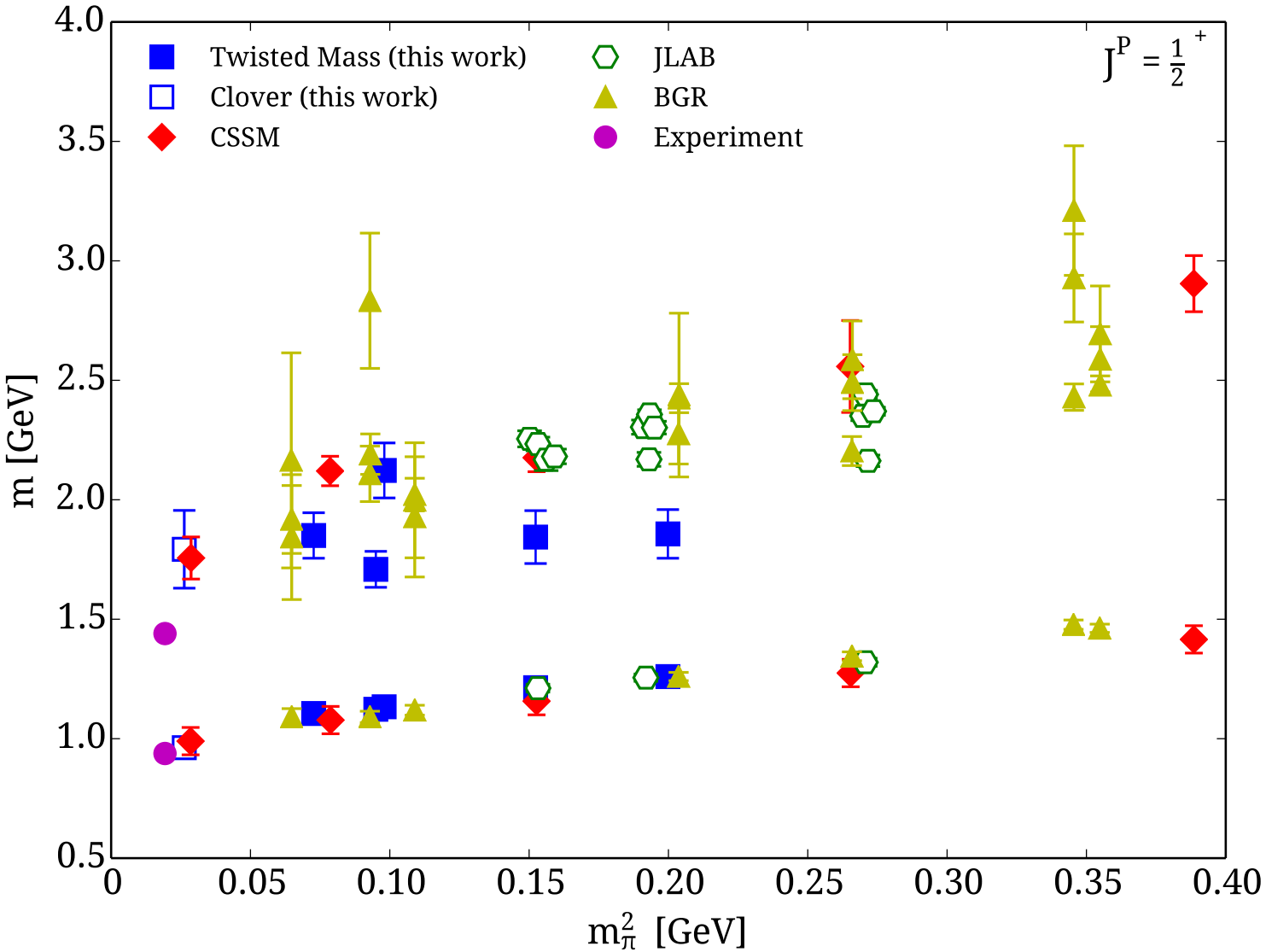

Negative Parity Nucleon Spectrum: Cyprus

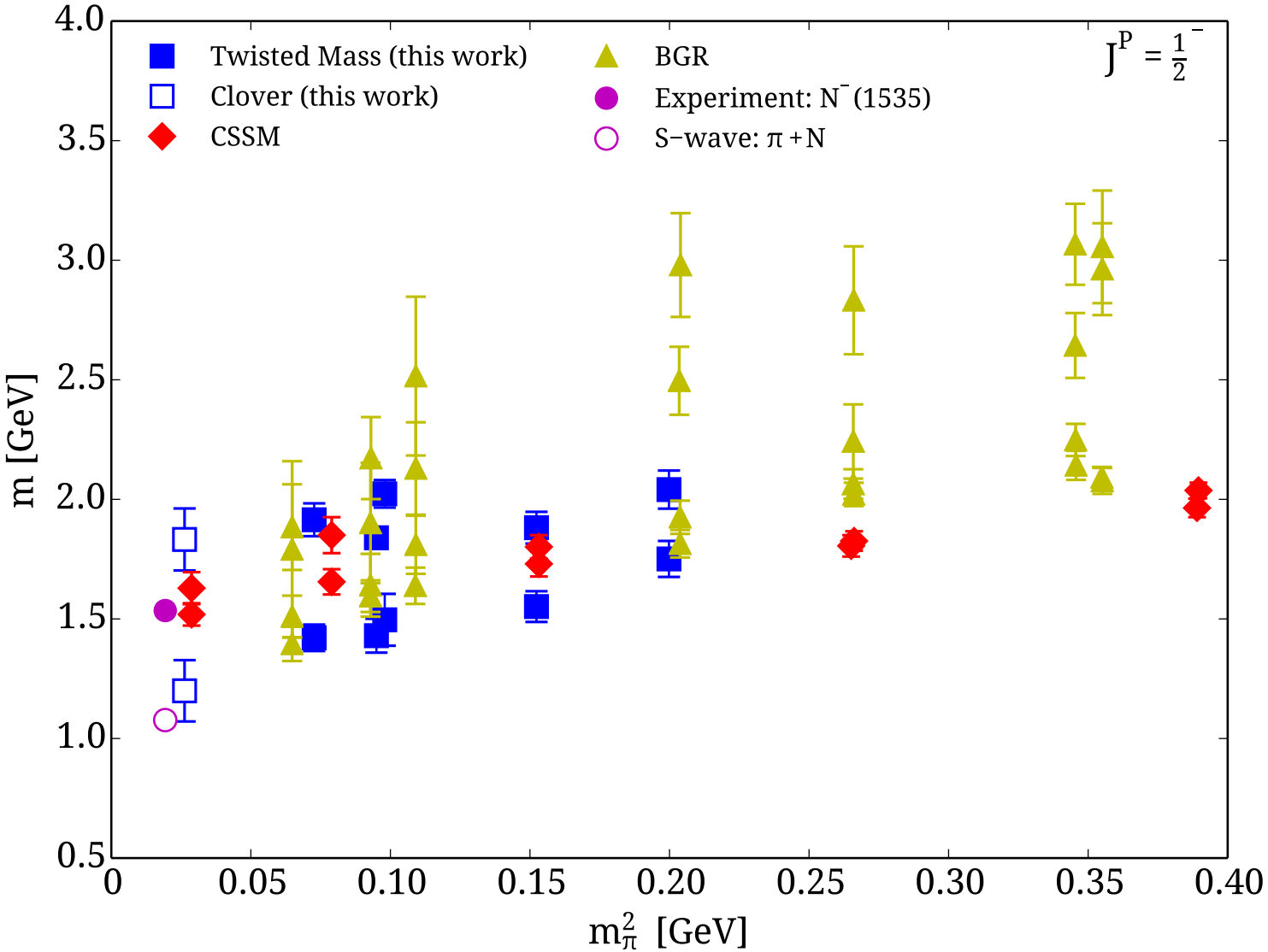

Outline

Variational Analysis

- Consider a basis of interpolating fields χ_i

Variational Analysis

- Consider a basis of interpolating fields χ_i
- Construct the correlation matrix

$$G_{ij}(\mathbf{p};t) = \sum_{\mathbf{x}} \mathrm{e}^{-\mathrm{i}\,\mathbf{p}\cdot\mathbf{x}}\,\mathrm{tr}\left(\,\Gamma\,\left\langle\Omega\right|\chi_i(x)\,\overline{\chi}_j(0)\left|\Omega\right\rangle\,\right).$$

Variational Analysis

- Consider a basis of interpolating fields χ_i
- Construct the correlation matrix

$$G_{ij}(\mathbf{p};t) = \sum_{\mathbf{x}} \mathrm{e}^{-\mathrm{i}\,\mathbf{p}\cdot\mathbf{x}}\,\mathrm{tr}\left(\,\Gamma\,\left\langle\Omega\right|\chi_i(x)\,\overline{\chi}_j(0)\left|\Omega\right\rangle\,\right).$$

- Seek linear combinations of the interpolators $\{\,\chi_i\,\}$ that isolate individual energy eigenstates, α, at momentum $\mathbf{p}$:

$$\phi^\alpha = v_i^\alpha(\mathbf{p})\,\chi_i\,, \qquad \overline{\phi}^\alpha = u_i^\alpha(\mathbf{p})\,\overline{\chi}_i\,.$$

Variational Analysis

- When successful, only state α participates in the correlation function, and one can write recurrence relations

$$G(\mathbf{p}; t_0 + \delta t)\, \mathbf{u}^{\alpha}(\mathbf{p}) = \mathrm{e}^{-E_{\alpha}(\mathbf{p})\, \delta t}\, G(\mathbf{p}; t_0)\, \mathbf{u}^{\alpha}(\mathbf{p})$$

$$\mathbf{v}^{\alpha \mathrm{T}}(\mathbf{p})\, G(\mathbf{p}; t_0 + \delta t) = \mathrm{e}^{-E_{\alpha}(\mathbf{p})\, \delta t}\, \mathbf{v}^{\alpha \mathrm{T}}(\mathbf{p})\, G(\mathbf{p}; t_0)$$

  a Generalised Eigenvalue Problem (GEVP).

Variational Analysis

- When successful, only state α participates in the correlation function, and one can write recurrence relations

$$G(\mathbf{p}; t_0 + \delta t)\, \mathbf{u}^{\alpha}(\mathbf{p}) = \mathrm{e}^{-E_{\alpha}(\mathbf{p})\, \delta t}\, G(\mathbf{p}; t_0)\, \mathbf{u}^{\alpha}(\mathbf{p})$$

$$\mathbf{v}^{\alpha \mathrm{T}}(\mathbf{p})\, G(\mathbf{p}; t_0 + \delta t) = \mathrm{e}^{-E_{\alpha}(\mathbf{p})\, \delta t}\, \mathbf{v}^{\alpha \mathrm{T}}(\mathbf{p})\, G(\mathbf{p}; t_0)$$

  a Generalised Eigenvalue Problem (GEVP).
- Solve for the left, $\mathbf{v}^{\alpha}(\mathbf{p})$, and right, $\mathbf{u}^{\alpha}(\mathbf{p})$, generalised eigenvectors of $G(\mathbf{p}; t_0 + \delta t)$ and $G(\mathbf{p}; t_0)$.

Eigenstate-Projected Correlation Functions

- Using these optimal eigenvectors, create eigenstate-projected correlation functions

$$
\begin{aligned}
G^{\alpha}(\mathbf{p};t) &= \sum_{\mathbf{x}} \mathrm{e}^{-\mathrm{i}\,\mathbf{p}\cdot\mathbf{x}} \left\langle \Omega \middle| \phi^{\alpha}(x)\, \overline{\phi}^{\alpha}(0) \middle| \Omega \right\rangle \ , \\
&= \sum_{\mathbf{x}} \mathrm{e}^{-\mathrm{i}\,\mathbf{p}\cdot\mathbf{x}} \left\langle \Omega \middle| v_i^{\alpha}(\mathbf{p})\, \chi_i(x)\, \overline{\chi}_j(0)\, u_j^{\alpha}(\mathbf{p}) \middle| \Omega \right\rangle \ , \\
&= \mathbf{v}^{\alpha\mathsf{T}}(\mathbf{p})\, G(\mathbf{p};t)\, \mathbf{u}^{\alpha}(\mathbf{p}) \, .
\end{aligned}
$$

$$
G^{\alpha}(\mathbf{p};t) = A_{\alpha}\ \exp\left(-E_{\alpha}(\mathbf{p})\, t\right) \ .
$$

Eigenstate-Projected Correlation Functions

- Using these optimal eigenvectors, create eigenstate-projected correlation functions

$$
\begin{aligned}
G^{\alpha}(\mathbf{p};t) &= \sum_{\mathbf{x}} \mathrm{e}^{-\mathrm{i}\,\mathbf{p}\cdot\mathbf{x}} \,\langle\Omega|\phi^{\alpha}(x)\,\overline{\phi}^{\alpha}(0)|\Omega\rangle \ , \\
&= \sum_{\mathbf{x}} \mathrm{e}^{-\mathrm{i}\,\mathbf{p}\cdot\mathbf{x}} \,\langle\Omega|v_i^{\alpha}(\mathbf{p})\,\chi_i(x)\,\overline{\chi}_j(0)\,u_j^{\alpha}(\mathbf{p})|\Omega\rangle \ , \\
&= \mathbf{v}^{\alpha\mathsf{T}}(\mathbf{p})\,G(\mathbf{p};t)\,\mathbf{u}^{\alpha}(\mathbf{p}) \,.
\end{aligned}
$$

$$
G^{\alpha}(\mathbf{p};t) = A_{\alpha}\,\exp\left(-E_{\alpha}(\mathbf{p})\,t\right) \ .
$$

- Here t is different from t_0 and δt and can become large.

Defining the Effective Mass

- At zero momentum, the projected correlator is

$$G^{\alpha}(\mathbf{0}; t) = A_{\alpha} \exp\left(-M_{\alpha}\, t\right) .$$

Defining the Effective Mass

- At zero momentum, the projected correlator is

$$G^{\alpha}(\mathbf{0}; t) = A_{\alpha} \exp\left(-M_{\alpha}\, t\right) .$$

- Taking the log

$$\ln G^{\alpha}(\mathbf{0}; t) = \ln\left(A_{\alpha}\right) - M_{\alpha}\, t\, .$$

Defining the Effective Mass

- At zero momentum, the projected correlator is

$$G^{\alpha}(\mathbf{0}; t) = A_{\alpha} \exp\left(-M_{\alpha}\, t\right) .$$

- Taking the log

$$\ln G^{\alpha}(\mathbf{0}; t) = \ln\left(A_{\alpha}\right) - M_{\alpha}\, t\,.$$

- The effective mass is defined as

$$M^{\alpha}_{\text{eff}}(t) = \frac{1}{\Delta t} \ln\left(\frac{G^{\alpha}(t)}{G^{\alpha}(t+\Delta t)}\right) .$$

Defining the Effective Mass

- At zero momentum, the projected correlator is

$$G^{\alpha}(\mathbf{0}; t) = A_{\alpha} \exp\left(-M_{\alpha}\, t\right) .$$

- Taking the log

$$\ln G^{\alpha}(\mathbf{0}; t) = \ln\left(A_{\alpha}\right) - M_{\alpha}\, t\,.$$

- The effective mass is defined as

$$M^{\alpha}_{\text{eff}}(t) = \frac{1}{\Delta t} \ln\left(\frac{G^{\alpha}(t)}{G^{\alpha}(t+\Delta t)}\right) .$$

- $\Delta t = 1$ or 2 is common.

Smeared Source to Point Sink Correlation Functions

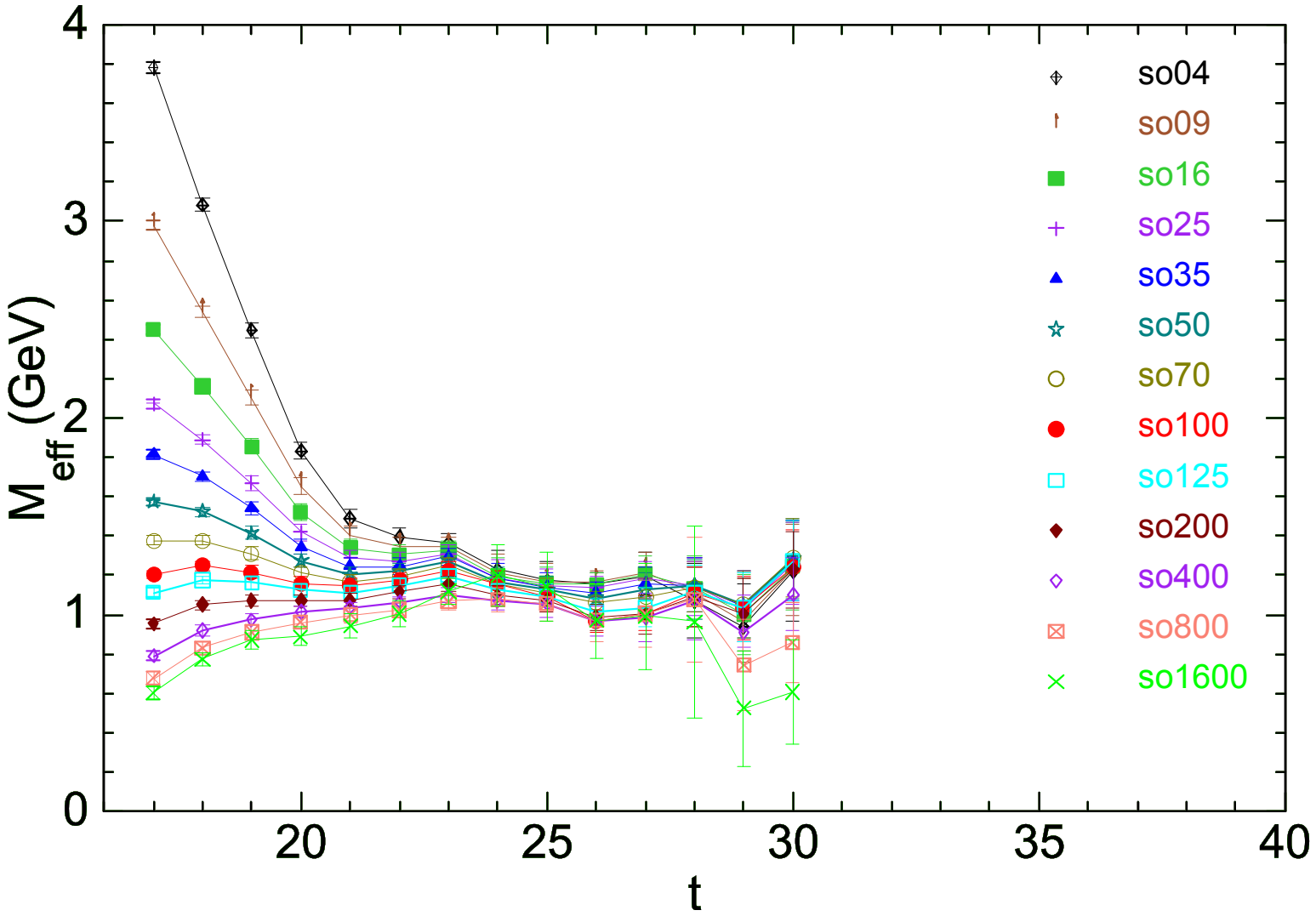

Positive Parity Nucleon - First Excited State - m_π: 296 MeV

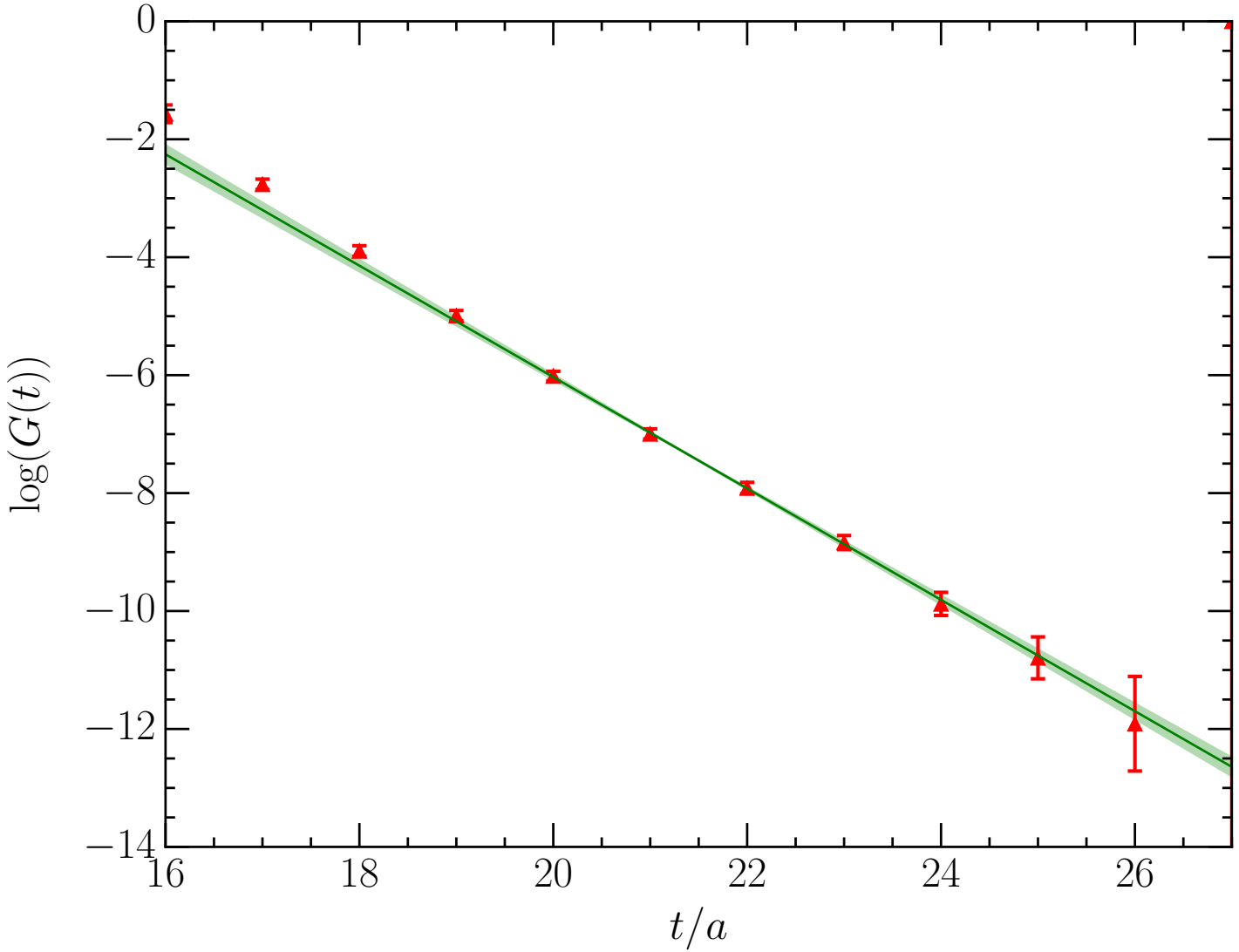

Positive Parity Nucleon - First Excited State - m_π: 296 MeV - χ^2_{dof}: 0.67

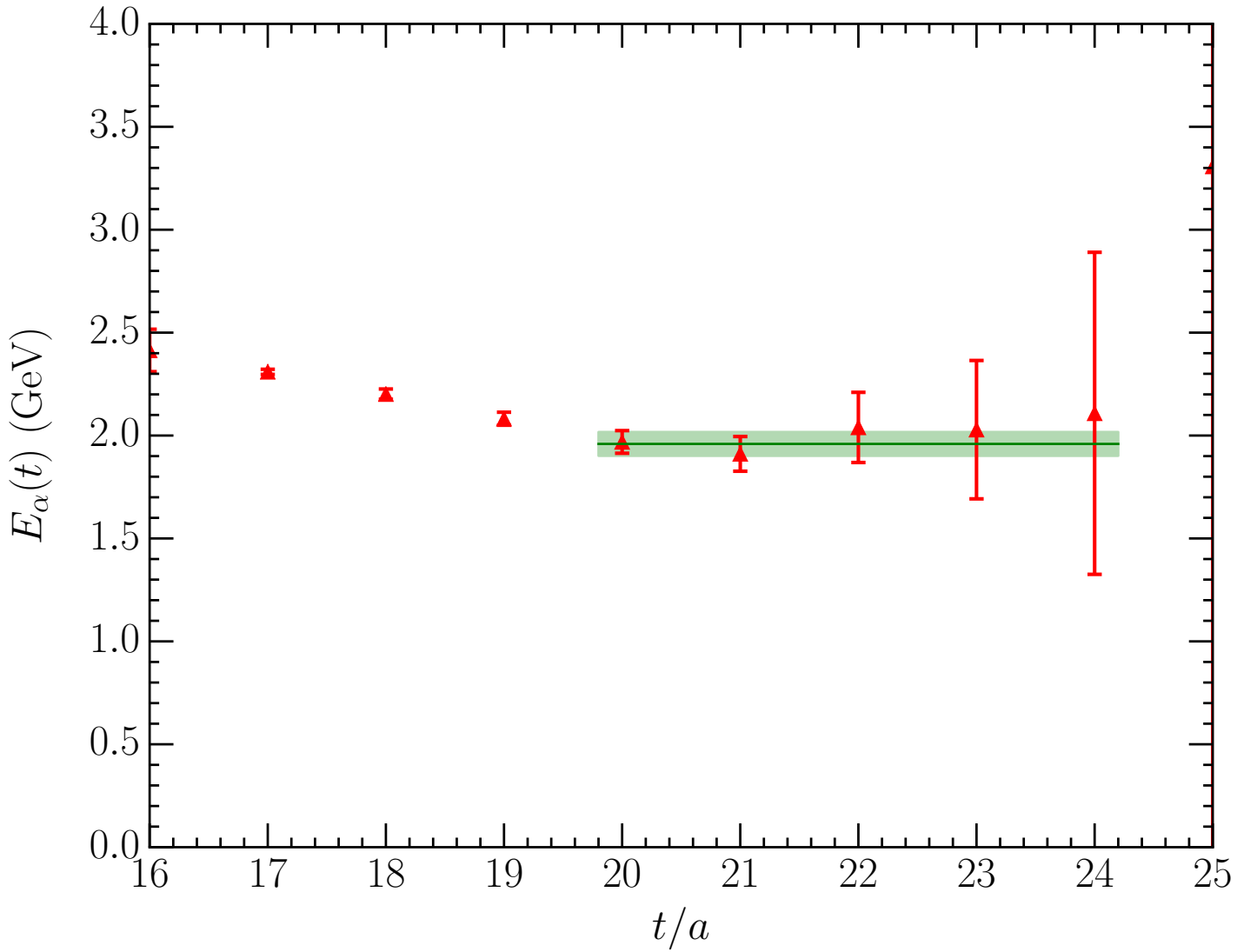

Negative Parity Nucleon - 2nd Excited State - m_π: 156 MeV

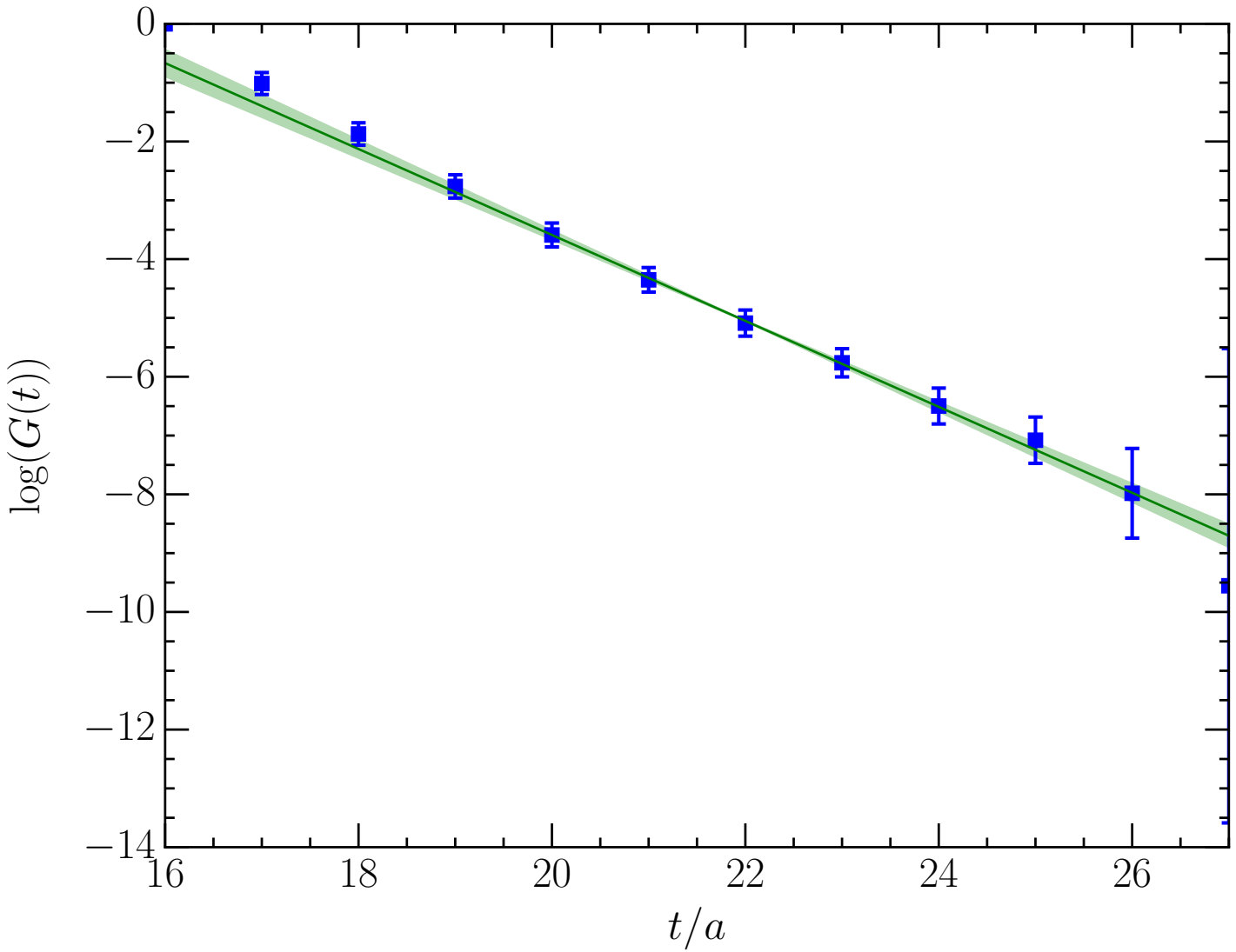

Negative Parity Nucleon - 2nd Excited State - m_π: 156 MeV - χ^2_{dof}: 0.88

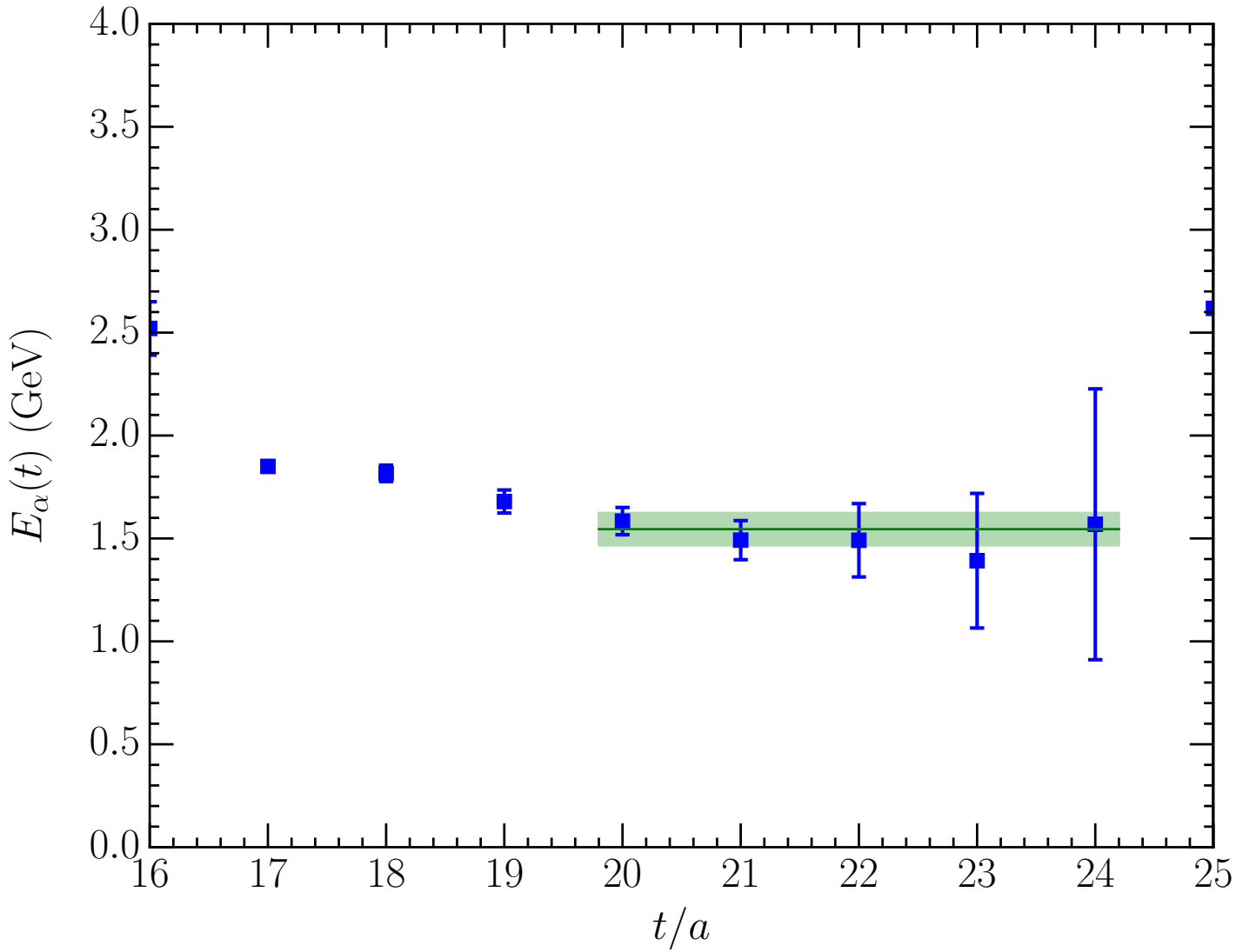

Further Information

- "Roper Resonance in 2+1 Flavor QCD,"
  M. S. Mahbub, *et al.* [CSSM],
  Phys. Lett. B **707** (2012) 389
  arXiv:1011.5724 [hep-lat],

- "Low-lying Odd-parity States of the Nucleon in Lattice QCD,"
  M. Selim Mahbub, *et al.* [CSSM],
  Phys. Rev. D Rapid Comm. **87** (2013) 011501,
  arXiv:1209.0240 [hep-lat]

- "Structure and Flow of the Nucleon Eigenstates in Lattice QCD,"
  M. S. Mahbub, *et al.* [CSSM],
  Phys. Rev. D **87** (2013) 9, 094506
  arXiv:1302.2987 [hep-lat].

CSSM Simulation Details

Based on the PACS-CS $(2+1)$-flavour ensembles, available through the ILDG.

S. Aoki *et al* (PACS-CS Collaboration), Phys. Rev. D **79**, 034503 (2009)

- Lattice size of $32^3 \times 64$ with $\beta = 1.90$. $L \simeq 3$ fm.

CSSM Simulation Details

Based on the PACS-CS $(2+1)$-flavour ensembles, available through the ILDG.

S. Aoki *et al* (PACS-CS Collaboration), Phys. Rev. D **79**, 034503 (2009)

- Lattice size of $32^3 \times 64$ with $\beta = 1.90$. $L \simeq 3$ fm.
- 5 pion masses, ranging from 640 MeV down to 156 MeV.

CSSM Simulation Details

Based on the PACS-CS $(2+1)$-flavour ensembles, available through the ILDG.

S. Aoki *et al* (PACS-CS Collaboration), Phys. Rev. D **79**, 034503 (2009)

- Lattice size of $32^3 \times 64$ with $\beta = 1.90$. $L \simeq 3$ fm.
- 5 pion masses, ranging from 640 MeV down to 156 MeV.
- The strange quark κ_s is held fixed as the light quark masses vary.
  - Changes in the strange quark contributions are environmental effects.

Positive Parity Nucleon Spectrum: CSSM

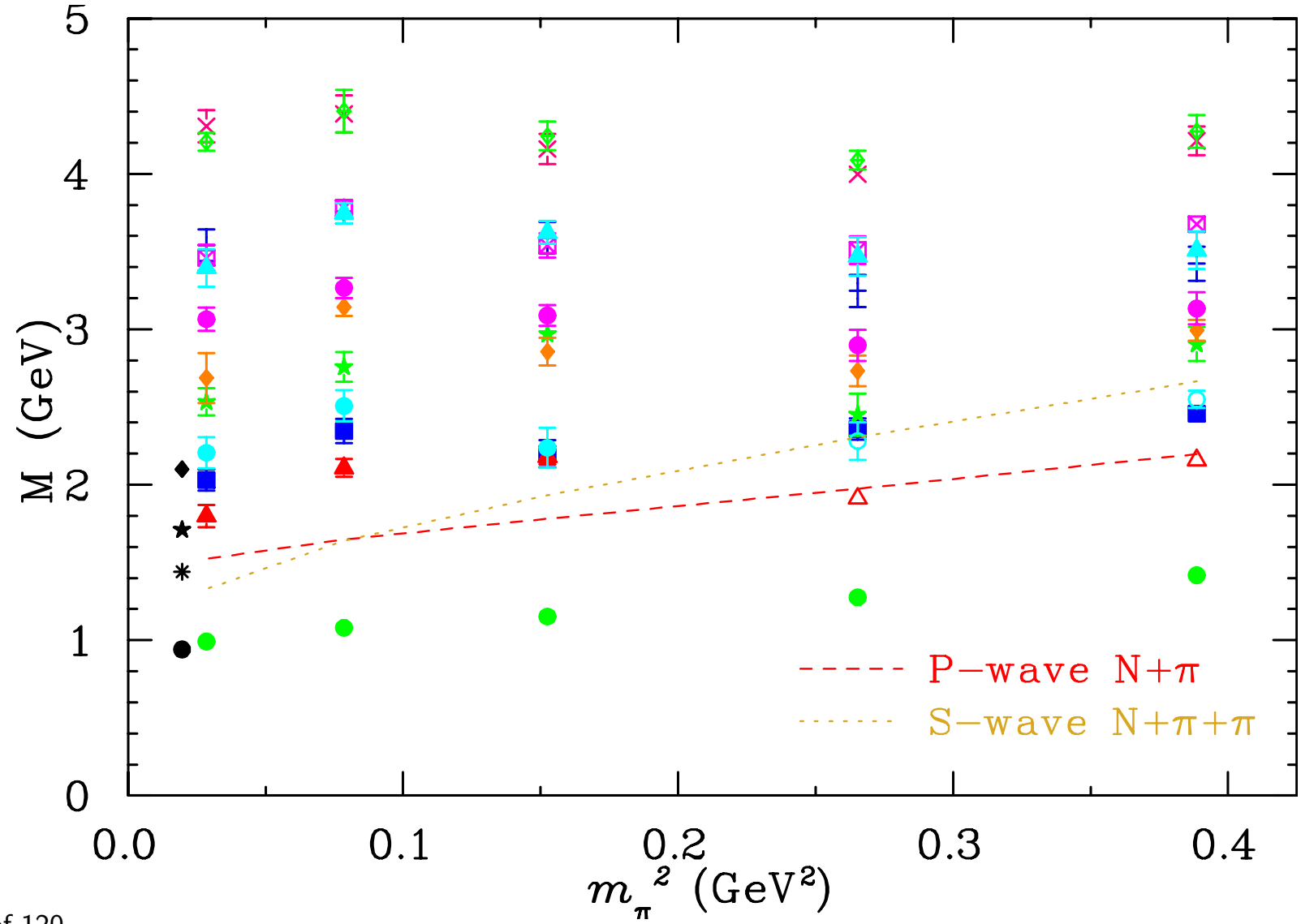

States Tracked via Orthogonal Eigenvectors

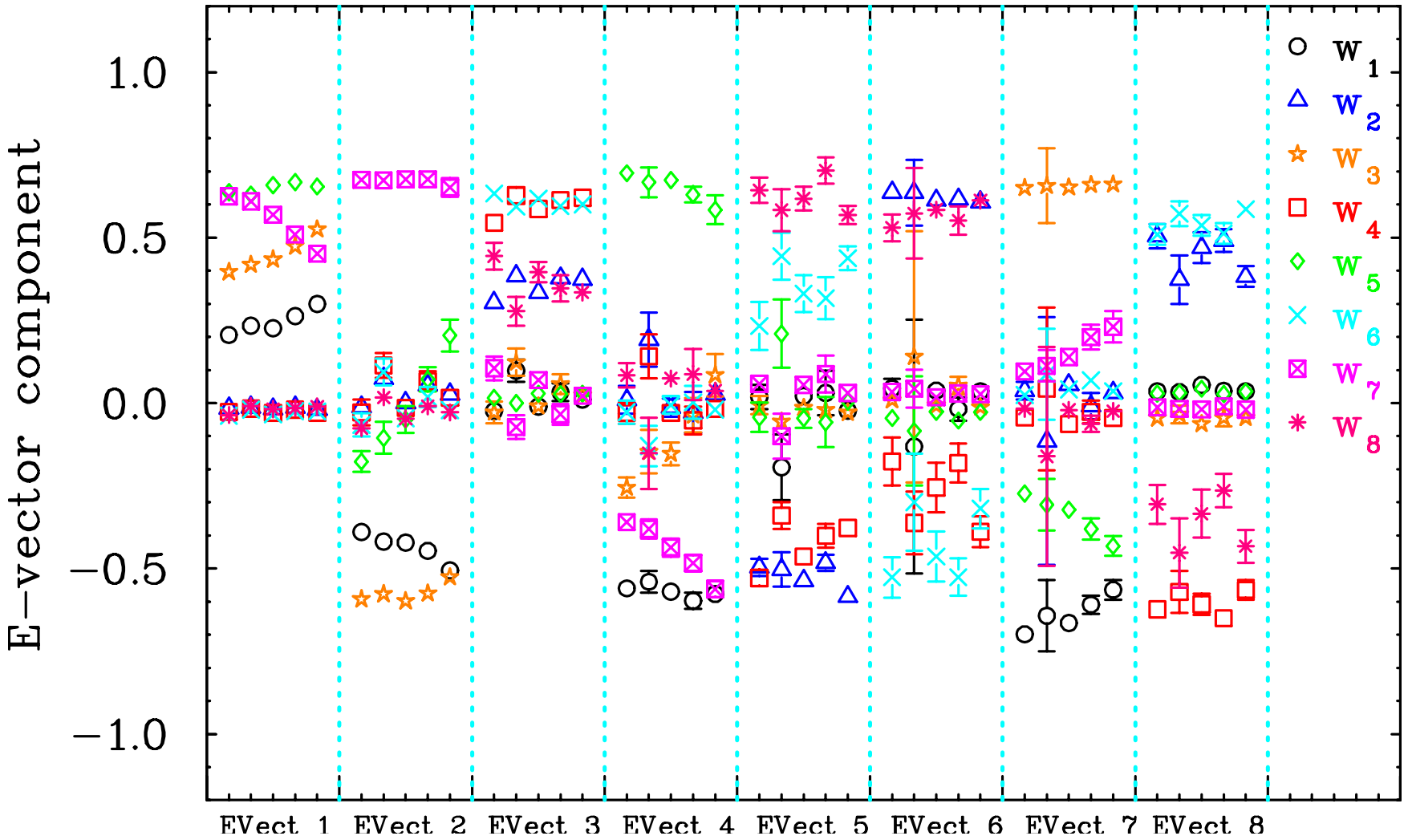

Positive Parity Nucleon Spectrum: CSSM

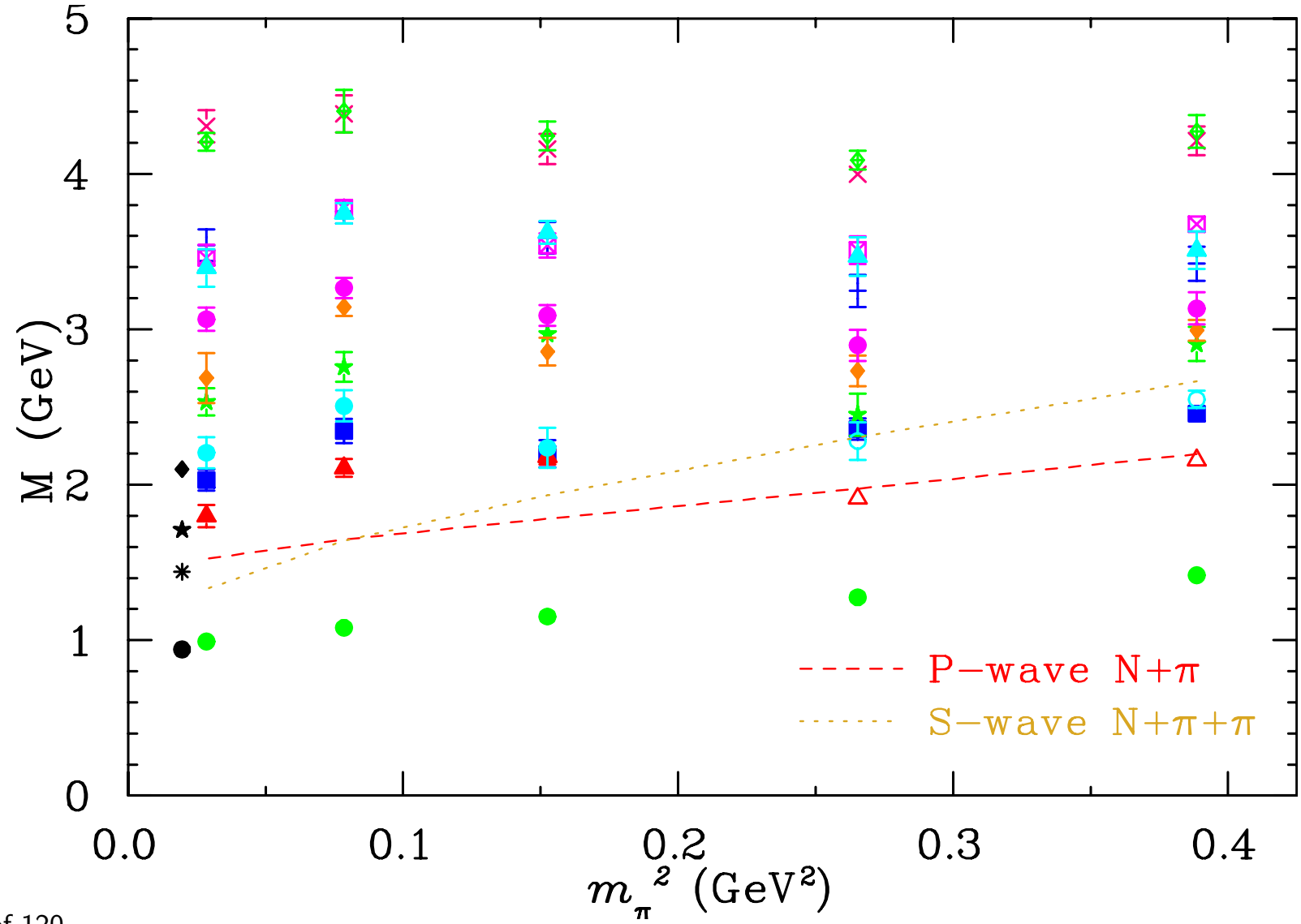

Comparison: Hadron Spectrum Collaboration (HSC)

- "Excited state baryon spectroscopy from lattice QCD," R. G. Edwards, J. J. Dudek, D. G. Richards and S. J. Wallace, Phys. Rev. D **84** (2011) 074508 arXiv:1104.5152 [hep-ph].

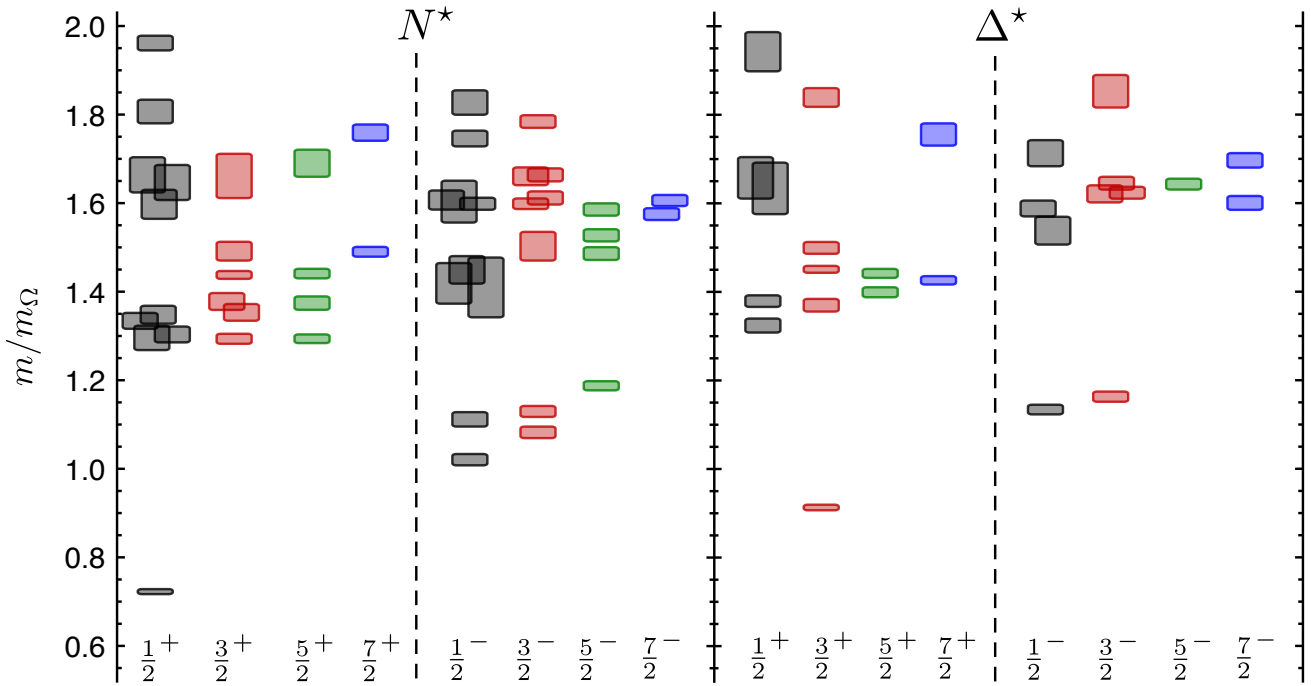

CSSM & HSC Comparison: Positive Parity CSSM

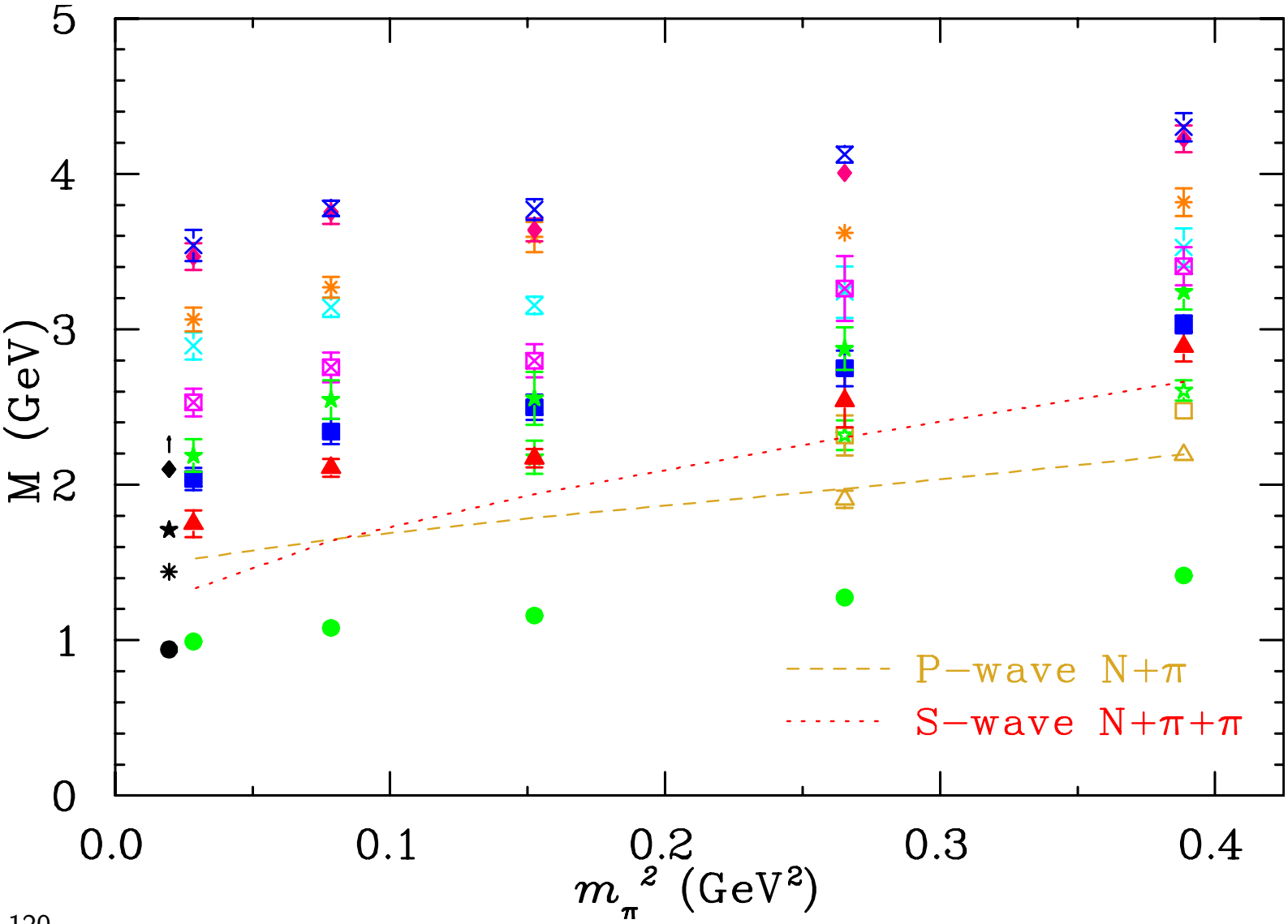

CSSM & HSC Comparison: Positive Parity CSSM

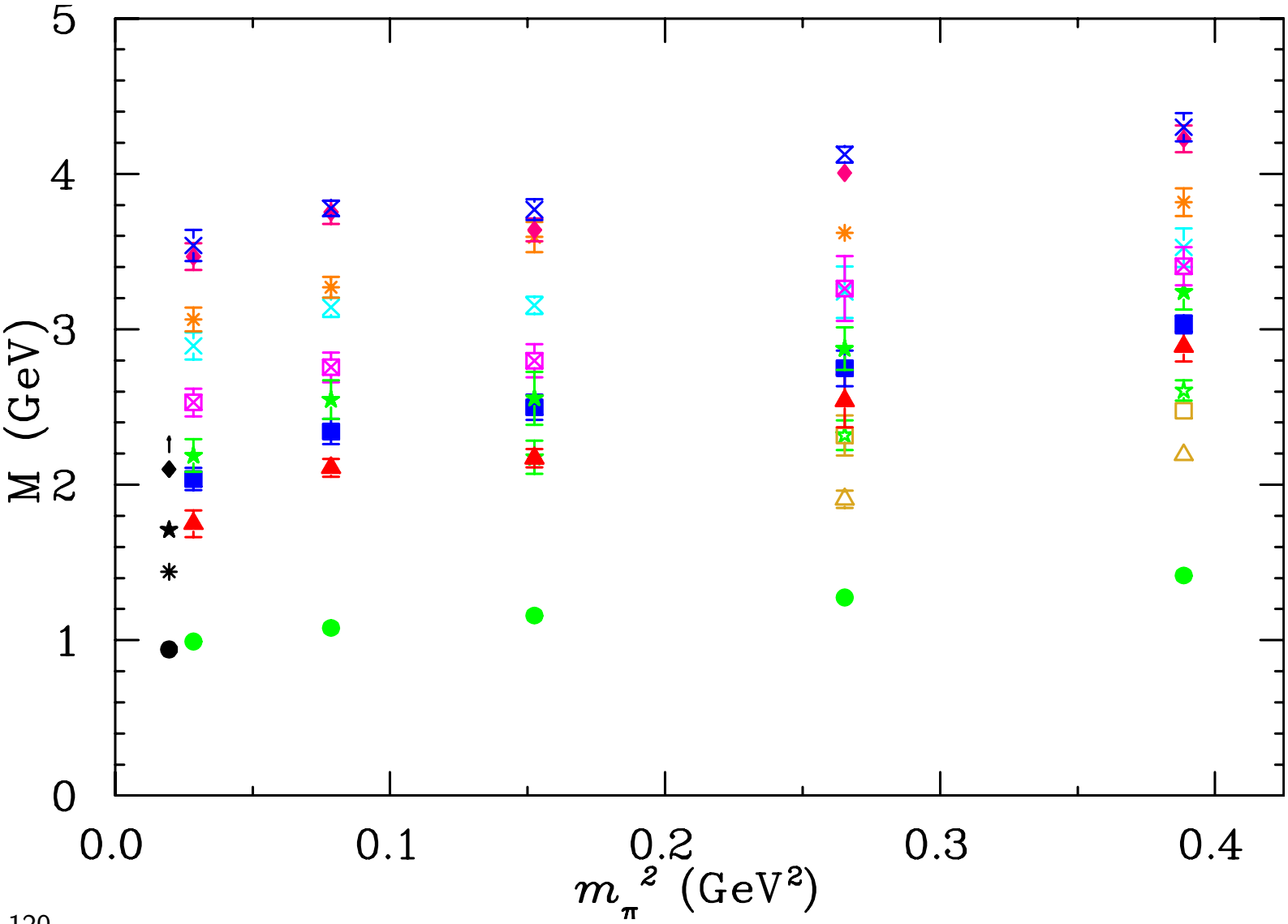

CSSM & HSC Comparison: Positive Parity

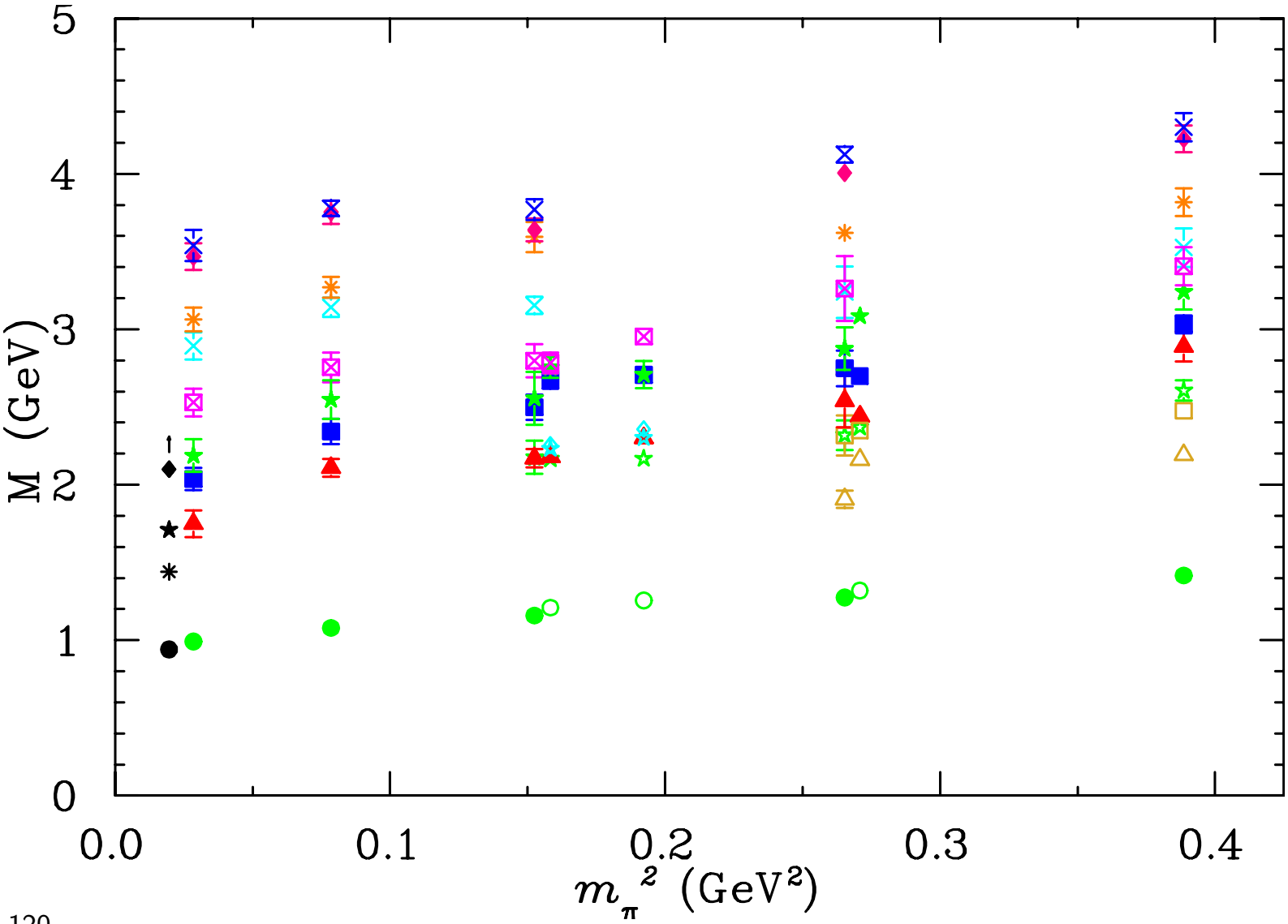

CSSM & HSC Comparison: Negative Parity CSSM

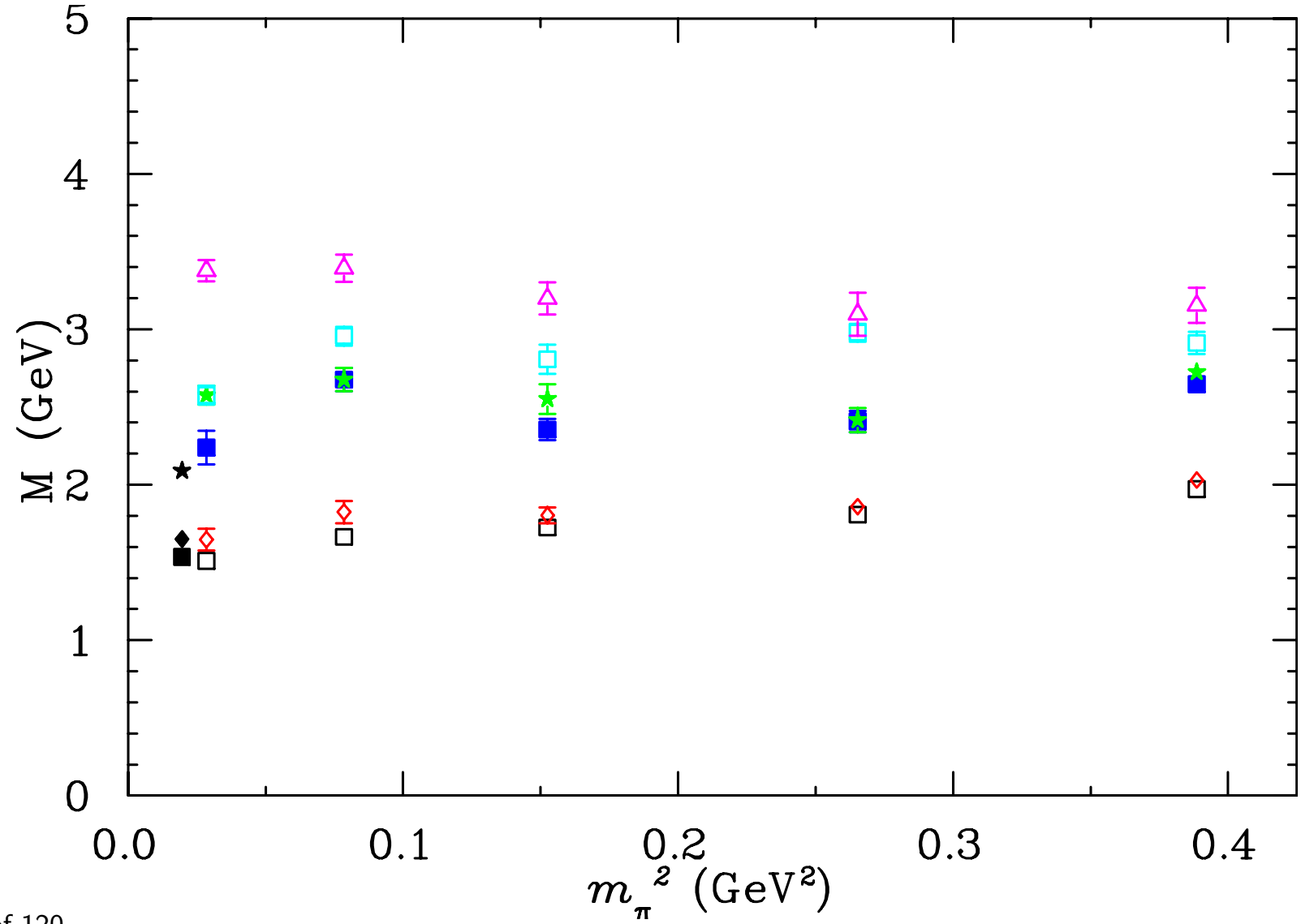

CSSM & HSC Comparison: Negative Parity

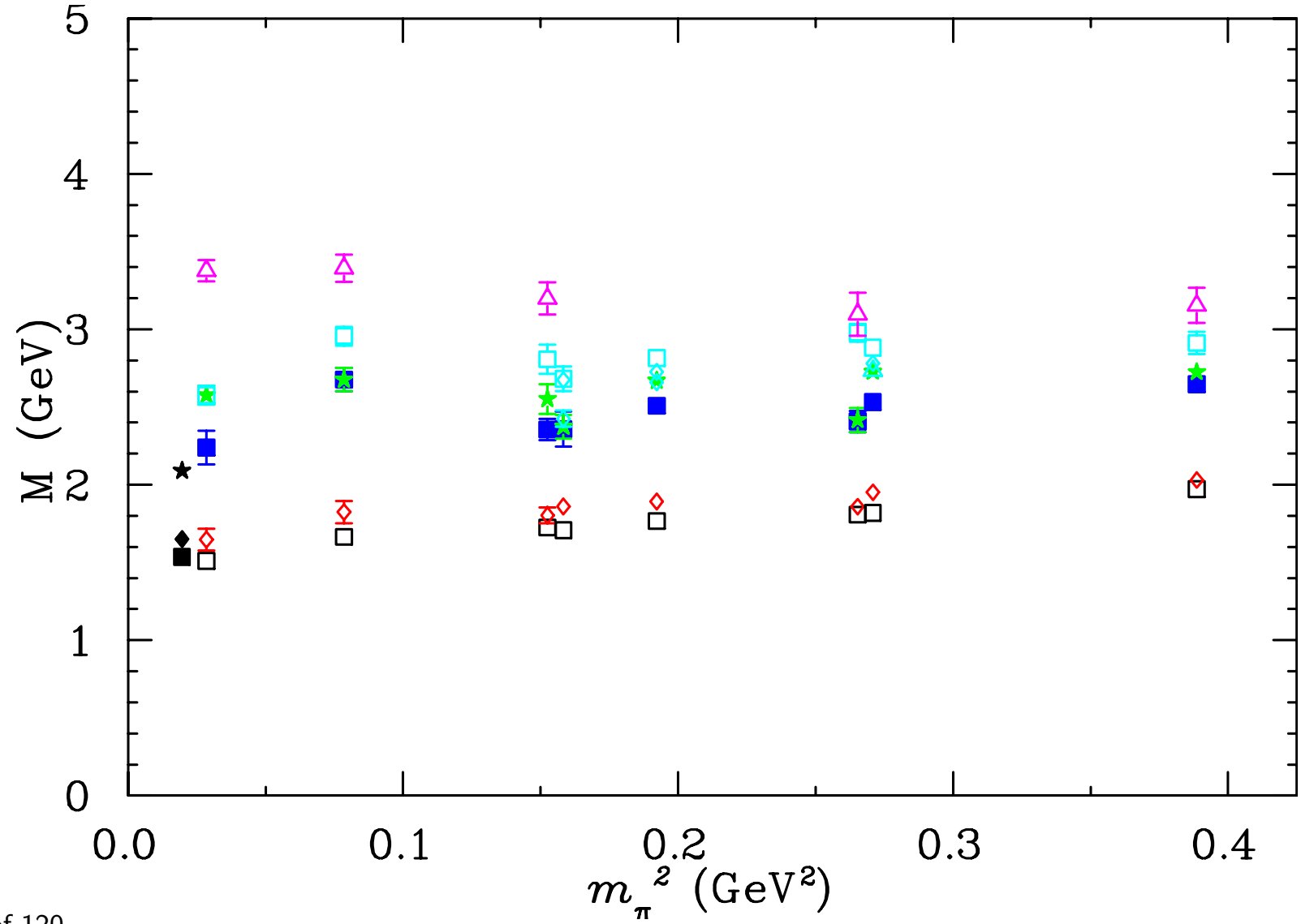

Positive Parity Nucleon Spectrum: χQCD (U. Kentucky) Collaboration

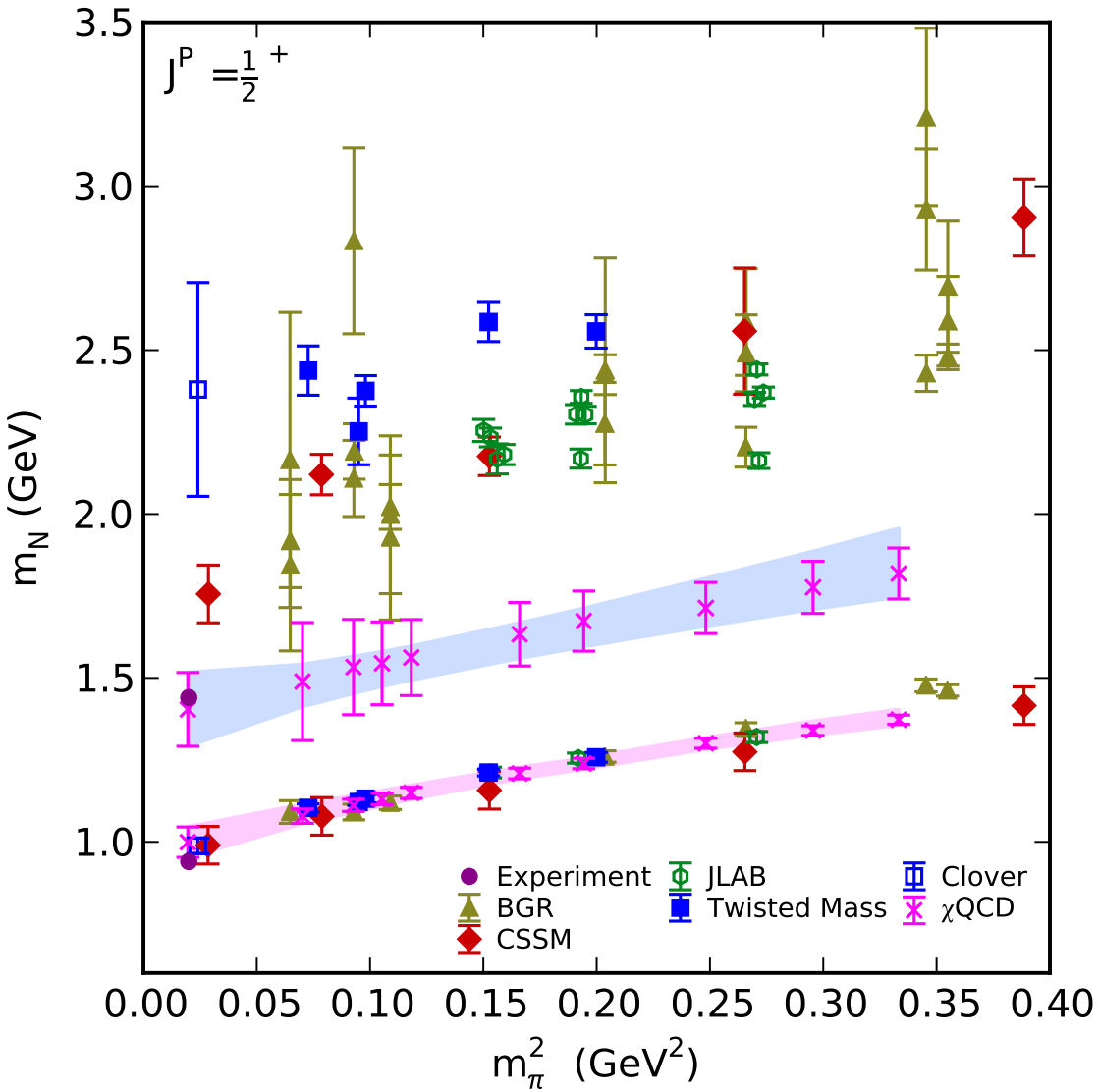

Positive Parity Nucleon Spectrum: χQCD (U. Kentucky) Collaboration

- "The Roper Puzzle,"
  K. F. Liu, Y. Chen, M. Gong, R. Sufian, M. Sun and A. Li,
  PoS LATTICE **2013** (2014) 507
  arXiv:1403.6847 [hep-ph].

Essence of the Sequential Empirical Bayesian (SEB) Analysis

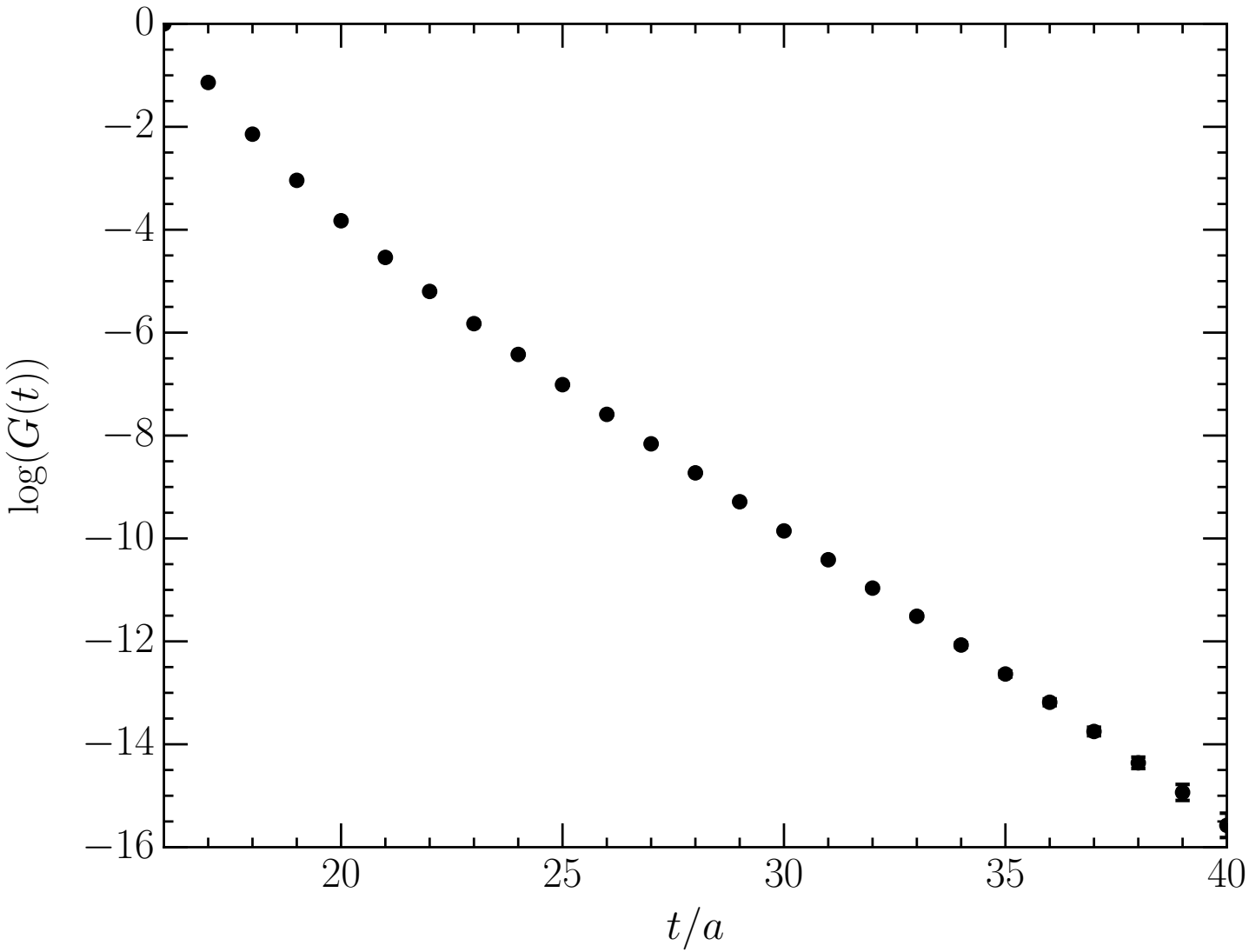

Essence of the Sequential Empirical Bayesian (SEB) Analysis

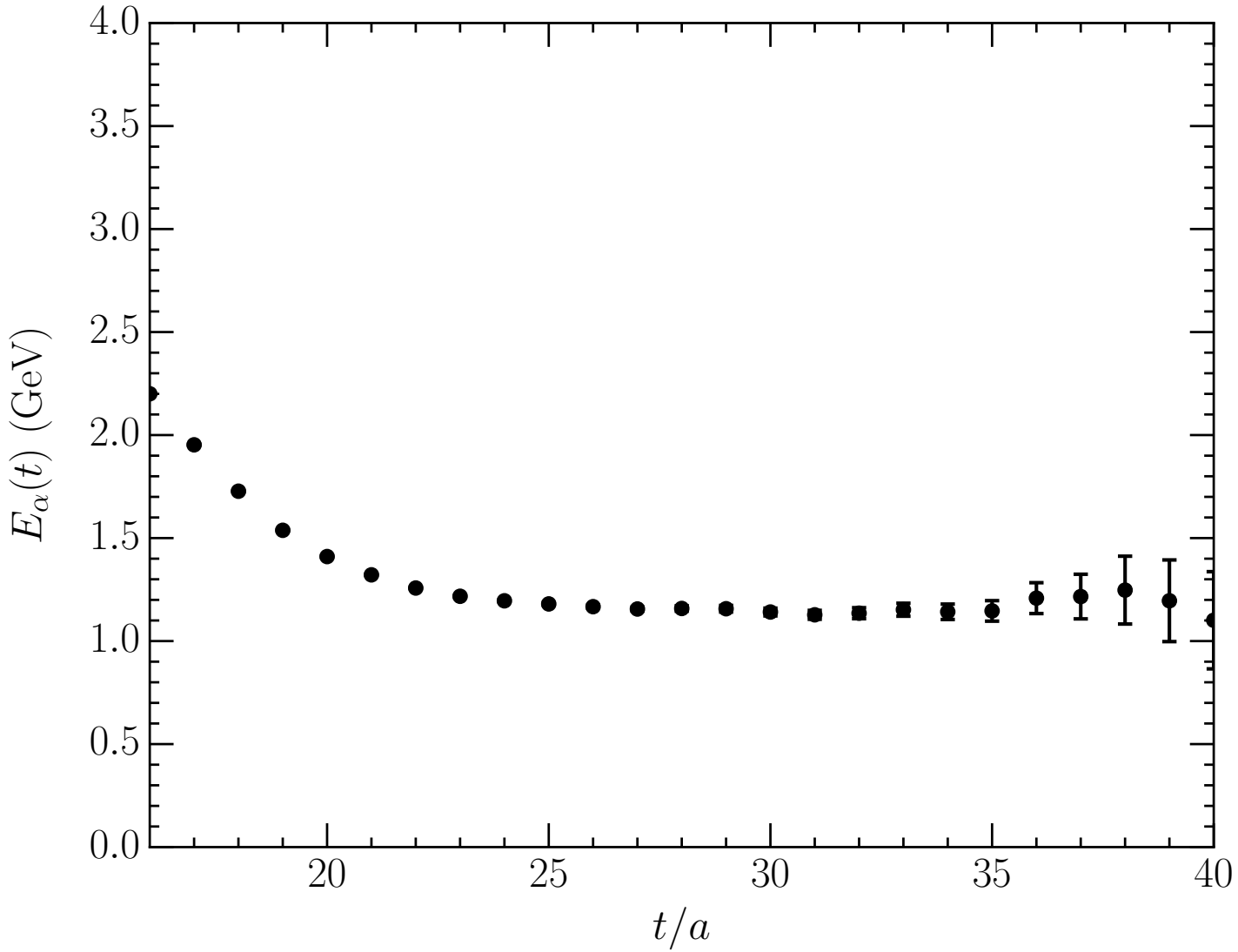

χQCD & HSC Systematic Comparison - Same Correlators Examined

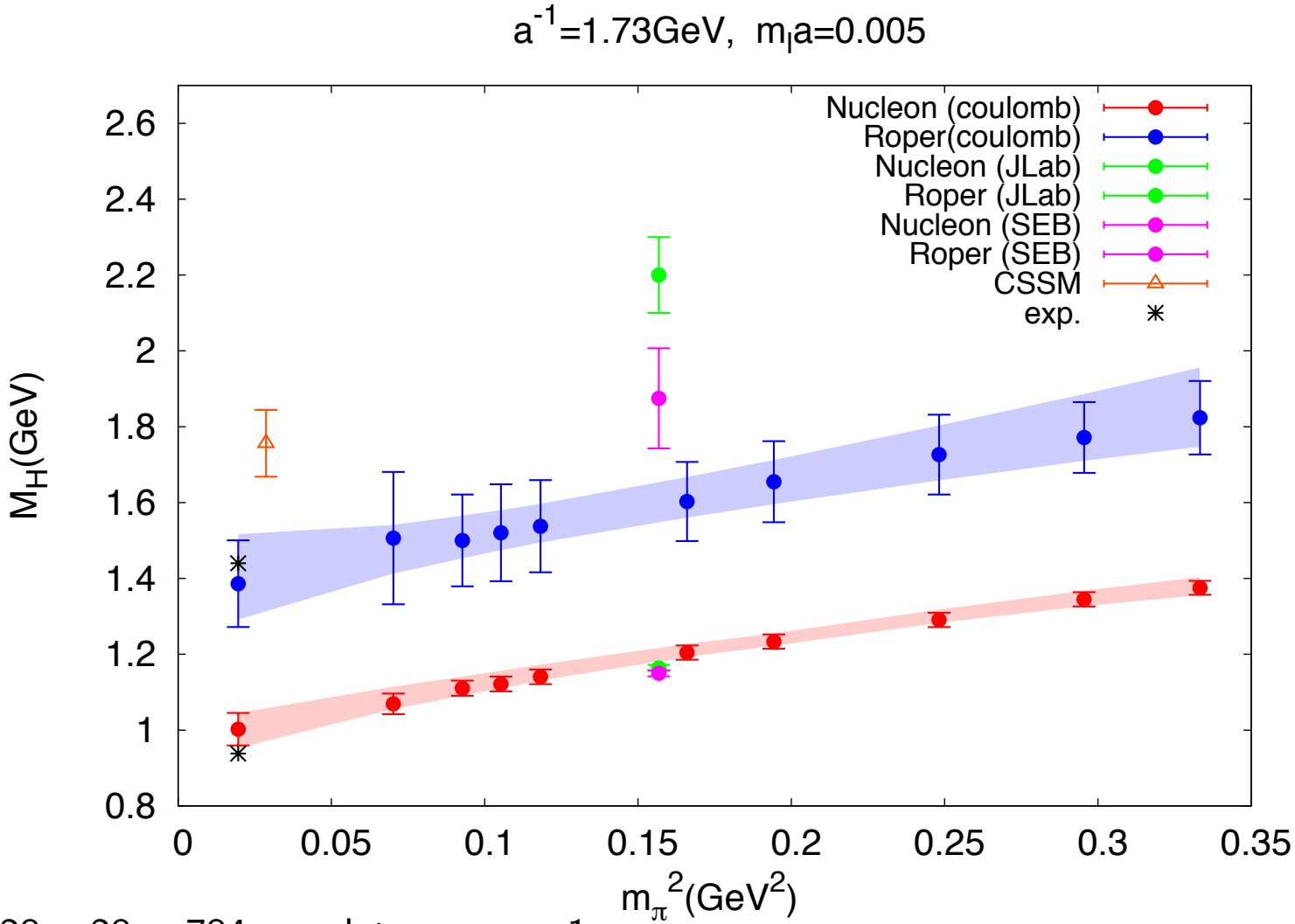

Note: $28 \times 28 = 784$ correlators versus 1.

Positive Parity Spectrum: Cyprus (Twisted Mass) Collaboration: Feb. '13

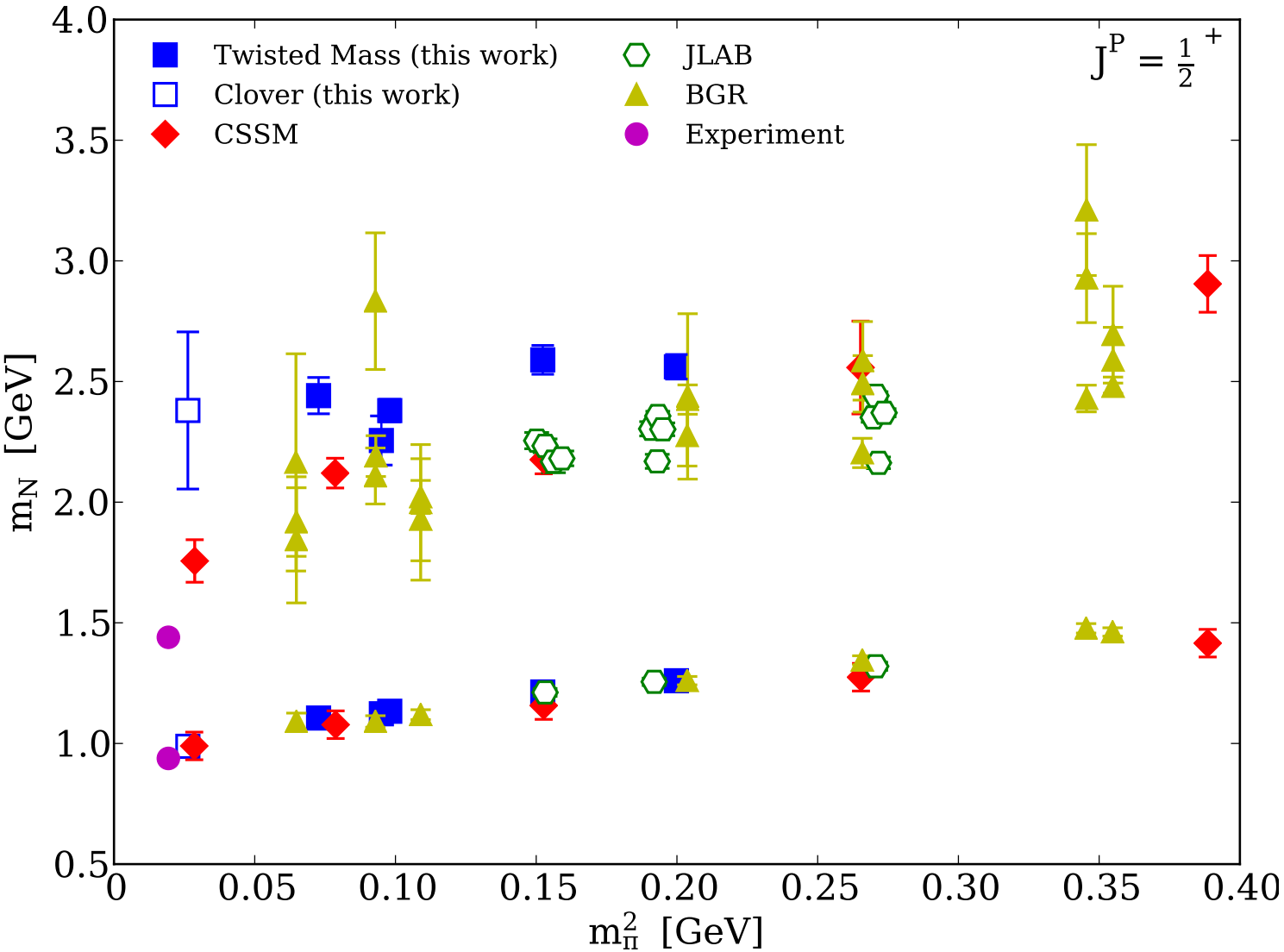

Positive Parity Spectrum: Cyprus (Twisted Mass) Collaboration: Jan. '14

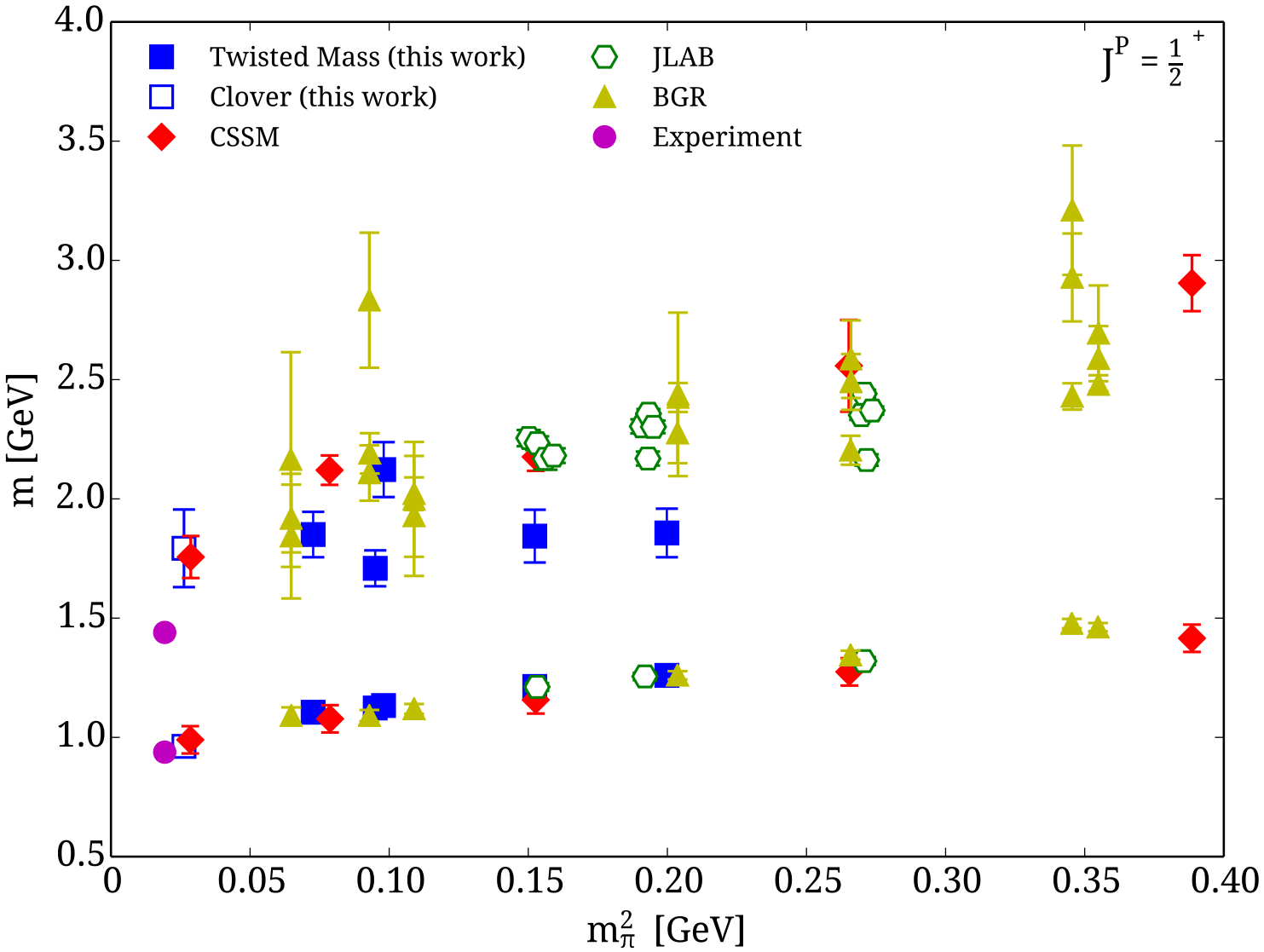

d-quark probability density in ground state proton: $m_\pi = 156$ MeV (CSSM)

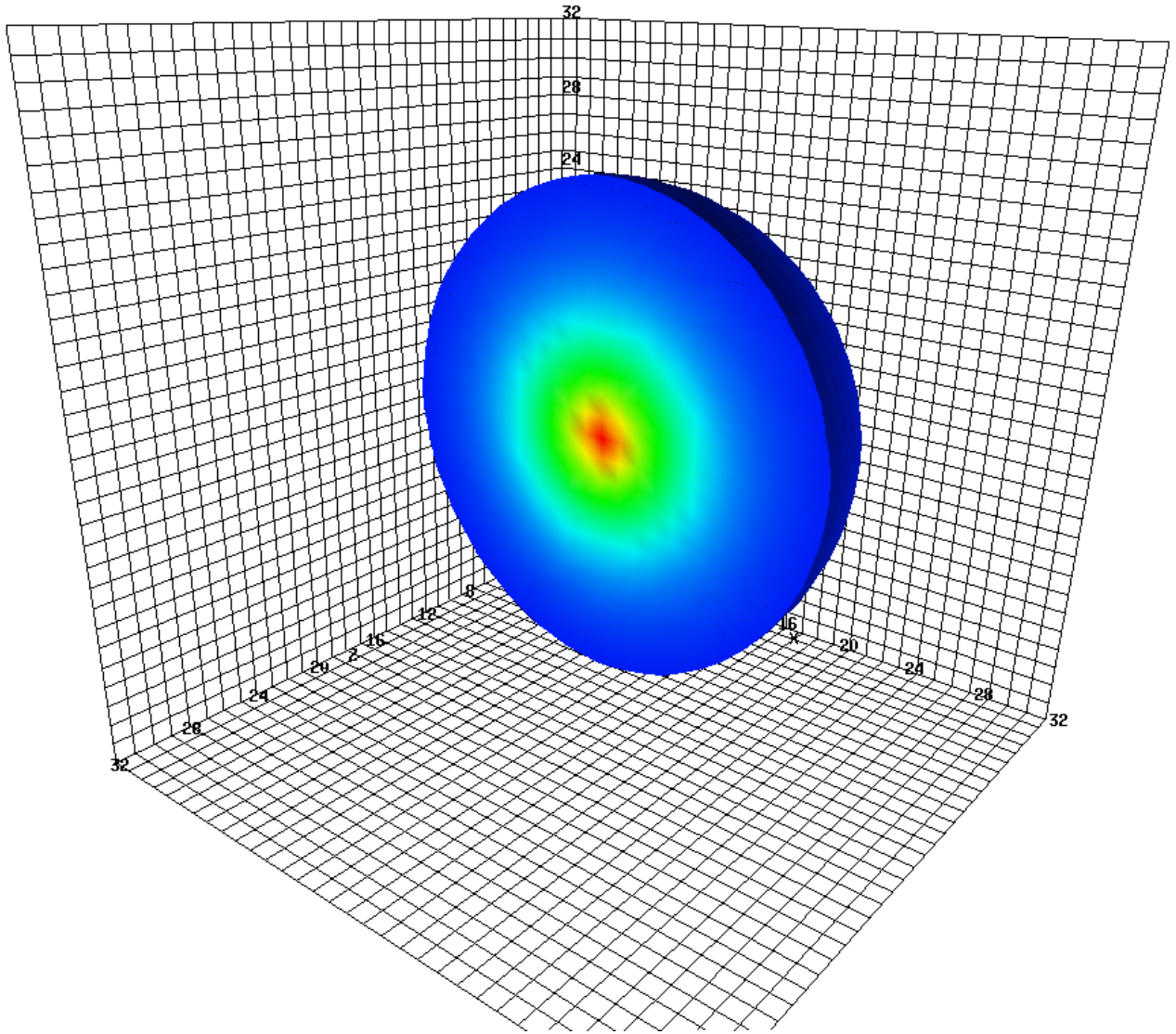

d-quark probability density in first excited proton: $m_\pi = 156$ MeV (CSSM)

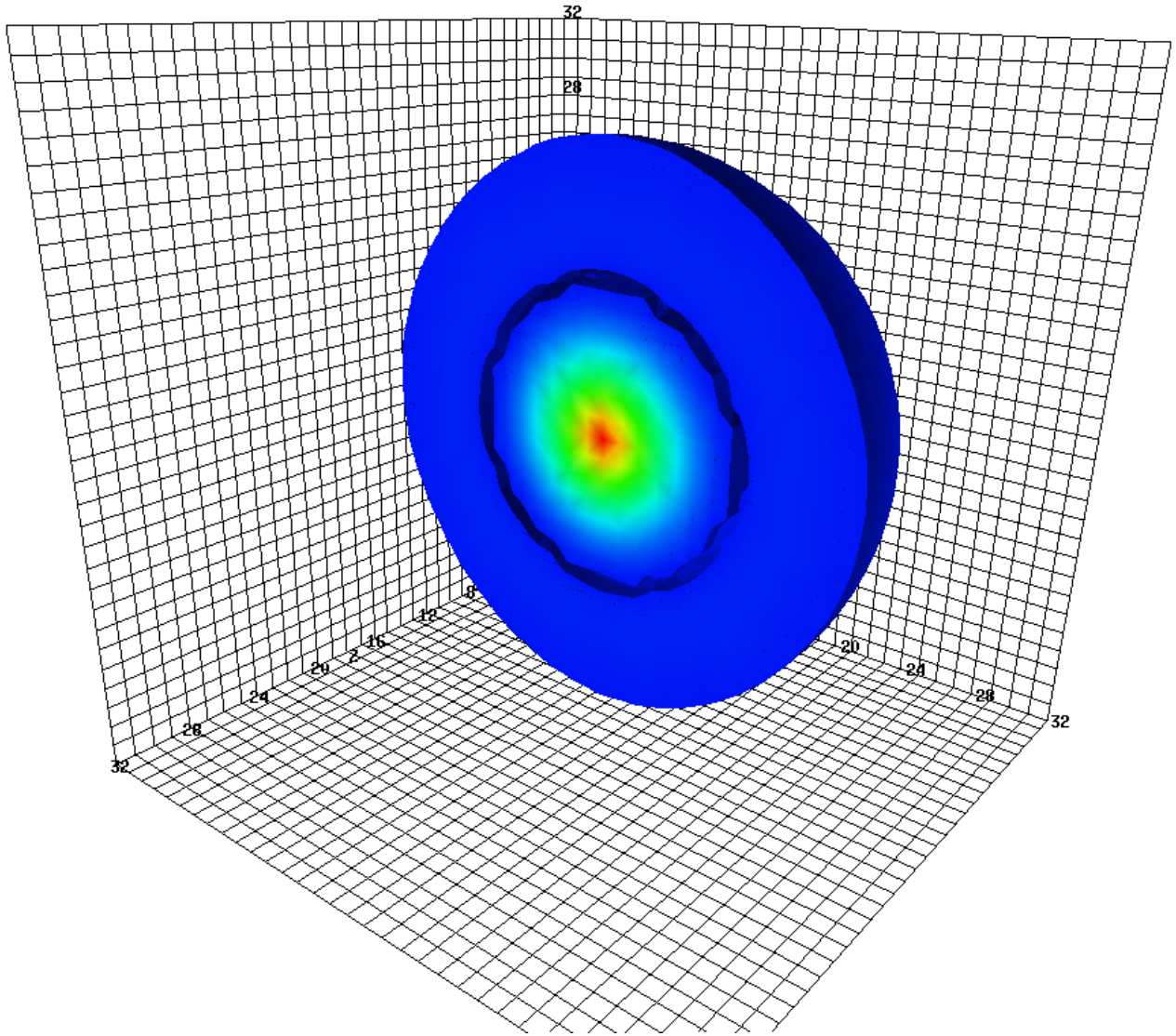

Positive Parity Nucleon Spectrum: only small smearing: Cyprus

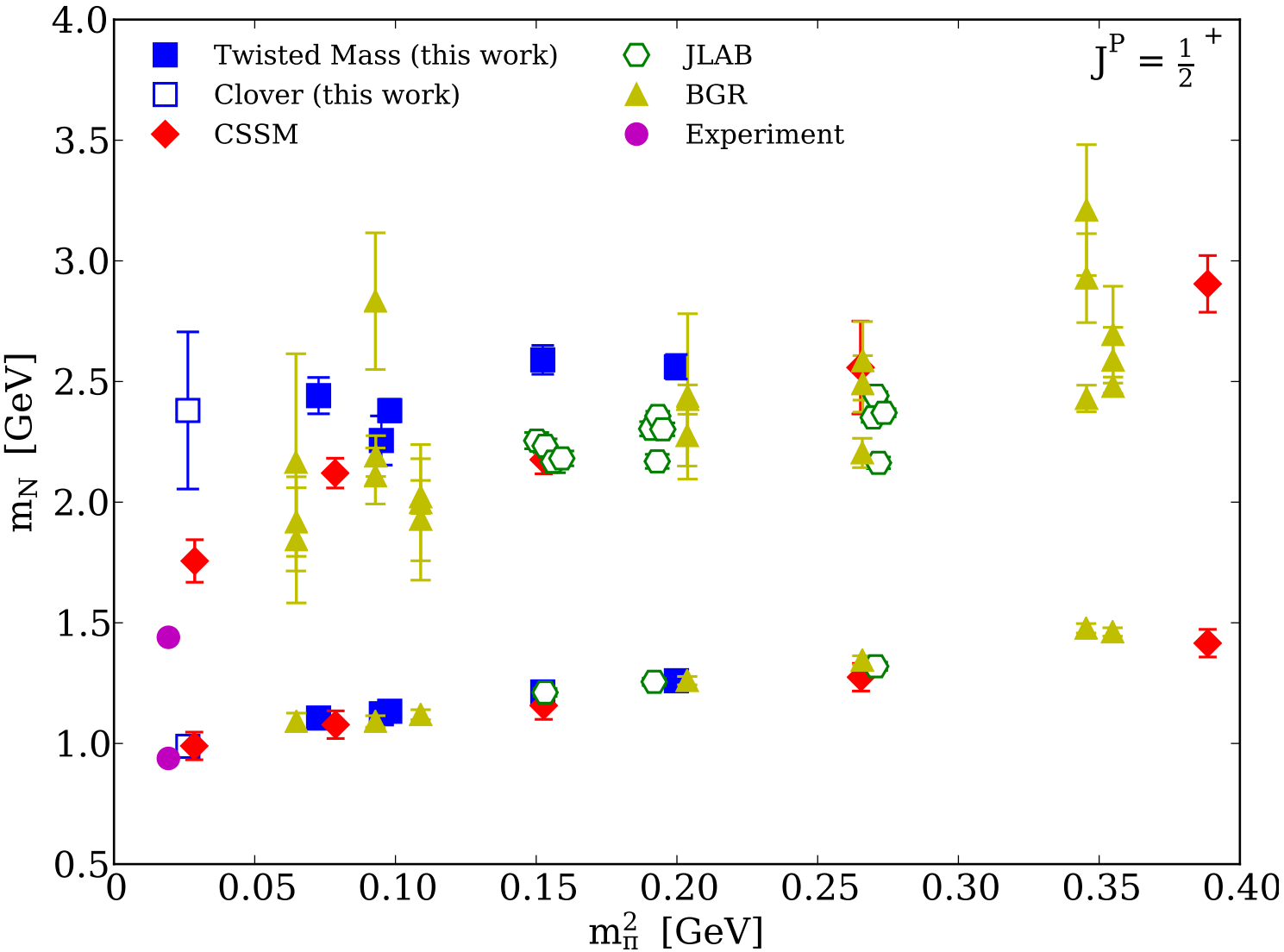

Positive Parity Nucleon Spectrum: r_{RMS} smearing of 8.6 lu: Cyprus

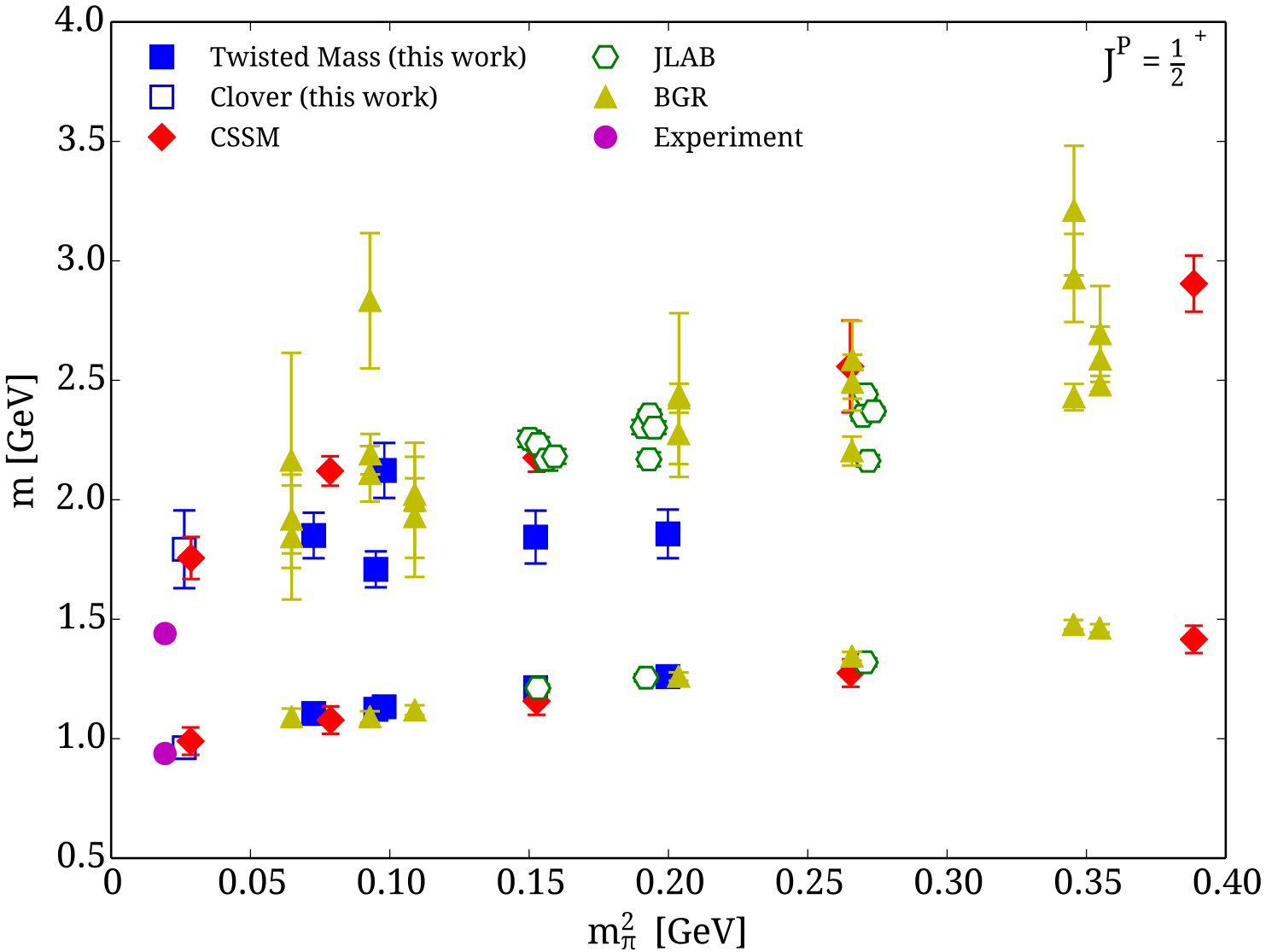

Athens Model Independent Analysis Scheme (AMIAS)

- "Novel analysis method for excited states in lattice QCD: The nucleon case,"
  C. Alexandrou, T. Leontiou, C. N. Papanicolas and E. Stiliaris,
  Phys. Rev. D **91** (2015) 1, 014506
  arXiv:1411.6765 [hep-lat].

Athens Model Independent Analysis Scheme (AMIAS)

- Does not rely on plateau identification of effective masses

Athens Model Independent Analysis Scheme (AMIAS)

- Does not rely on plateau identification of effective masses
- Exploits small time separations where the excited states contribute and statistical errors are small.

Athens Model Independent Analysis Scheme (AMIAS)

- Does not rely on plateau identification of effective masses
- Exploits small time separations where the excited states contribute and statistical errors are small.
- The Correlation matrix has the spectral decomposition

$$G_{ij}(t) = \sum_{\alpha=0}^{N_{\rm states}} A_i^{\alpha} \, A_j^{\dagger\alpha} \, e^{-E_\alpha \, t} \, . \quad i,j = 1, \ldots, N_{\rm interpolators} \, .$$

Athens Model Independent Analysis Scheme (AMIAS)

- Does not rely on plateau identification of effective masses
- Exploits small time separations where the excited states contribute and statistical errors are small.
- The Correlation matrix has the spectral decomposition

$$G_{ij}(t) = \sum_{\alpha=0}^{N_{\text{states}}} A_i^{\alpha} \, A_j^{\dagger\alpha} \, e^{-E_\alpha \, t} \, . \quad i,j = 1, \ldots, N_{\text{interpolators}} \, .$$

- Importance sampling is used to select fit parameters, A_i^{α} and E_α, with the probability $\exp(-\chi^2/2)$.

Athens Model Independent Analysis Scheme (AMIAS)

- Does not rely on plateau identification of effective masses
- Exploits small time separations where the excited states contribute and statistical errors are small.
- The Correlation matrix has the spectral decomposition

$$G_{ij}(t) = \sum_{\alpha=0}^{N_{\text{states}}} A_i^{\alpha} \, A_j^{\dagger\alpha} \, e^{-E_\alpha \, t} \, . \quad i,j = 1, \ldots, N_{\text{interpolators}} \, .$$

- Importance sampling is used to select fit parameters, A_i^{α} and E_α, with the probability $\exp(-\chi^2/2)$.
  - A parallel tempering algorithm is used to avoid local minima traps.

Athens Model Independent Analysis Scheme (AMIAS)

- Does not rely on plateau identification of effective masses
- Exploits small time separations where the excited states contribute and statistical errors are small.
- The Correlation matrix has the spectral decomposition

$$G_{ij}(t) = \sum_{\alpha=0}^{N_{\text{states}}} A_i^{\alpha} A_j^{\dagger\alpha} e^{-E_\alpha t} . \quad i,j = 1,\ldots,N_{\text{interpolators}} .$$

- Importance sampling is used to select fit parameters, A_i^{α} and E_α, with the probability $\exp(-\chi^2/2)$.
  - A parallel tempering algorithm is used to avoid local minima traps.
- Parameters are determined by fitting a Gaussian to their probability distributions.

Athens Model Independent Analysis Scheme (AMIAS)

- Does not rely on plateau identification of effective masses
- Exploits small time separations where the excited states contribute and statistical errors are small.
- The Correlation matrix has the spectral decomposition

$$G_{ij}(t) = \sum_{\alpha=0}^{N_{\rm states}} A_i^{\alpha} A_j^{\dagger\alpha} e^{-E_\alpha t} . \quad i,j = 1,\ldots,N_{\rm interpolators} .$$

- Importance sampling is used to select fit parameters, A_i^{α} and E_α, with the probability $\exp(-\chi^2/2)$.
  - A parallel tempering algorithm is used to avoid local minima traps.
- Parameters are determined by fitting a Gaussian to their probability distributions.
- Increase $N_{\rm states}$ until there is no sensitivity to additional exponentials.

Determining $N_{\text{states}} \equiv n_{\max}$ (Cyprus)

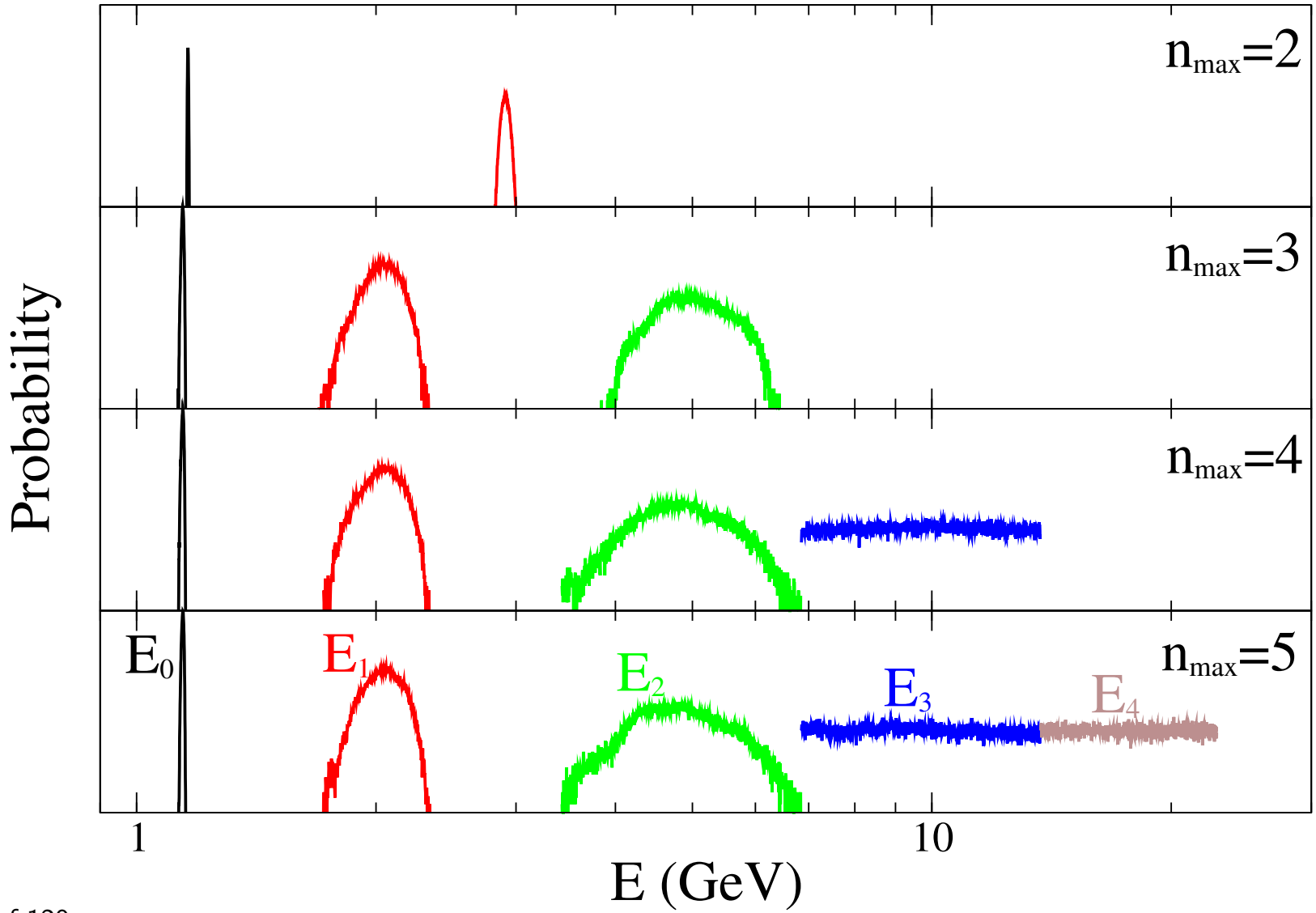

Analysis of Correlation Matrix is Essential

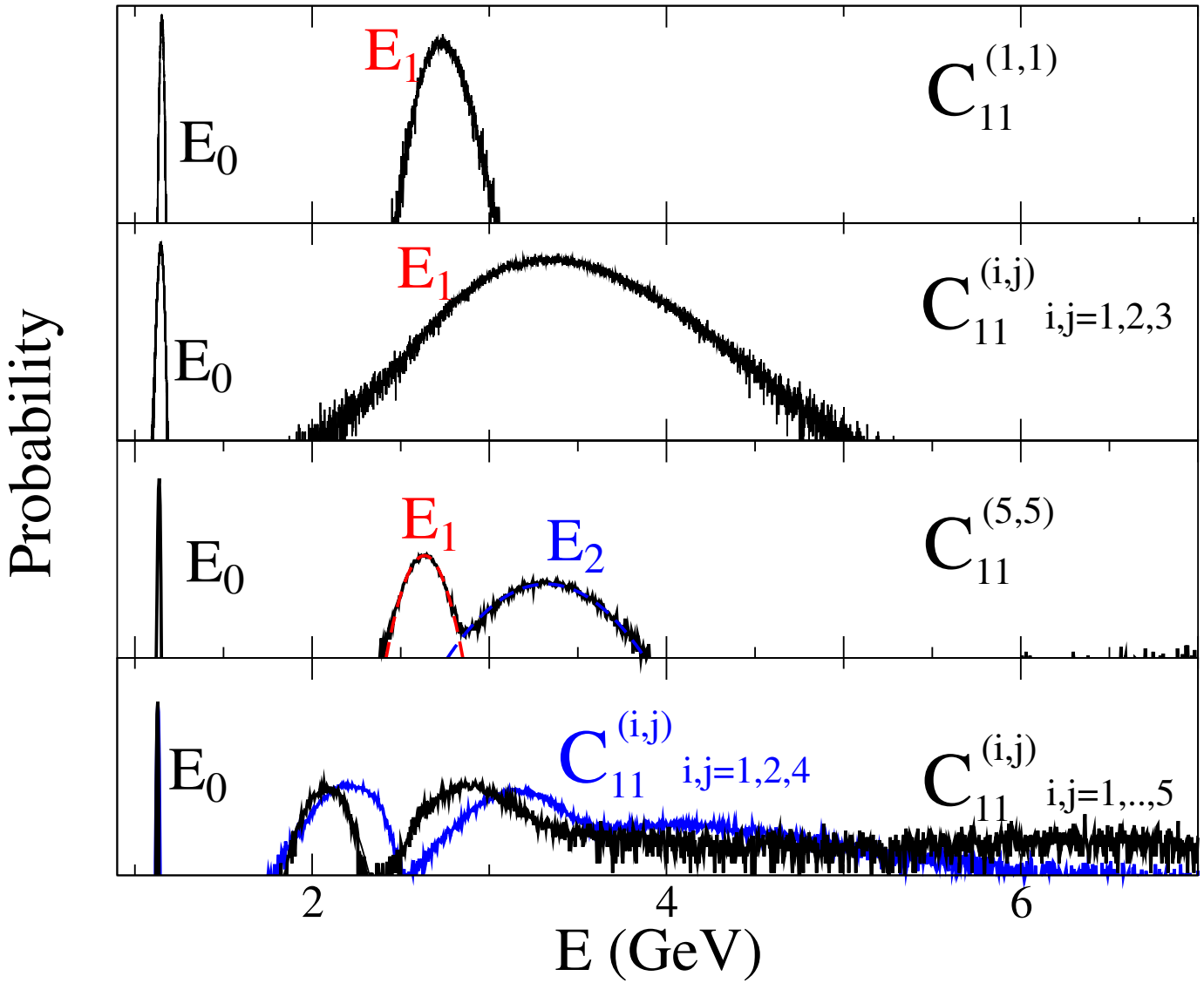

AMIAS applied to positive-parity Cyprus results

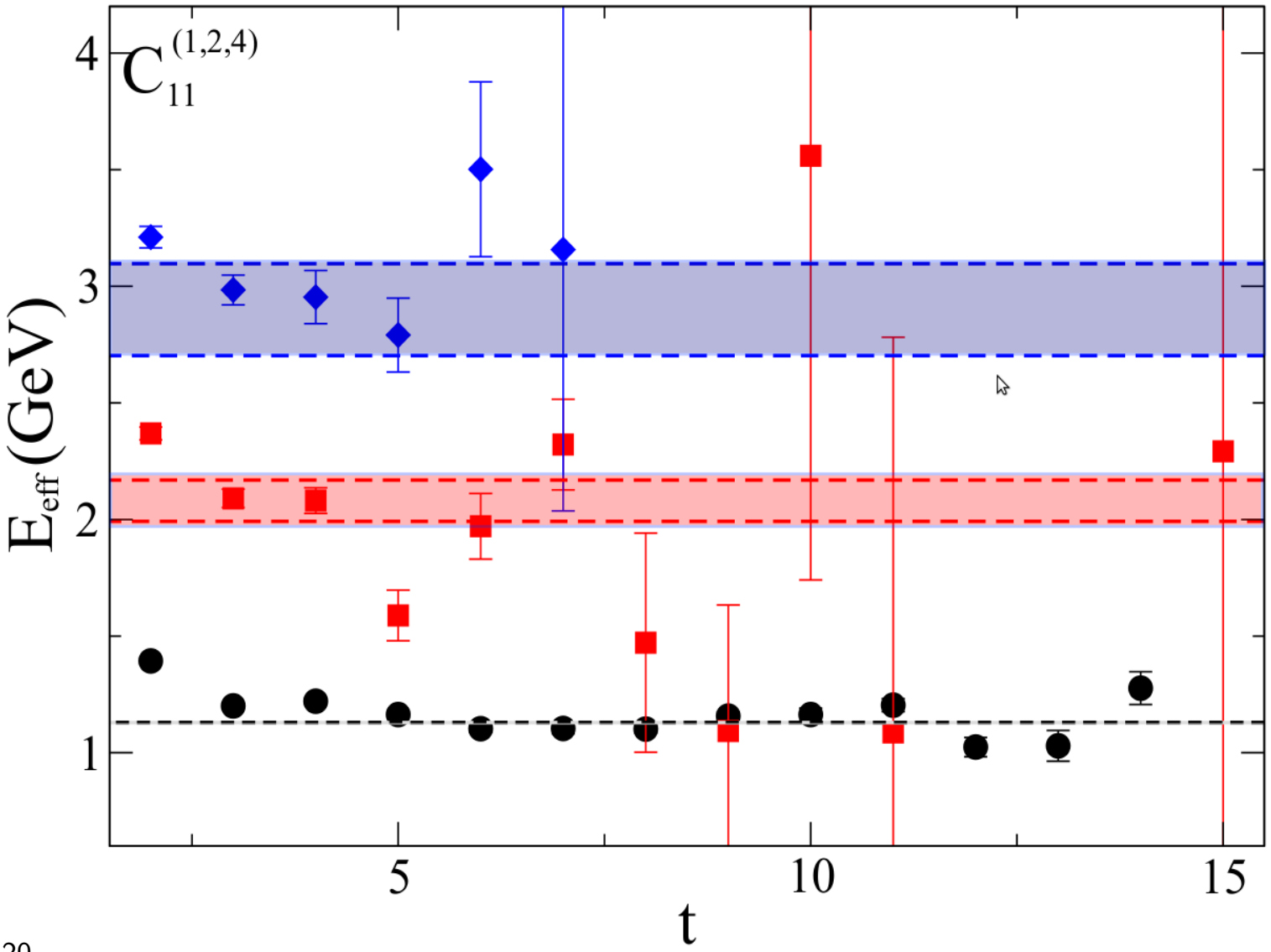

Lowest-lying positive-parity N^* Spectrum

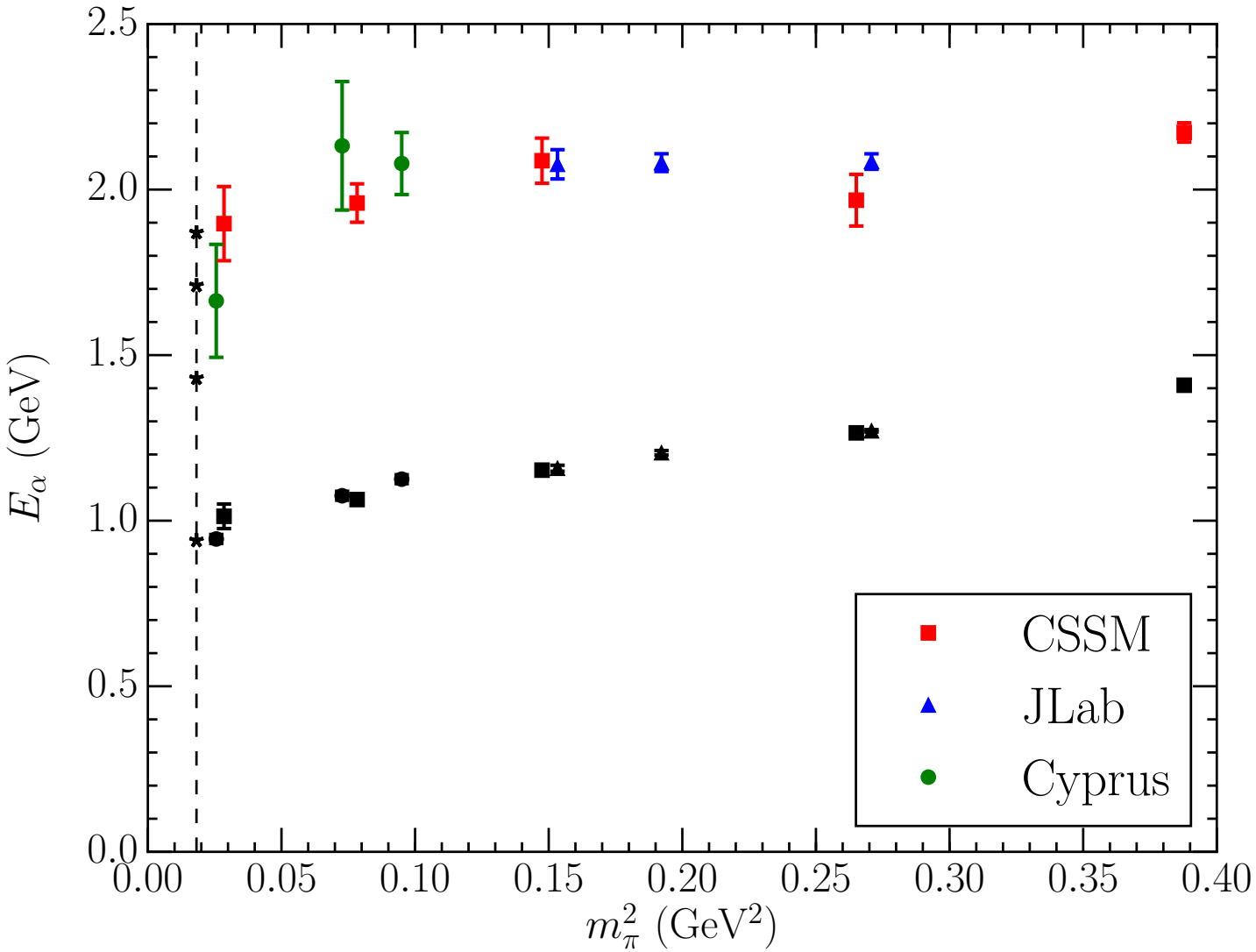

Properties of the Positive Parity Nucleon Spectrum

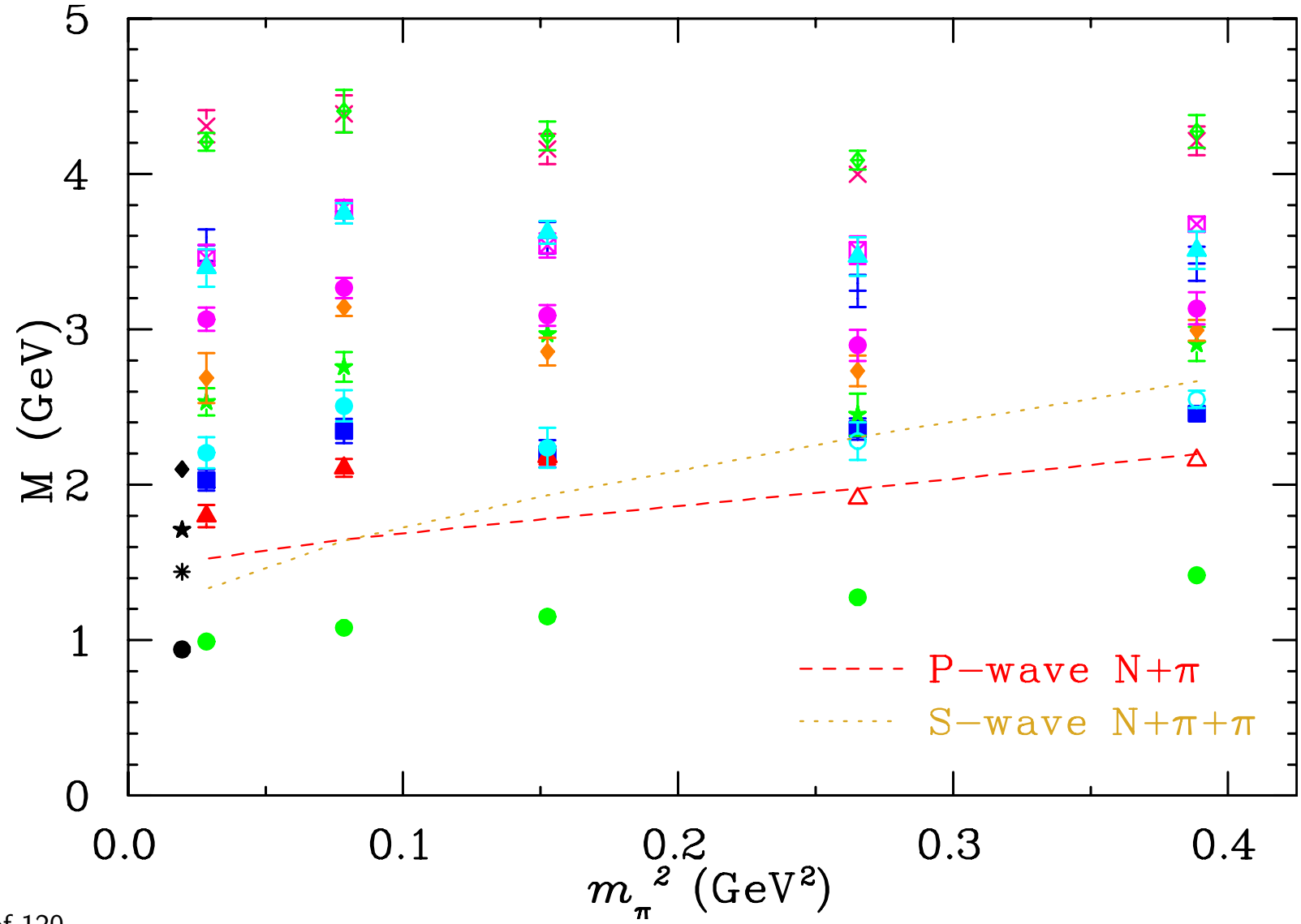

d-quark probability density in ground state proton (CSSM)

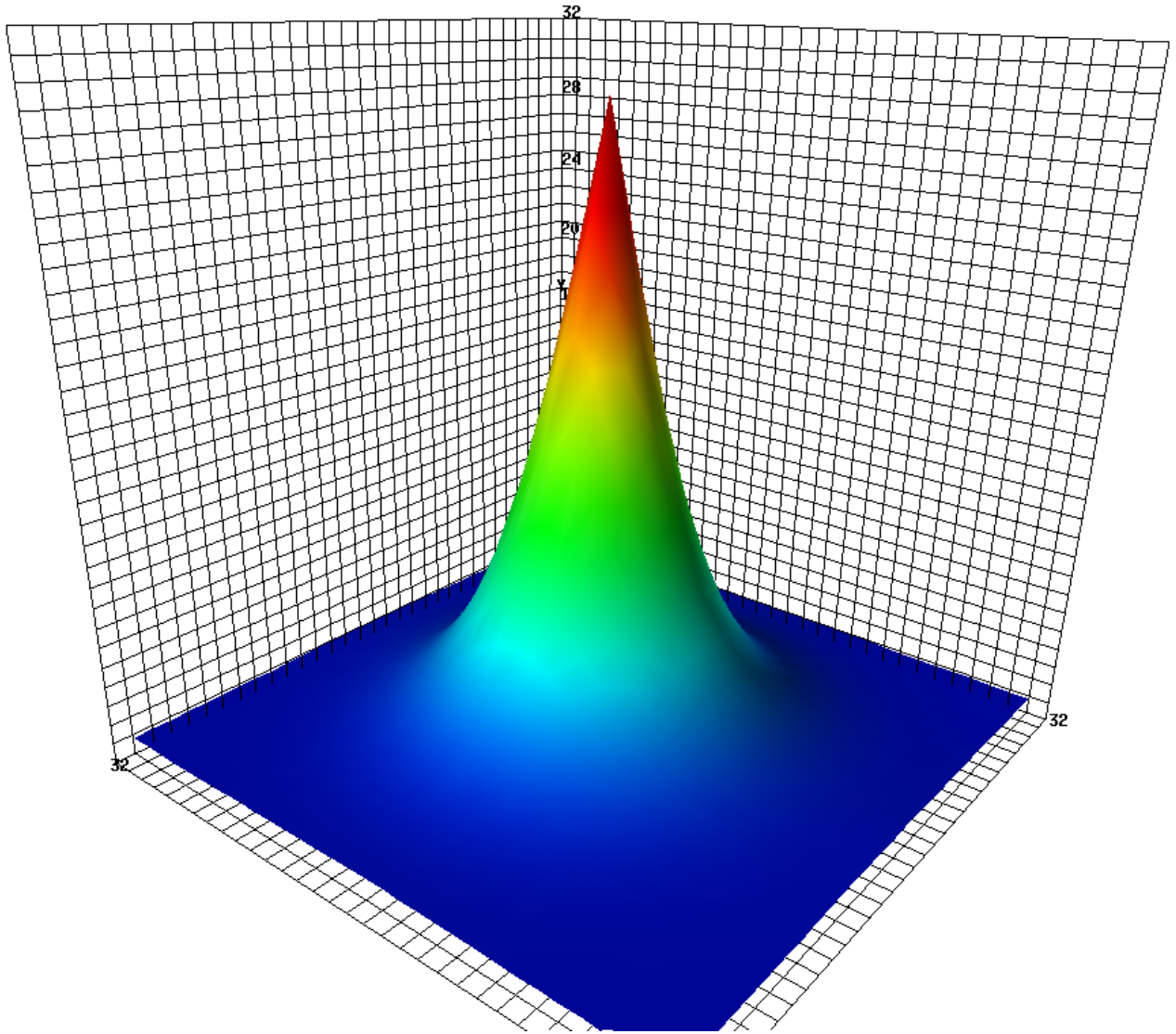

d-quark probability density in 1st excited state of proton (CSSM)

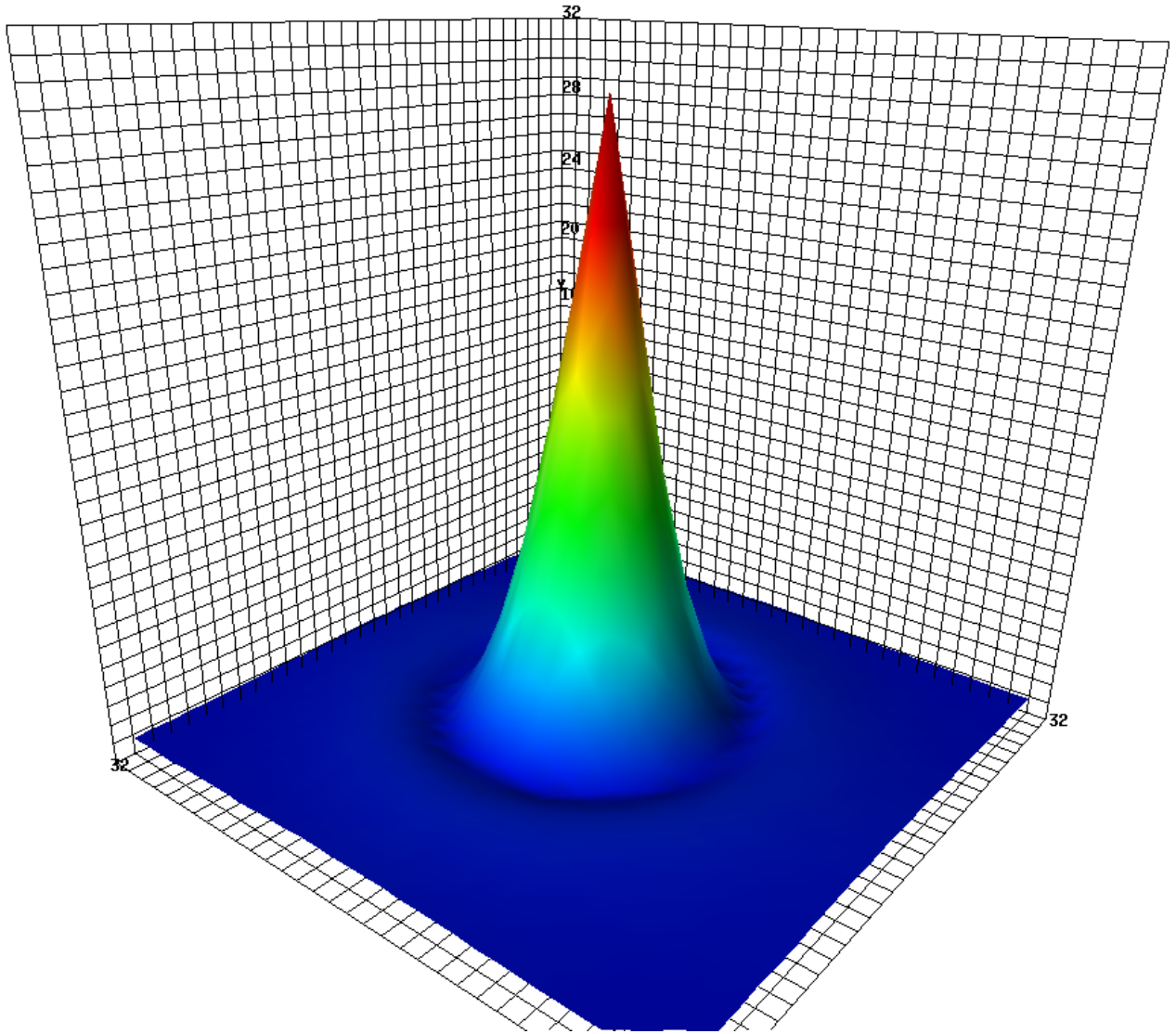

d-quark probability density in $N = 3$ excited state of proton (CSSM)

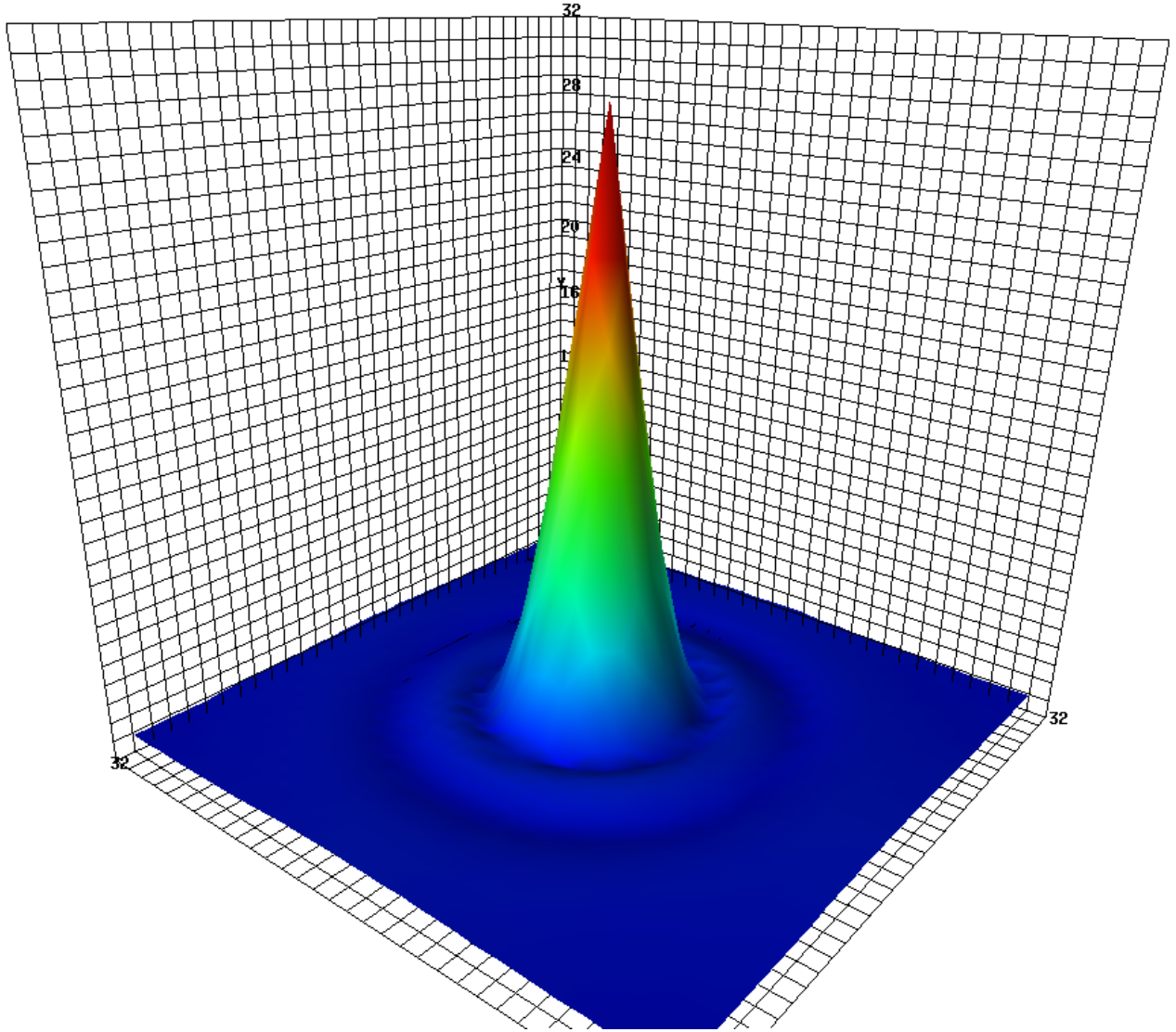

d-quark probability density in $N = 4$ excited state of proton (CSSM)

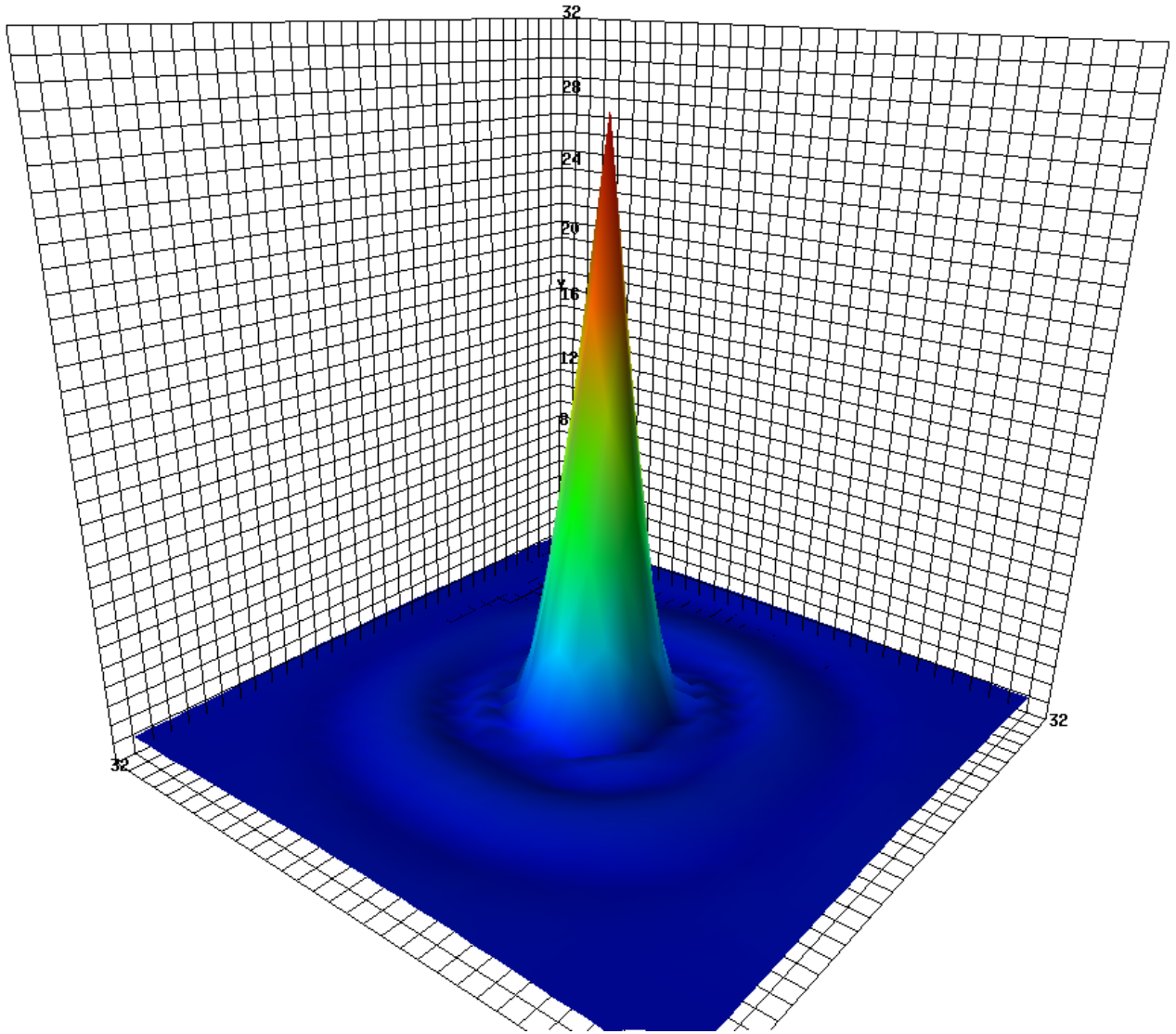

Comparison with the Simple Quark Model - CSSM

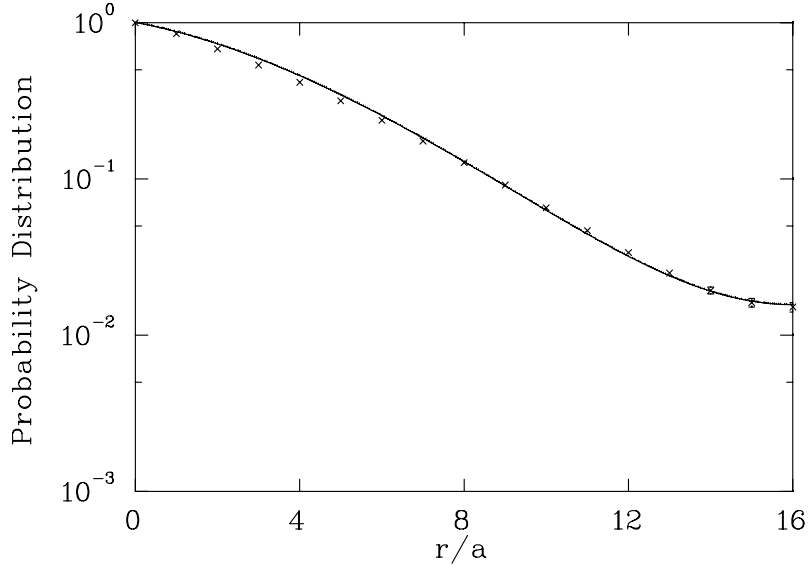

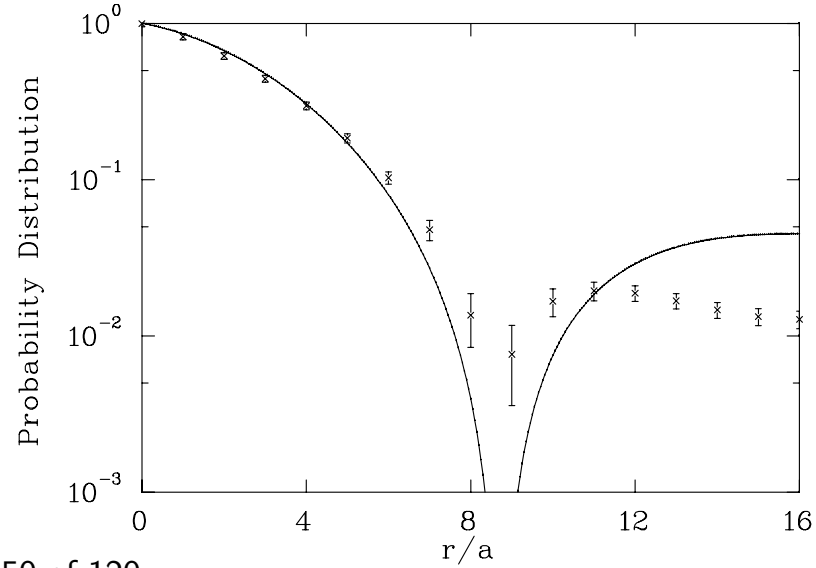

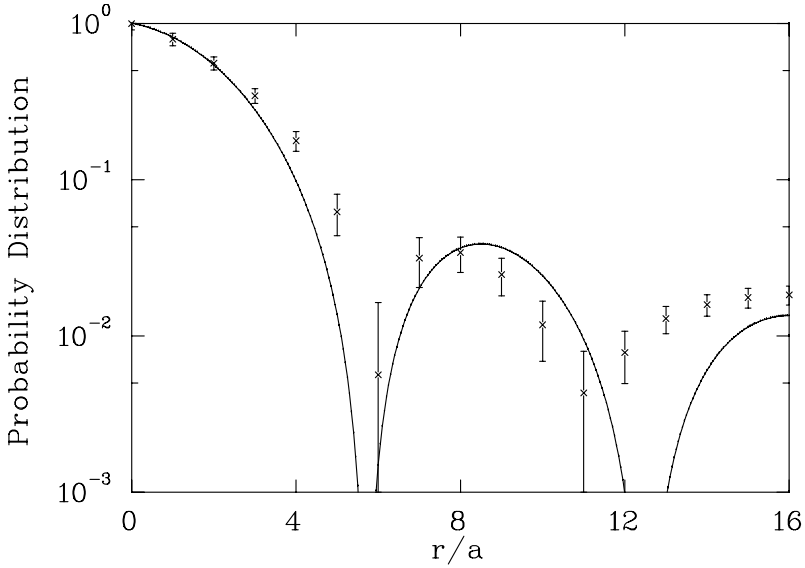

Properties of the Positive Parity Nucleon Spectrum

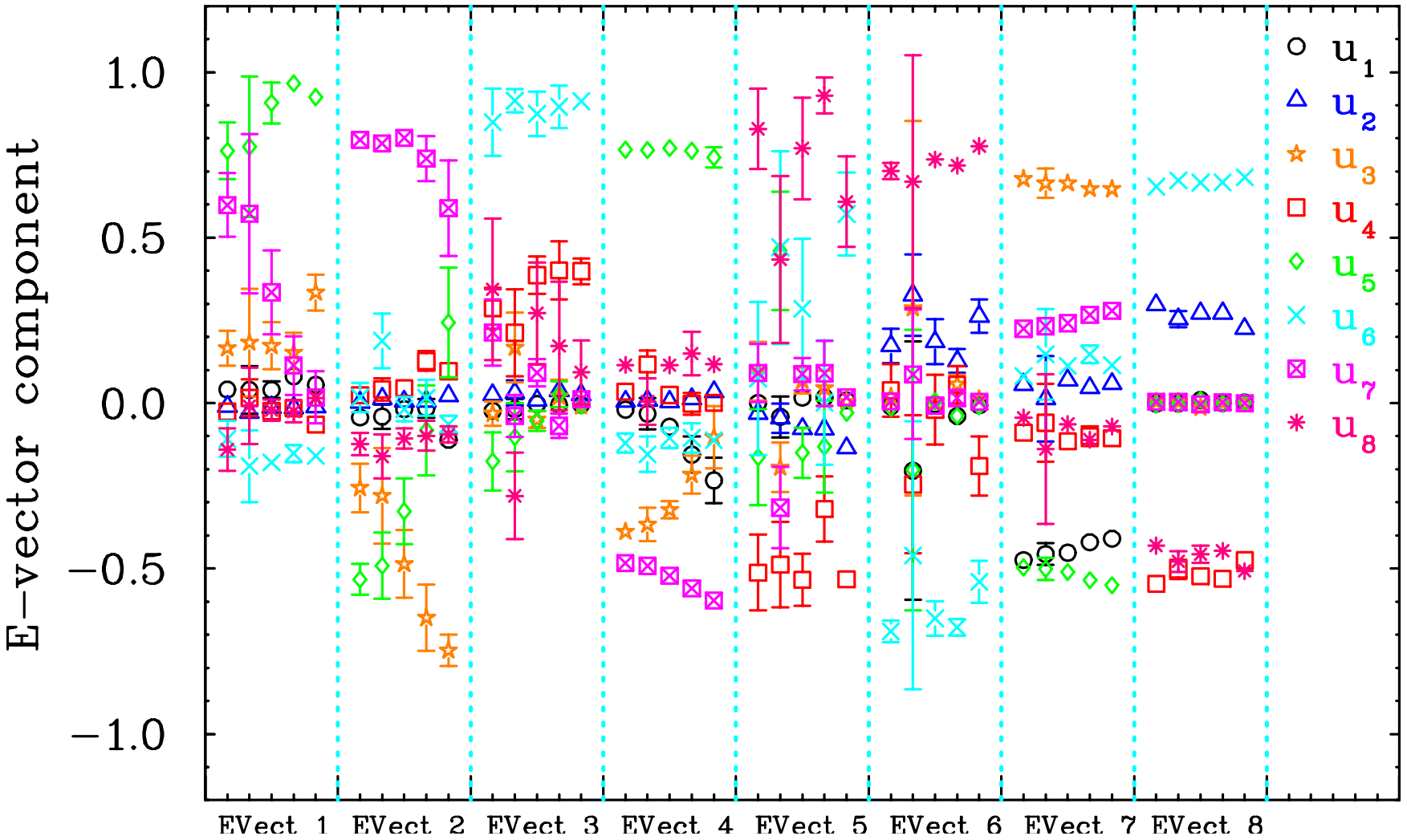

d-quark probability density in 1st excited state of proton (CSSM)

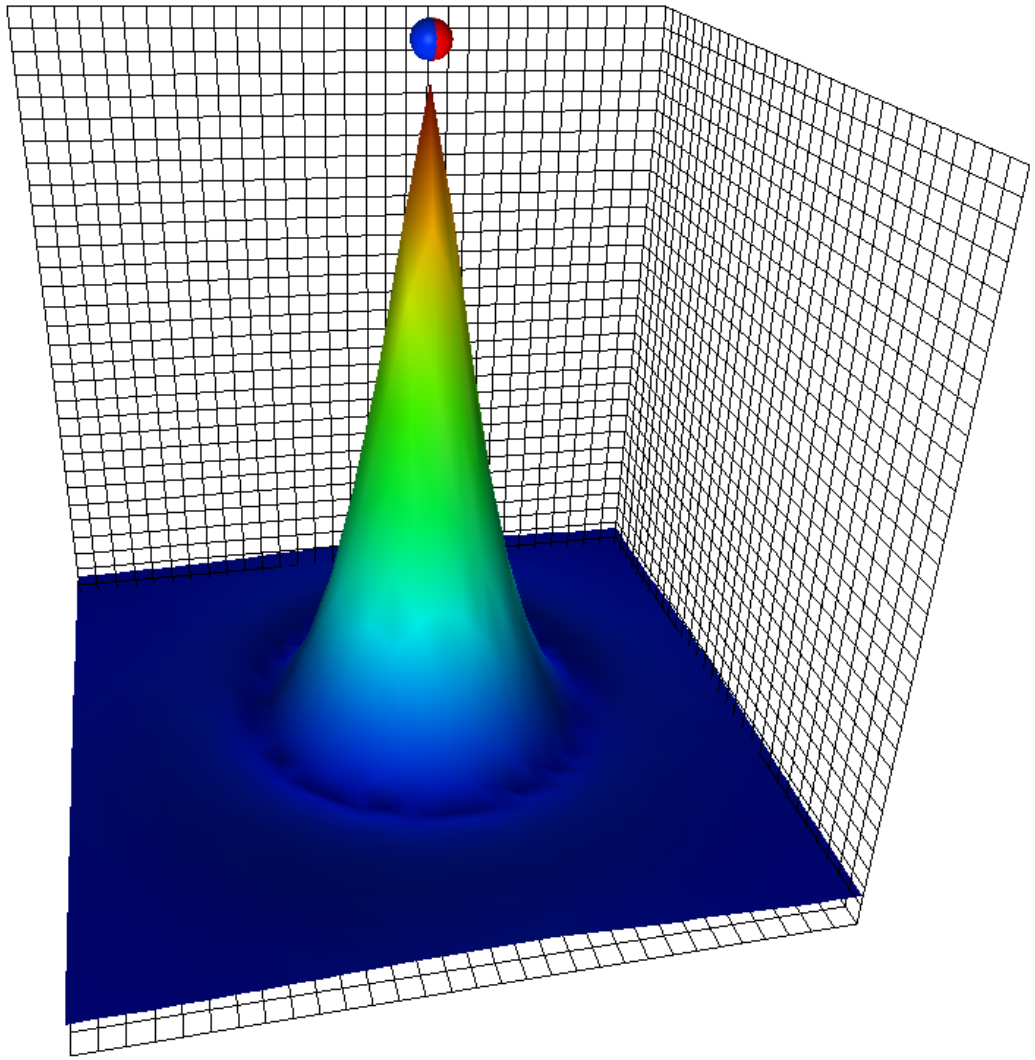

d-quark probability density in 1st excited state of proton (CSSM)

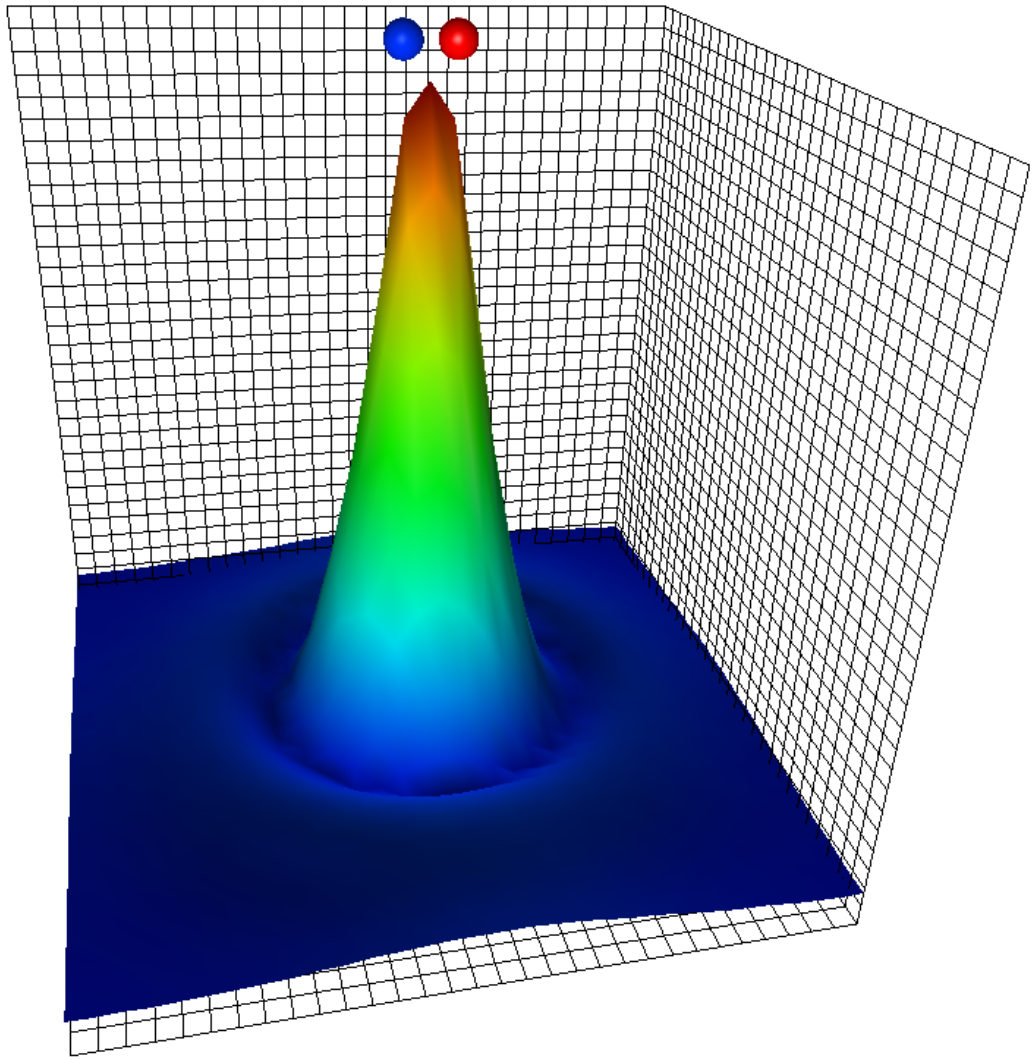

d-quark probability density in 1st excited state of proton (CSSM)

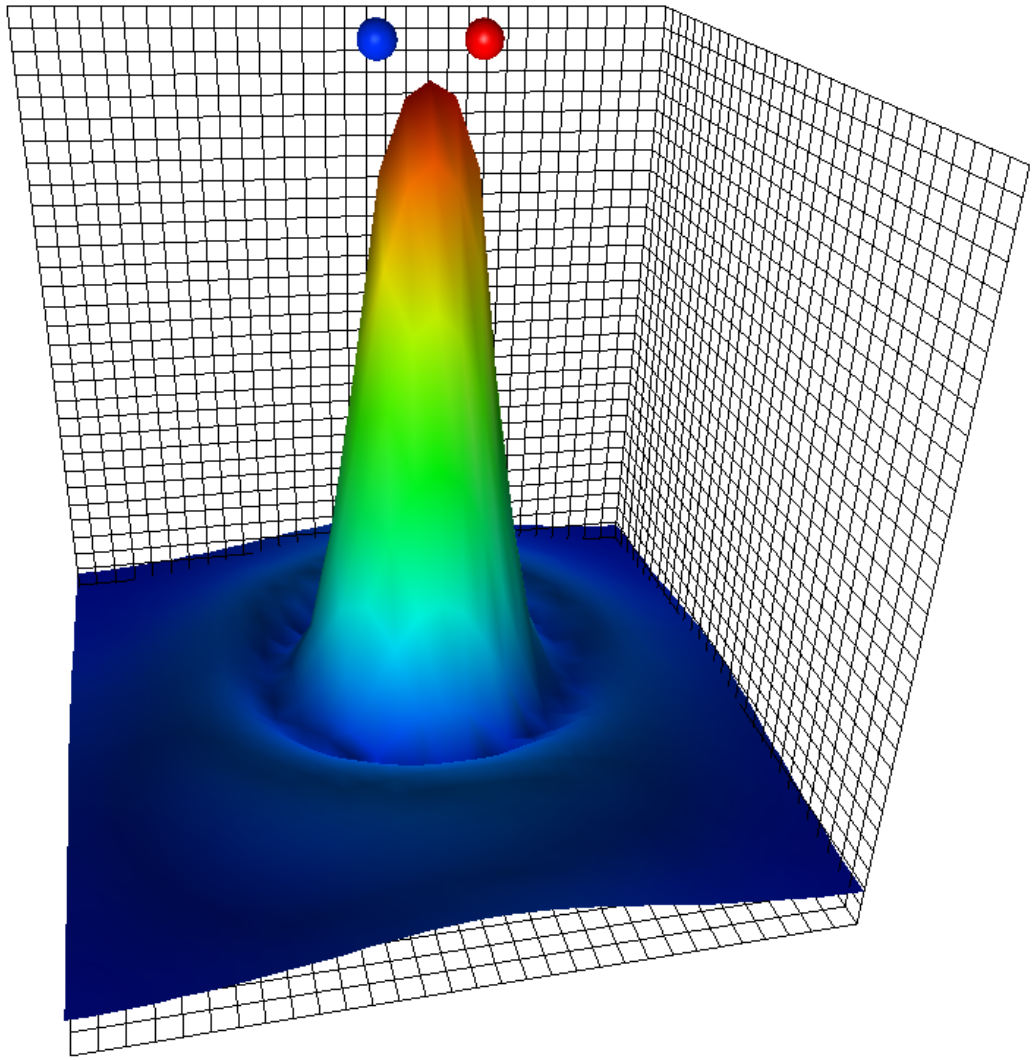

d-quark probability density in 1st excited state of proton (CSSM)

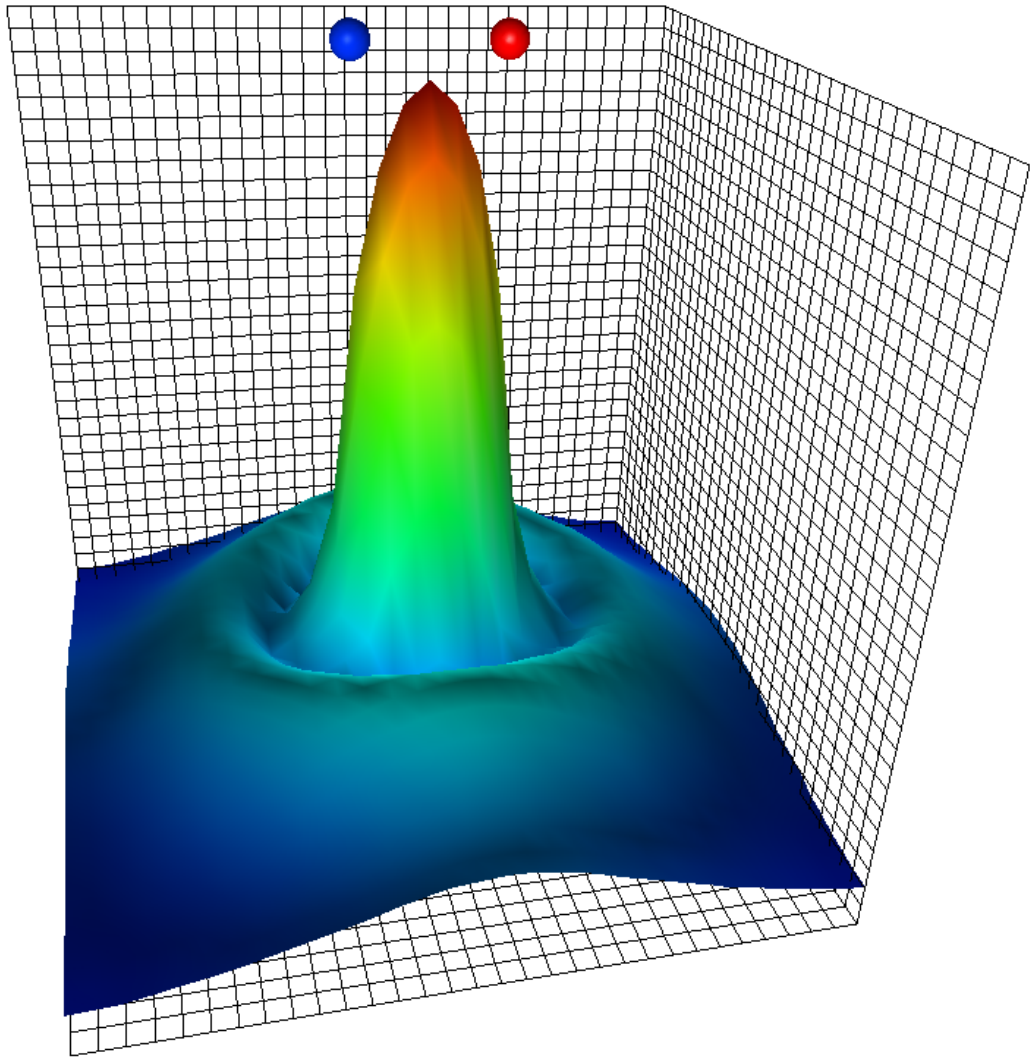

d-quark probability density in 1st excited state of proton (CSSM)

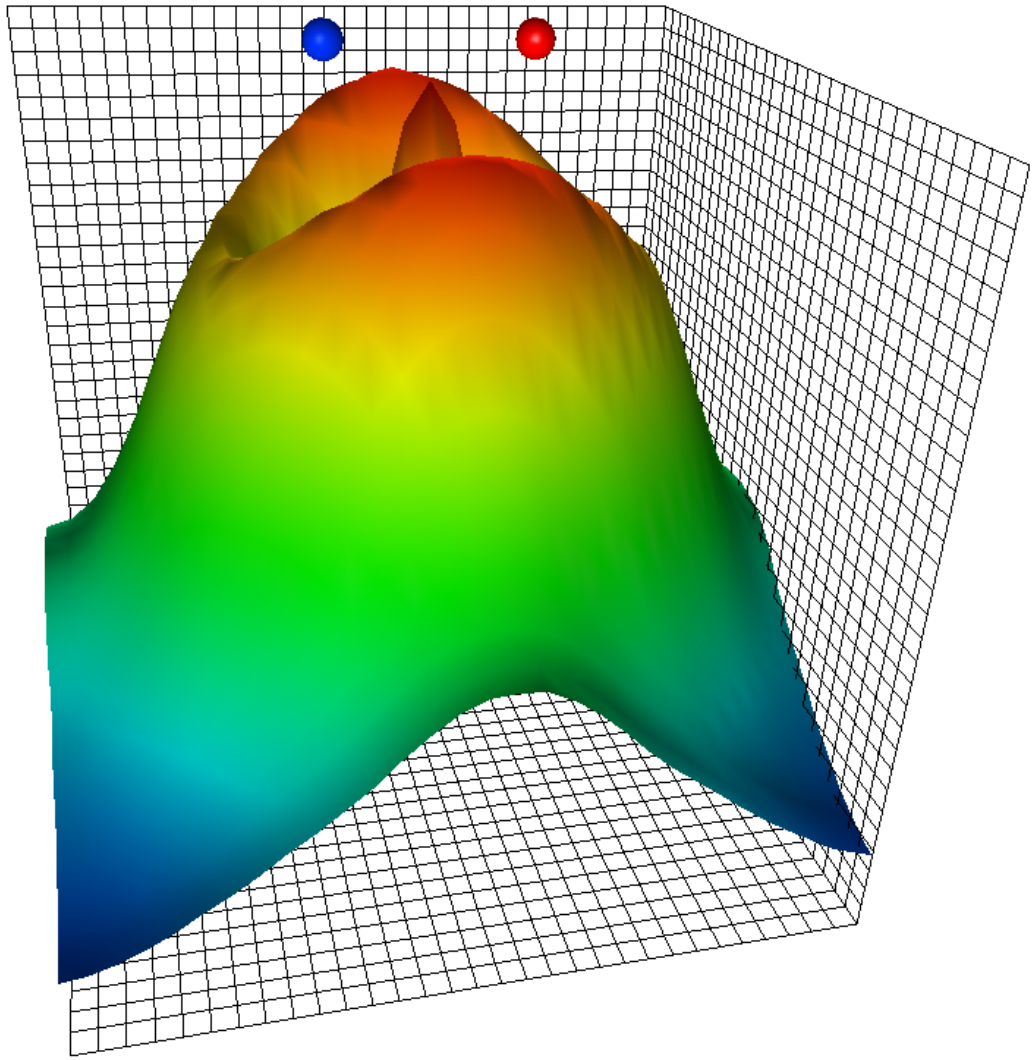

d-quark probability density in 1st excited state of proton (CSSM)

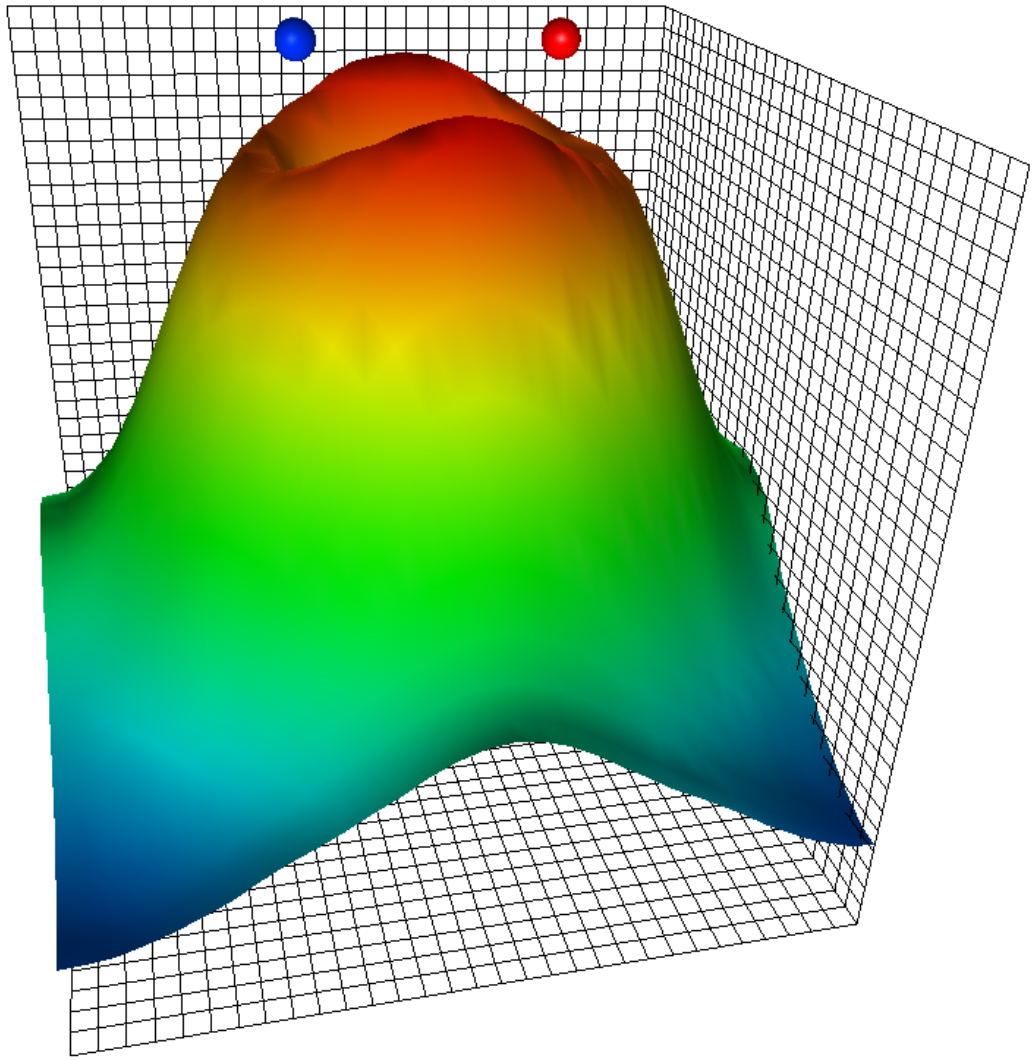

d-quark probability density in 1st excited state of proton (CSSM)

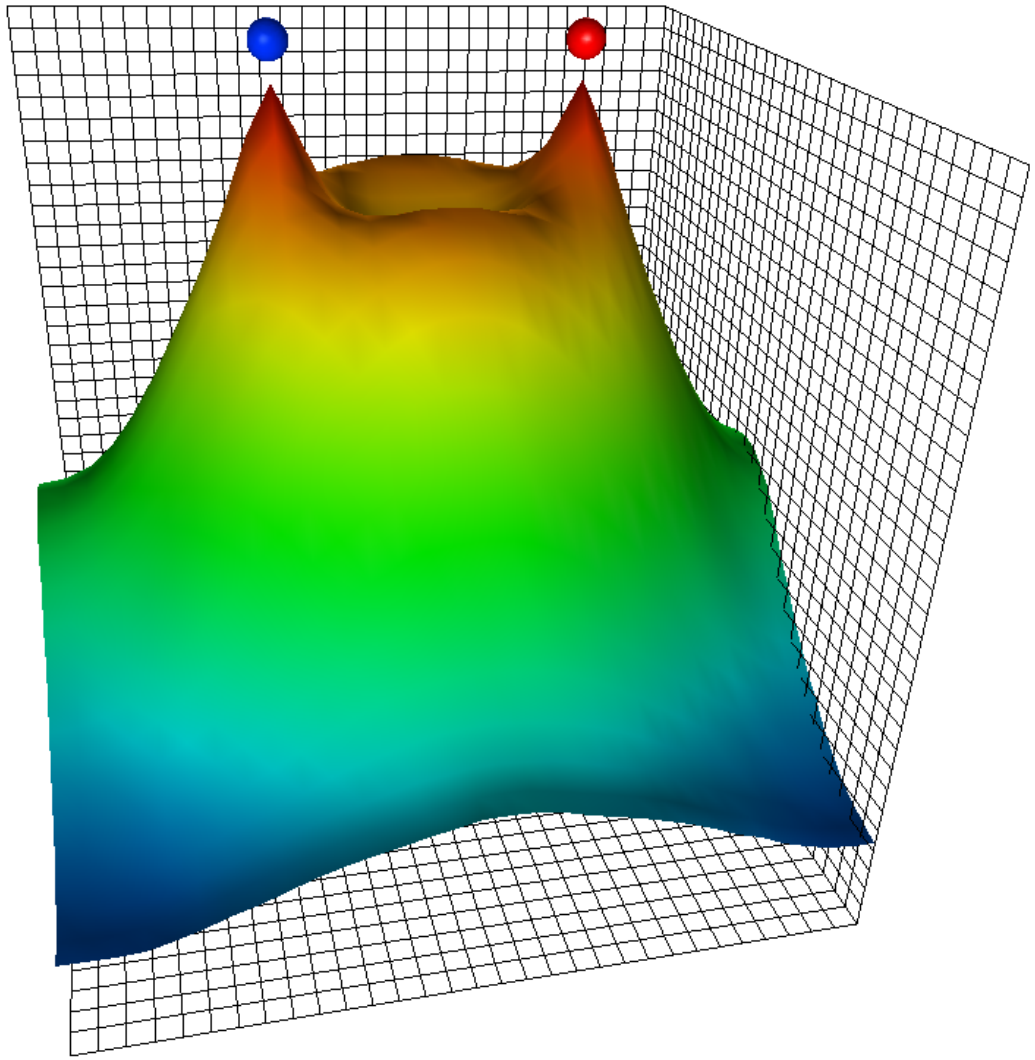

d-quark probability density in 1st excited state of proton (CSSM)

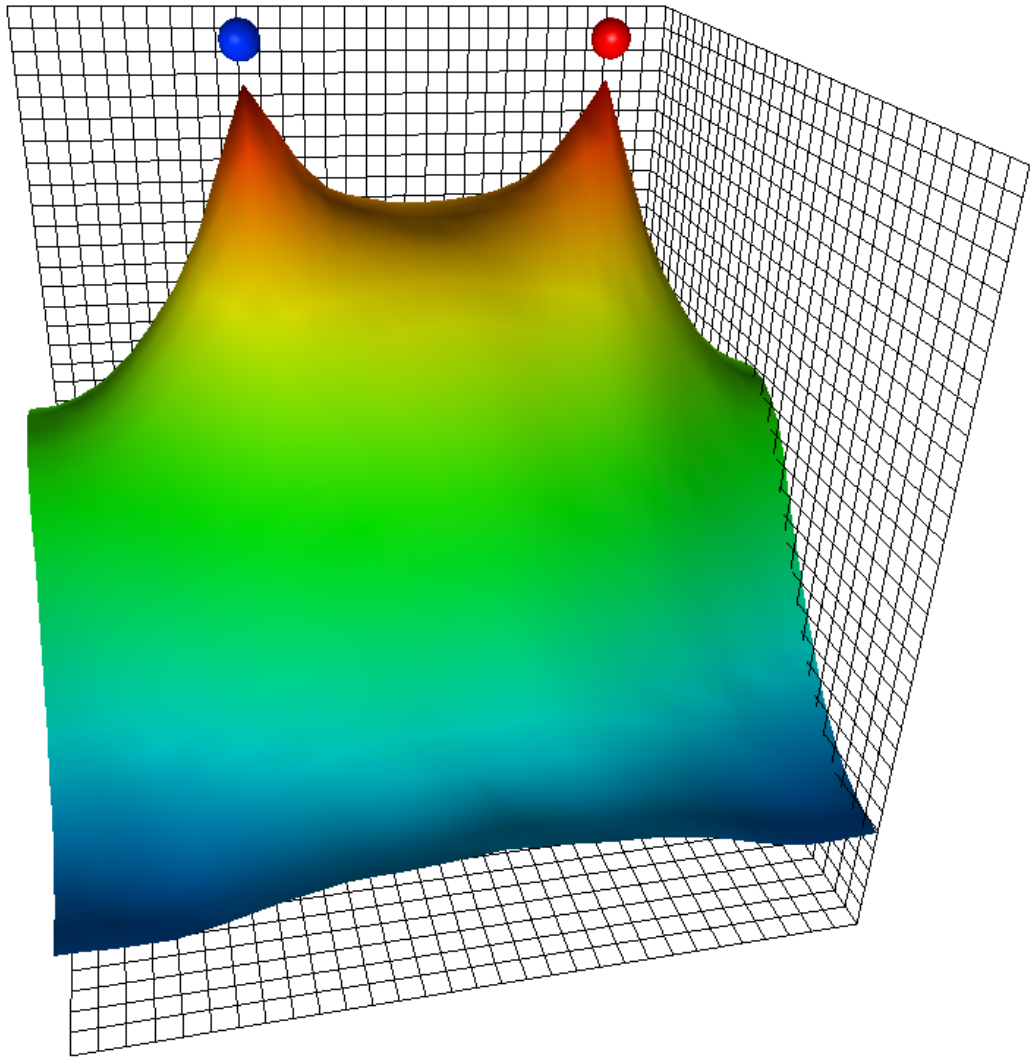

Form Factors of positive-parity nucleon excitations

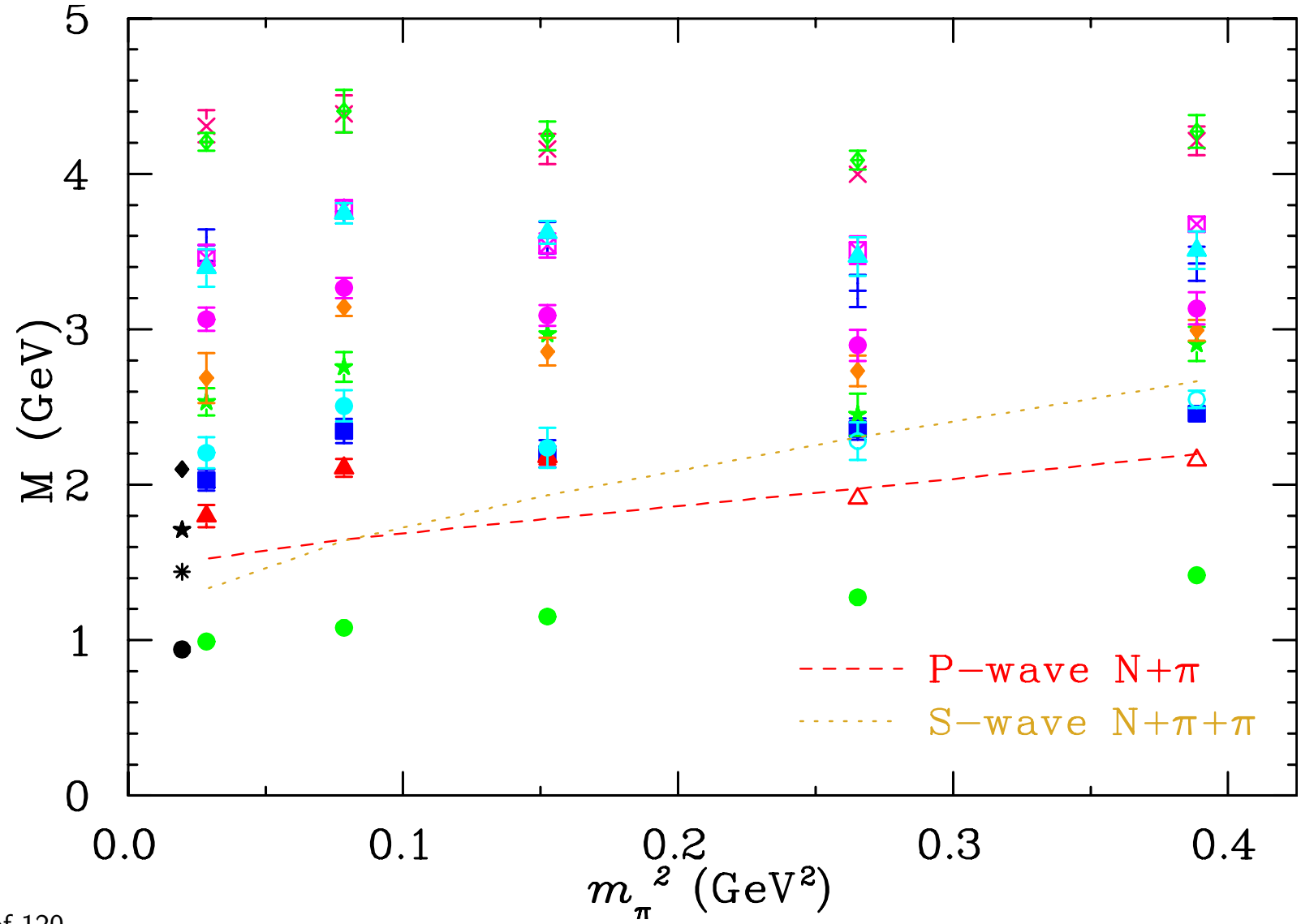

Charge Radii of the Proton, Delta and "Roper"

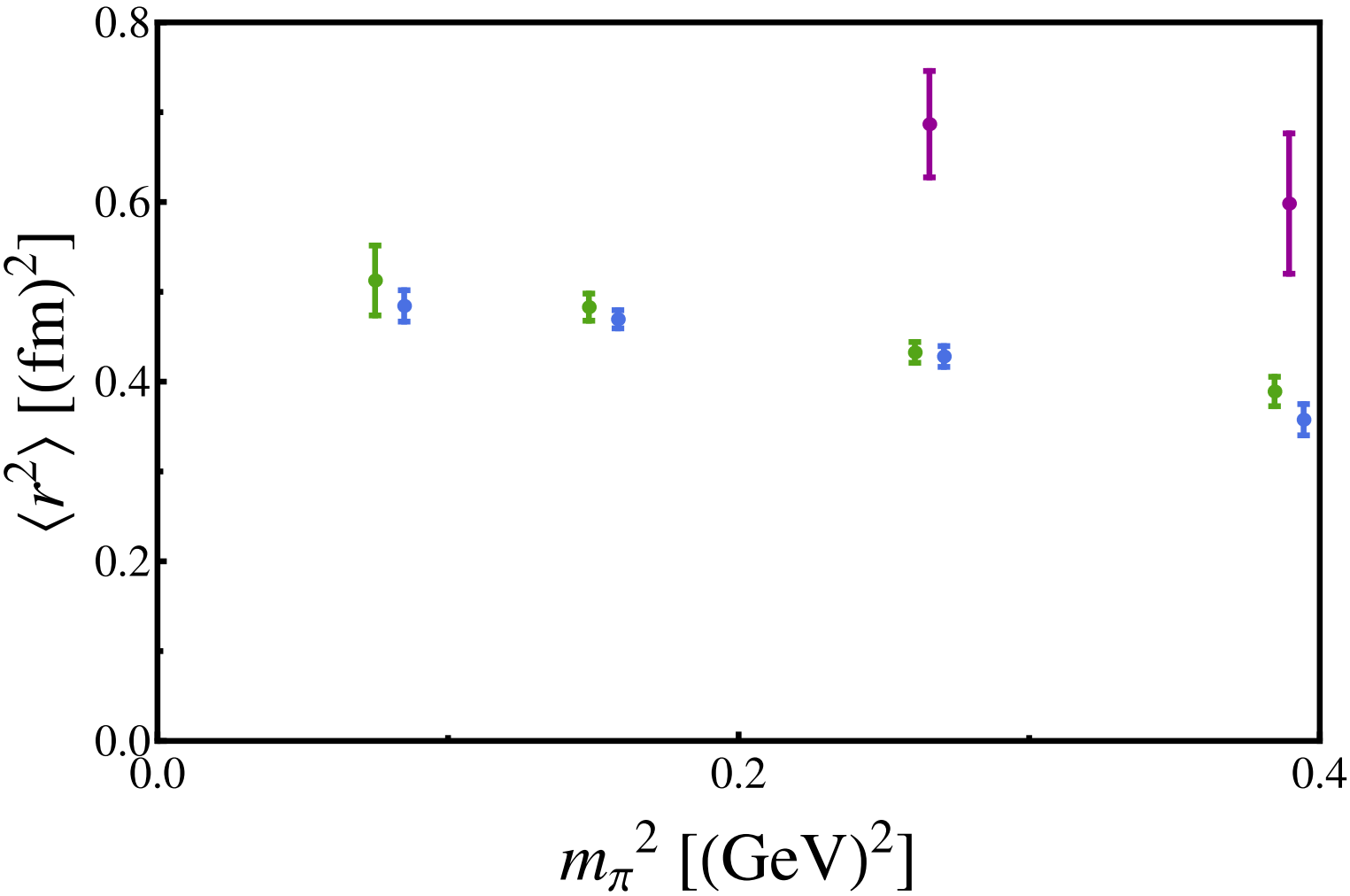

Magnetic Moments of the Proton, Delta and "Roper"

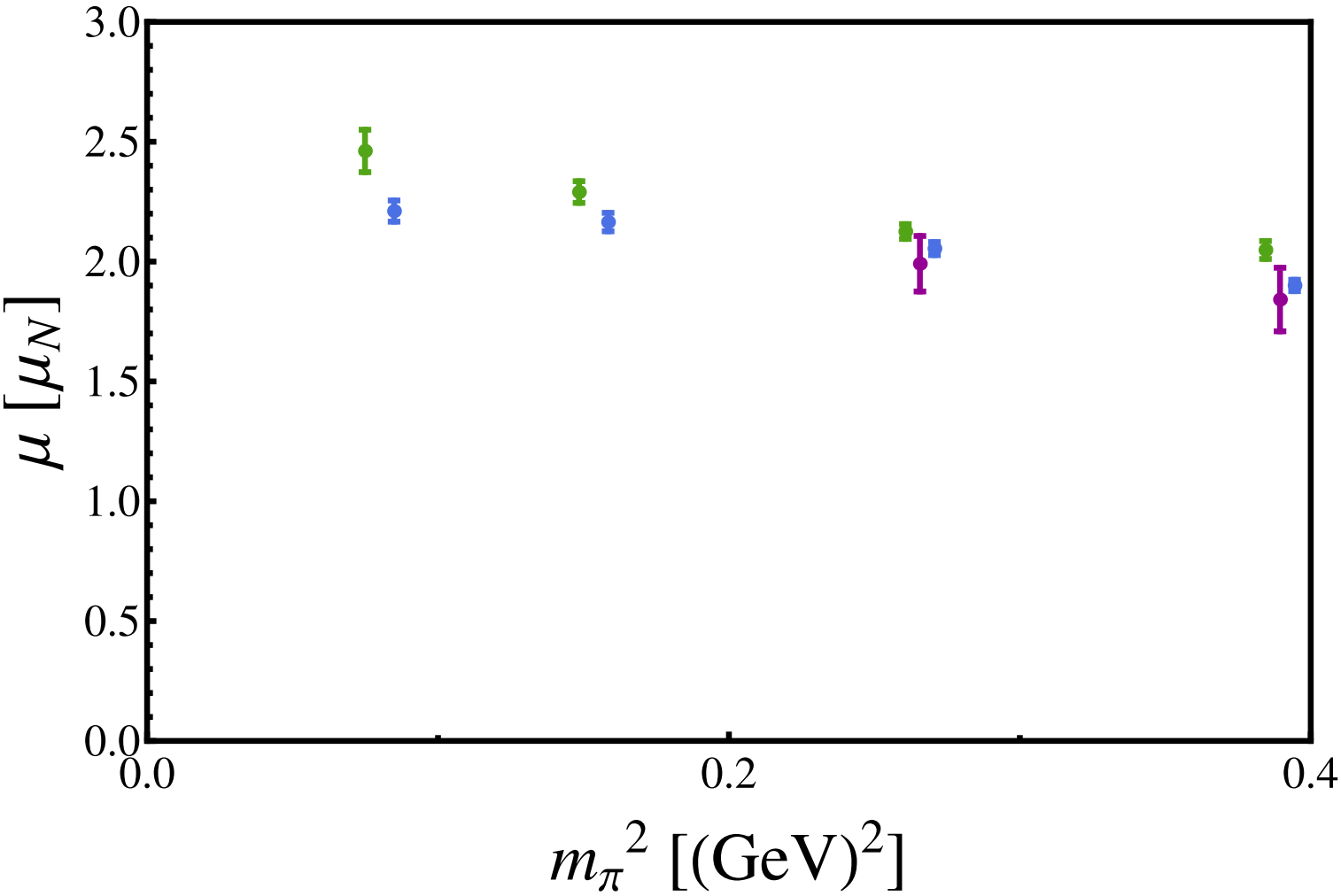

Magnetic Moments of the odd-parity p^*, and n^*

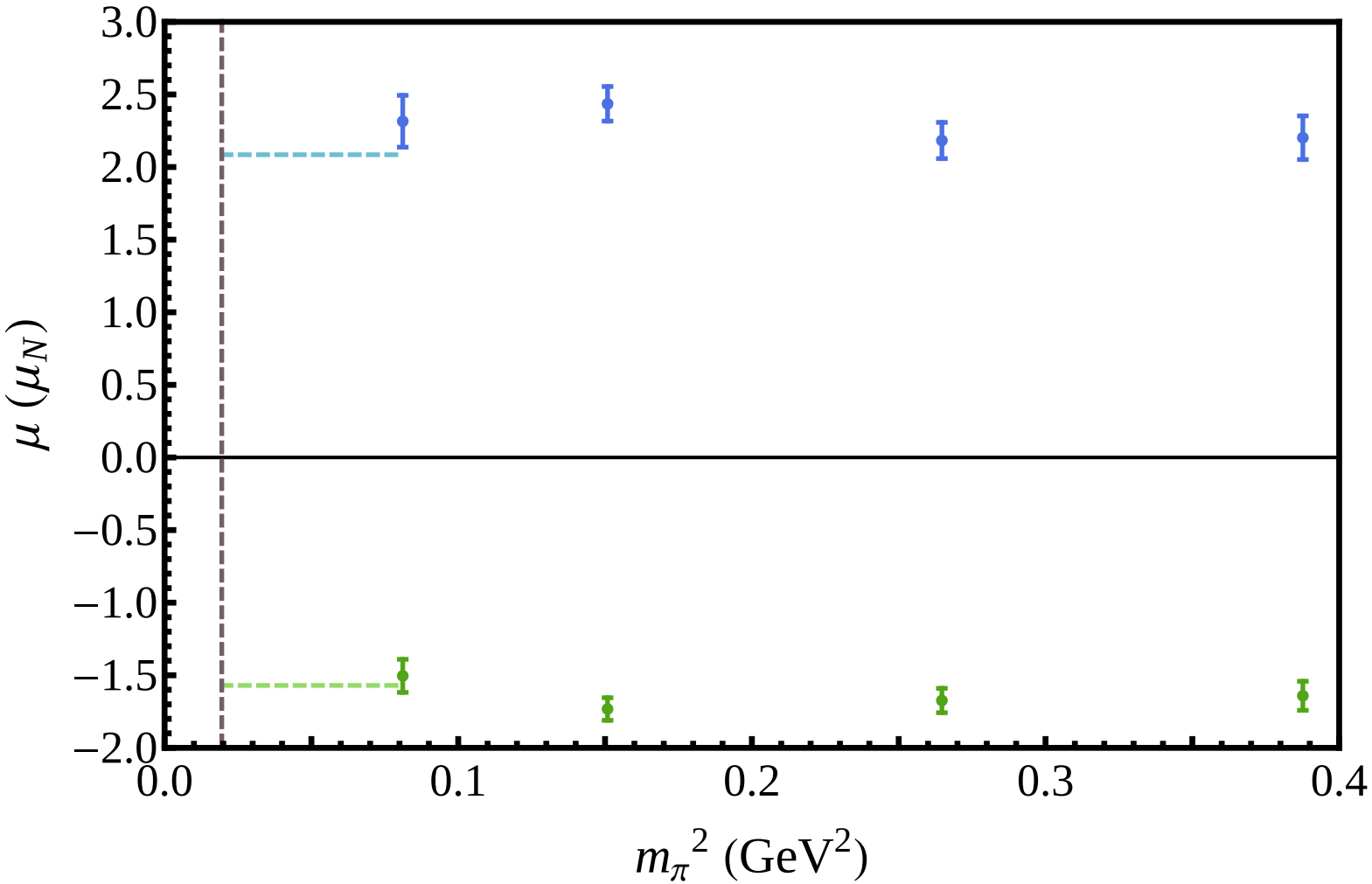

- Comparison with quark model result of N. Sharma, *et al.* (2013).

References

- "Nucleon Excited State Wave Functions from Lattice QCD,"
  D. S. Roberts, *et al.*
  Phys. Rev. **D89** (2014) 074501 arXiv:1311.6626 [hep-lat]

- "Electromagnetic matrix elements for negative parity nucleons,"
  B. Owen, *et al.*
  PoS LATTICE **2014** (2014) 159 arXiv:1412.4432 [hep-lat]

- "Probing the proton and its excitations in full QCD,"
  B. J. Owen, *et al.*
  PoS LATTICE **2013** (2013) 277 arXiv:1312.0291 [hep-lat]

References

- "Nucleon Excited State Wave Functions from Lattice QCD,"
  D. S. Roberts, *et al.*
  Phys. Rev. **D89** (2014) 074501 arXiv:1311.6626 [hep-lat]

- "Electromagnetic matrix elements for negative parity nucleons,"
  B. Owen, *et al.*
  PoS LATTICE **2014** (2014) 159 arXiv:1412.4432 [hep-lat]

- "Probing the proton and its excitations in full QCD,"
  B. J. Owen, *et al.*
  PoS LATTICE **2013** (2013) 277 arXiv:1312.0291 [hep-lat]

- "Magnetic moments of the low-lying $1/2^-$ octet baryon resonances,"
  N. Sharma, A. Martinez Torres, K. P. Khemchandani and H. Dahiya
  Eur. Phys. J. A **49** (2013) 11 [arXiv:1207.3311 [hep-ph]]

Have we seen the Roper?

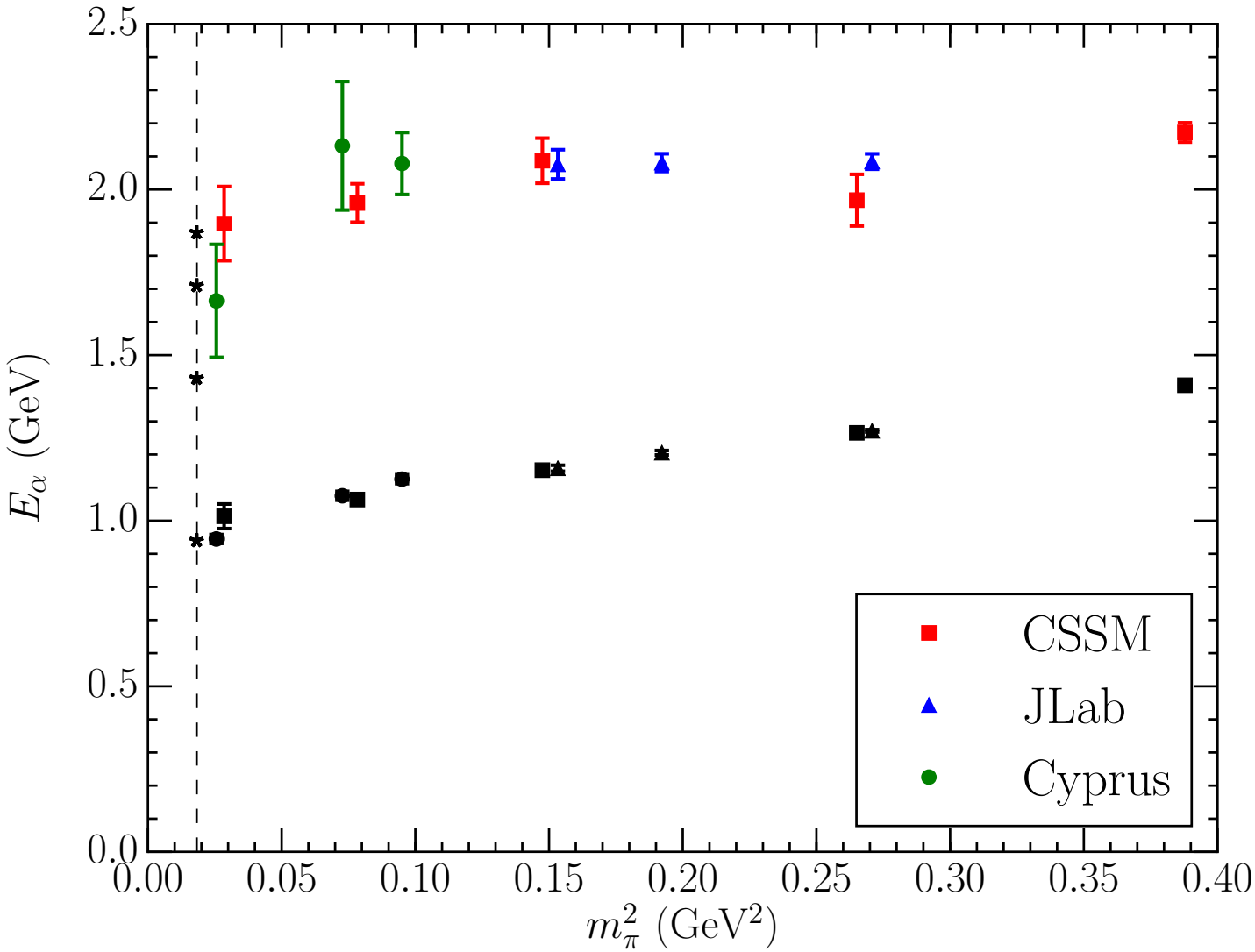

Finite-Volume Effect in $N = 2$ excited state: $m_\pi = 702$ MeV

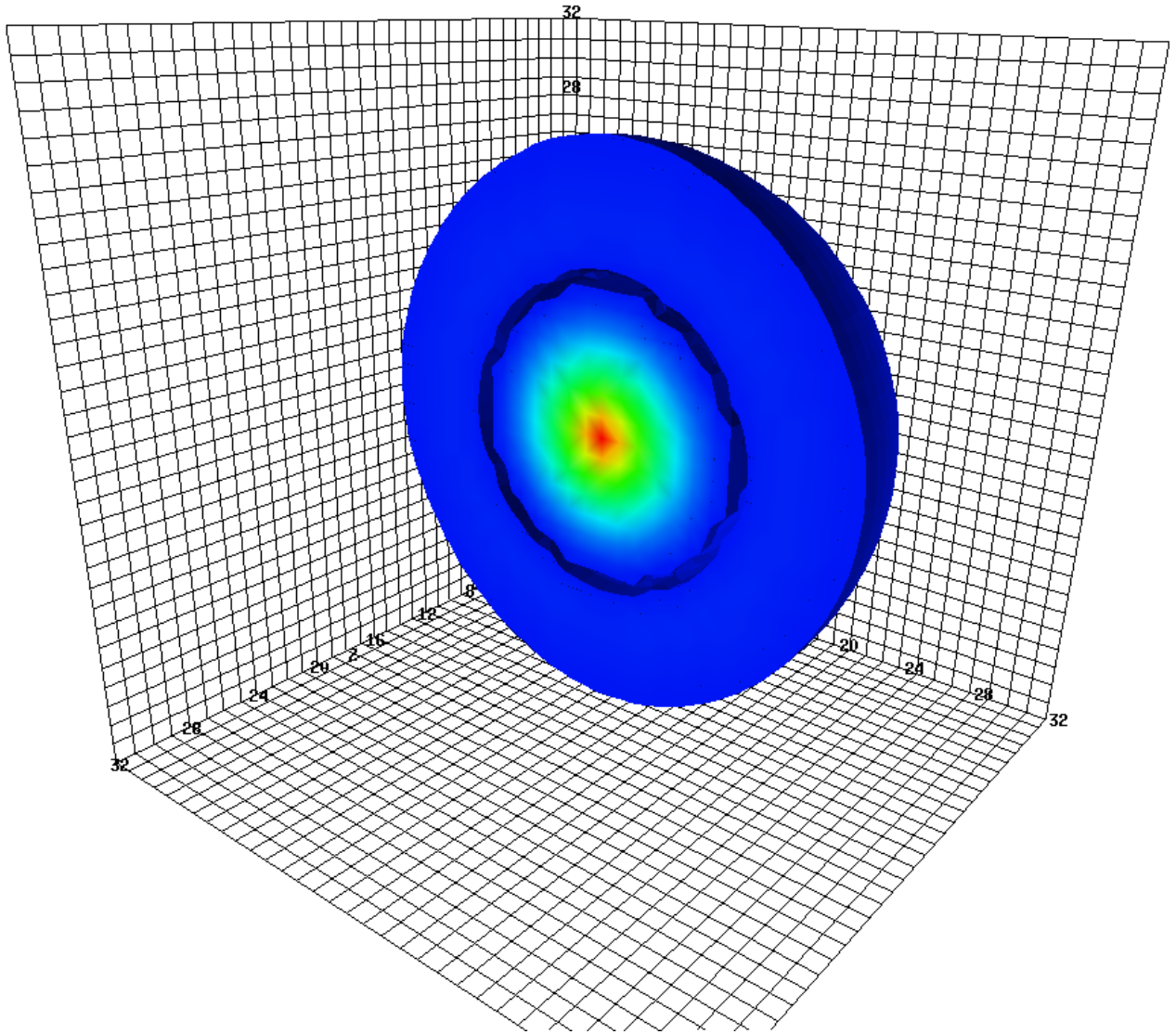

Finite-Volume Effect in $N = 2$ excited state: $m_\pi = 570$ MeV

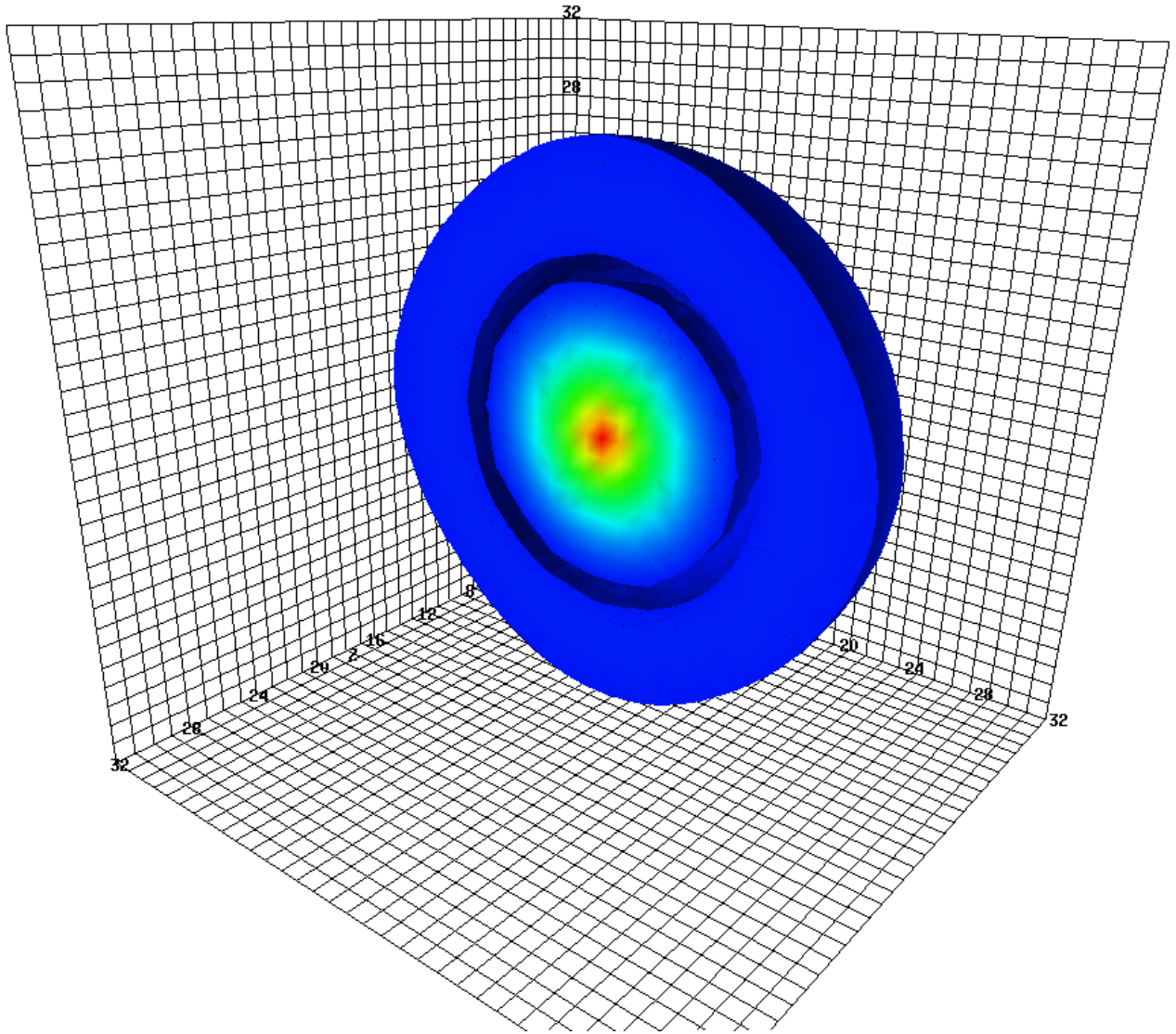

Finite-Volume Effect in $N = 2$ excited state: $m_\pi = 411$ MeV

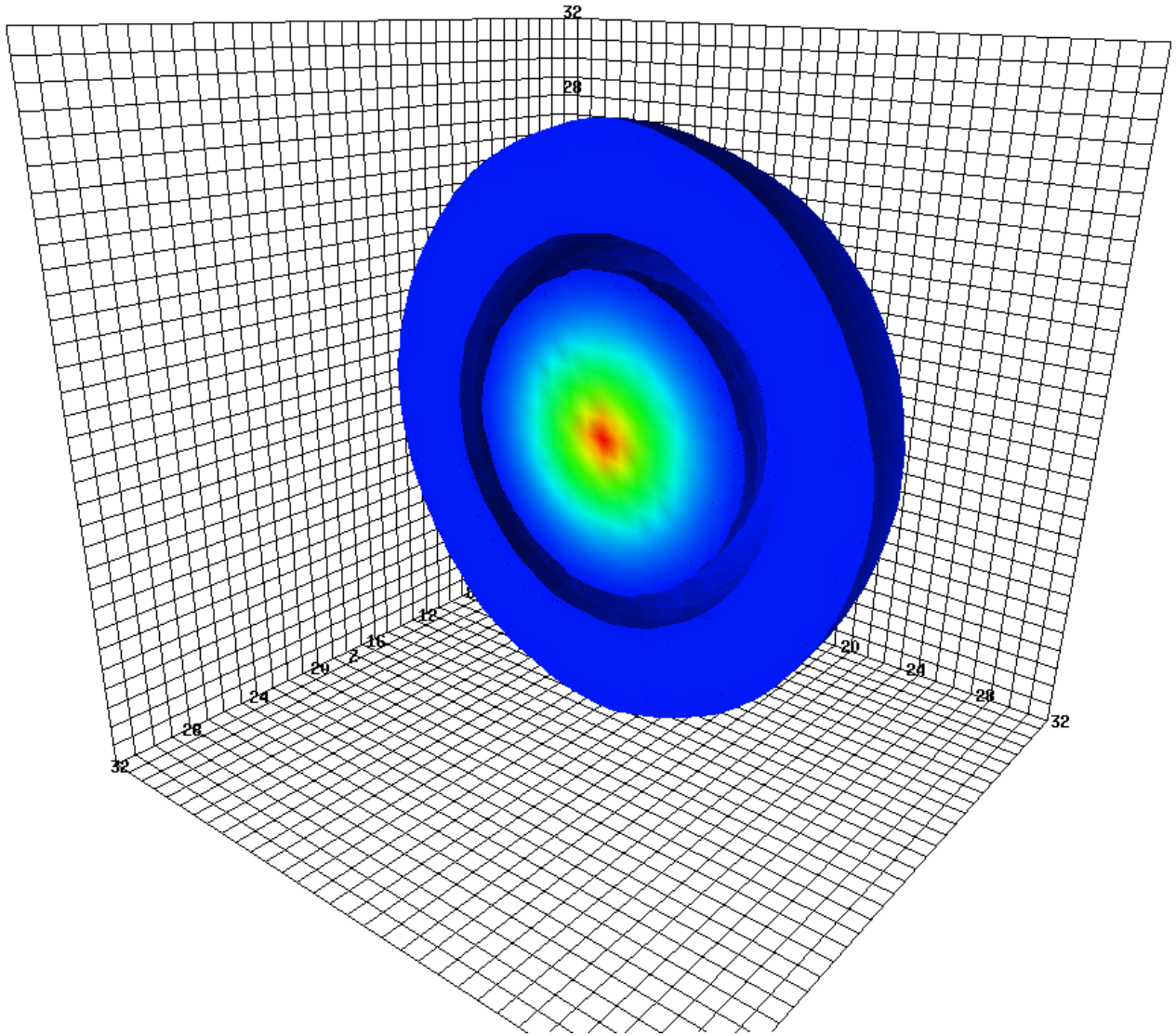

Finite-Volume Effect in $N = 2$ excited state: $m_\pi = 296$ MeV

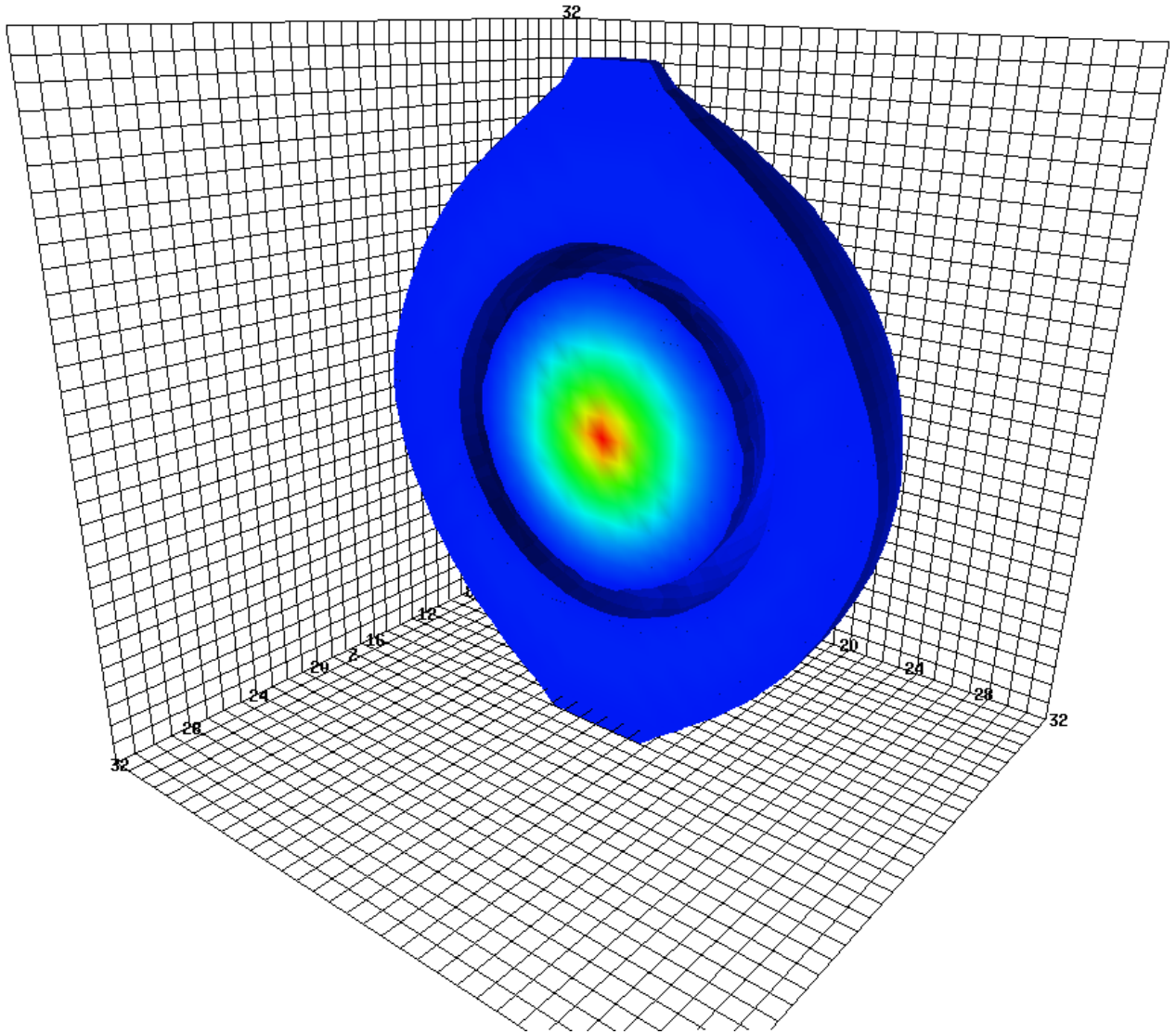

Finite-Volume Effect in $N = 2$ excited state: $m_\pi = 156$ MeV

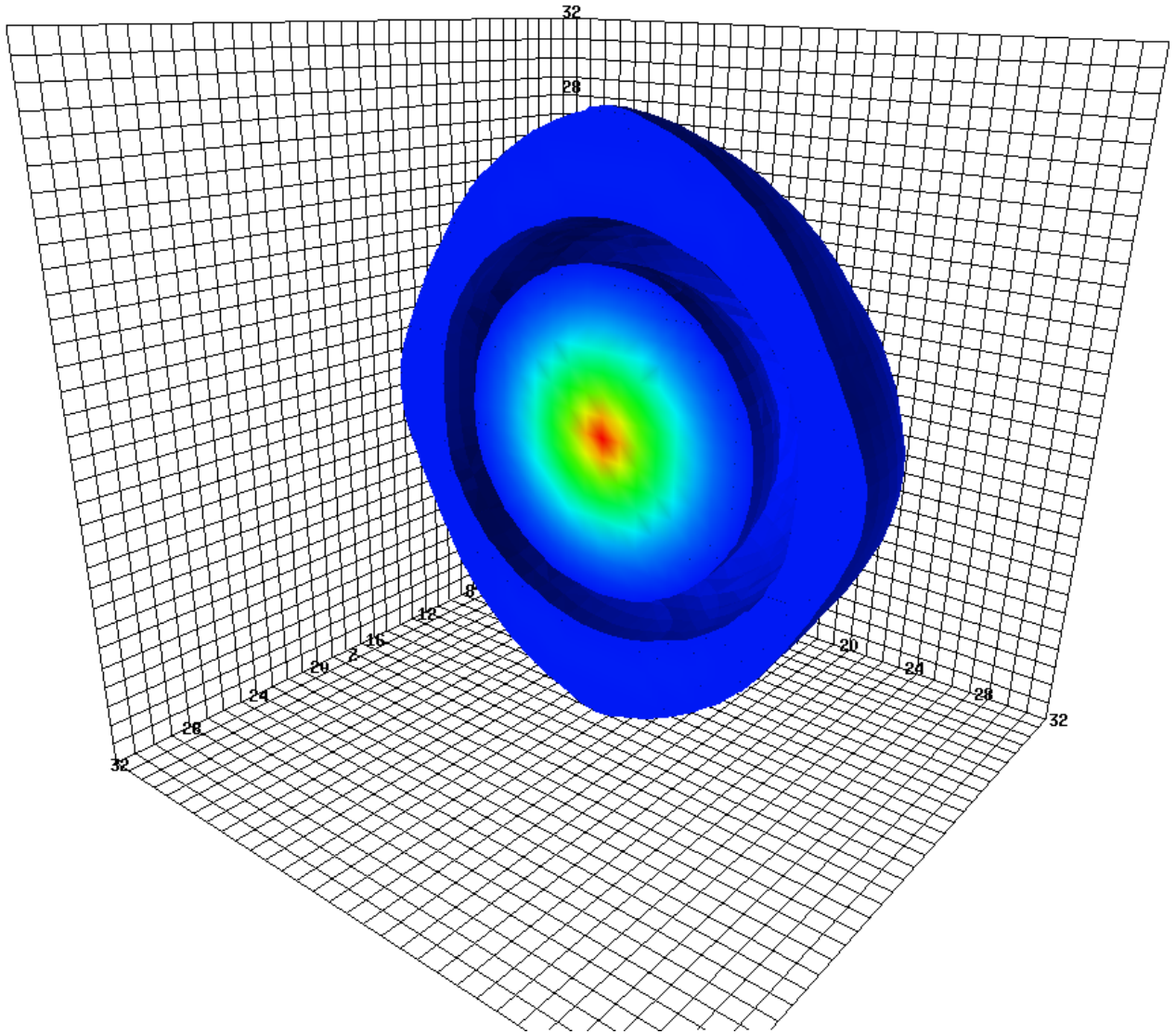

Have we seen the Roper?

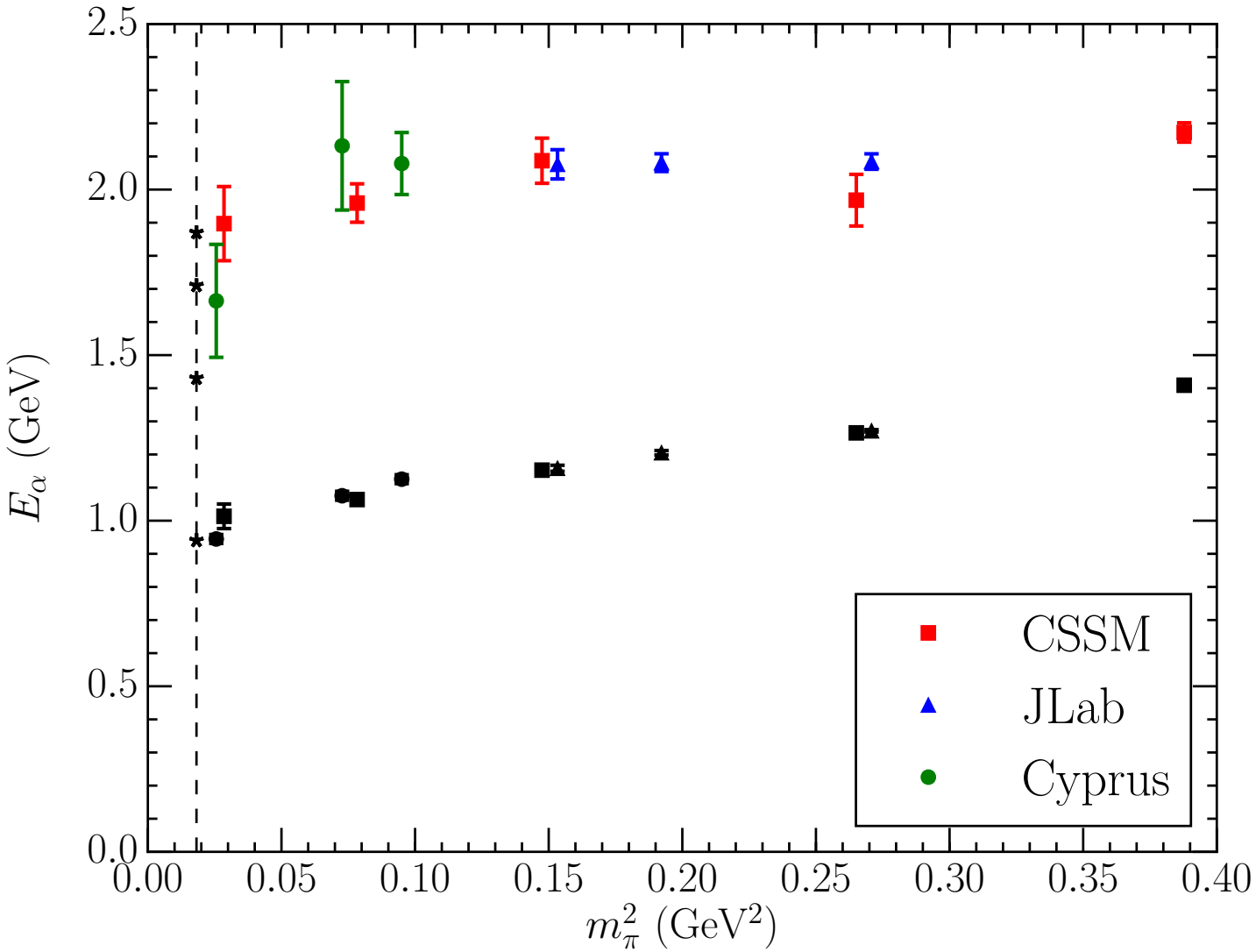

Hamiltonian Effective Field Theory

- Z. W. Liu, W. Kamleh, DBL, F. M. Stokes, A. W. Thomas and J. J. Wu, "Hamiltonian EFT study of the $N^*(1535)$ resonance in lattice QCD," Phys. Rev. Lett. **116** (2016) 082004. [arXiv:1512.00140 [hep-lat]].

Hamiltonian Effective Field Theory

- Z. W. Liu, W. Kamleh, DBL, F. M. Stokes, A. W. Thomas and J. J. Wu, "Hamiltonian EFT study of the $N^*(1535)$ resonance in lattice QCD," Phys. Rev. Lett. **116** (2016) 082004. [arXiv:1512.00140 [hep-lat]].

- Zhan-Wei Liu, Jiajun Wu, *et al.*
"Study of $N^*(1440)$ on the Lattice with Hamiltonian EFT,"
To be submitted to Phys. Rev. D.

Hamiltonian Effective Field Theory

- Z. W. Liu, W. Kamleh, DBL, F. M. Stokes, A. W. Thomas and J. J. Wu, "Hamiltonian EFT study of the $N^*(1535)$ resonance in lattice QCD," Phys. Rev. Lett. **116** (2016) 082004. [arXiv:1512.00140 [hep-lat]].

- Zhan-Wei Liu, Jiajun Wu, *et al.*
"Study of $N^*(1440)$ on the Lattice with Hamiltonian EFT,"
To be submitted to Phys. Rev. D.

- J. M. M. Hall, *et al.* [CSSM]
"Lattice QCD Evidence that the $\Lambda(1405)$ Resonance is an Antikaon-Nucleon Molecule"
Phys. Rev. Lett. **114**, 132002 (2015). arXiv:1411.3402 [hep-lat]

- "On the Structure of the $\Lambda(1405)$",
J. M. M. Hall, *et al.* [CSSM]
PoS LATTICE **2014**, 094 (2014). arXiv:1411.3781 [hep-lat]

Hamiltonian Effective Field Theory Model

- Consider the $\Lambda(1405)$.

Hamiltonian Effective Field Theory Model

- Consider the $\Lambda(1405)$.
- The four octet meson-baryon interaction channels of the $\Lambda(1405)$ are considered: $\pi\Sigma$, $\overline{K}N$, $K\Xi$ and $\eta\Lambda$.

Hamiltonian Effective Field Theory Model

- Consider the $\Lambda(1405)$.
- The four octet meson-baryon interaction channels of the $\Lambda(1405)$ are considered: $\pi\Sigma$, $\overline{K}N$, $K\Xi$ and $\eta\Lambda$.
- A single-particle state with bare mass, $m_0 + \alpha_0\, m_\pi^2$ is also included.

Hamiltonian Effective Field Theory Model

- Consider the $\Lambda(1405)$.
- The four octet meson-baryon interaction channels of the $\Lambda(1405)$ are considered: $\pi\Sigma$, $\overline{K}N$, $K\Xi$ and $\eta\Lambda$.
- A single-particle state with bare mass, $m_0 + \alpha_0\, m_\pi^2$ is also included.
- In a finite periodic volume, momentum is quantised to $n\,(2\pi/L)$.

Hamiltonian Effective Field Theory Model

- Consider the $\Lambda(1405)$.
- The four octet meson-baryon interaction channels of the $\Lambda(1405)$ are considered: $\pi\Sigma$, $\overline{K}N$, $K\Xi$ and $\eta\Lambda$.
- A single-particle state with bare mass, $m_0 + \alpha_0\, m_\pi^2$ is also included.
- In a finite periodic volume, momentum is quantised to $n\,(2\pi/L)$.
- Working on a cubic volume of extent L on each side, it is convenient to define the momentum magnitudes

$$k_n = \sqrt{n_x^2 + n_y^2 + n_z^2}\,\frac{2\pi}{L}\,,$$

with $n_i = 0, 1, 2, \ldots$ and integer $n = n_x^2 + n_y^2 + n_z^2$.

Hamiltonian model, H_0

Denoting each meson-baryon energy by $\omega_{MB}(k_n) = \omega_M(k_n) + \omega_B(k_n)$, with $\omega_A(k_n) \equiv \sqrt{k_n^2 + m_A^2}$, the non-interacting Hamiltonian takes the form

$$H_0 = \begin{pmatrix} m_0 + \alpha_0\, m_\pi^2 & & 0 & & 0 & \cdots \\ & \omega_{\pi\Sigma}(k_0) & & & & \\ 0 & & \ddots & & 0 & \cdots \\ & & & \omega_{\eta\Lambda}(k_0) & & \\ & & & & \omega_{\pi\Sigma}(k_1) & \\ 0 & & 0 & & \ddots & \cdots \\ & & & & & \omega_{\eta\Lambda}(k_1) \\ \vdots & & \vdots & & \vdots & \ddots \end{pmatrix}.$$

Hamiltonian model, H_I

- Interaction entries describe the coupling of the single-particle state to the two-particle meson-baryon states.

Hamiltonian model, H_I

- Interaction entries describe the coupling of the single-particle state to the two-particle meson-baryon states.
- Each entry represents the S-wave interaction energy of the $\Lambda(1405)$ with one of the four channels at a certain value for k_n.

$$H_I = \begin{pmatrix} 0 & g_{\pi\Sigma}(k_0) & \cdots & g_{\eta\Lambda}(k_0) & g_{\pi\Sigma}(k_1) & \cdots & g_{\eta\Lambda}(k_1)\cdots \\ g_{\pi\Sigma}(k_0) & 0 & \cdots & & & & \\ \vdots & \vdots & 0 & & & & \\ g_{\eta\Lambda}(k_0) & & & \ddots & & & \\ g_{\pi\Sigma}(k_1) & & & & & & \\ \vdots & & & & & & \\ g_{\eta\Lambda}(k_1) & & & & & & \\ \vdots & & & & & & \end{pmatrix}.$$

Eigenvalue Equation Form

- The eigenvalue equation corresponding to our Hamiltonian model is

$$\lambda = m_0 + \alpha_0\, m_\pi^2 - \sum_{M,B} \sum_{n=0}^{\infty} \frac{g_{MB}^2(k_n)}{\omega_{MB}(k_n) - \lambda}\,.$$

  with λ denoting the energy eigenvalue.

Eigenvalue Equation Form

- The eigenvalue equation corresponding to our Hamiltonian model is

$$\lambda = m_0 + \alpha_0\, m_\pi^2 - \sum_{M,B} \sum_{n=0}^{\infty} \frac{g_{MB}^2(k_n)}{\omega_{MB}(k_n) - \lambda}\,.$$

  with λ denoting the energy eigenvalue.
- As λ is finite, the pole in the denominator of the right-hand side is never accessed.
- The bare mass $m_0 + \alpha_0\, m_\pi^2$ encounters self-energy corrections that lead to avoided level-crossings in the finite-volume energy eigenstates.

Eigenvalue Equation Form

- The eigenvalue equation corresponding to our Hamiltonian model is

$$\lambda = m_0 + \alpha_0\, m_\pi^2 - \sum_{M,B} \sum_{n=0}^{\infty} \frac{g_{MB}^2(k_n)}{\omega_{MB}(k_n) - \lambda}\,.$$

  with λ denoting the energy eigenvalue.
- As λ is finite, the pole in the denominator of the right-hand side is never accessed.
- The bare mass $m_0 + \alpha_0\, m_\pi^2$ encounters self-energy corrections that lead to avoided level-crossings in the finite-volume energy eigenstates.
- Reference to chiral effective field theory provides the form of $g_{MB}(k_n)$.

Hamiltonian model solution and fit

- The LAPACK software library routine `dgeev` is used to obtain the eigenvalues and eigenvectors of H.

Hamiltonian model solution and fit

- The LAPACK software library routine `dgeev` is used to obtain the eigenvalues and eigenvectors of H.
- The bare mass parameters m_0 and α_0 are determined by a fit to the lattice QCD results.

Hamiltonian model fit

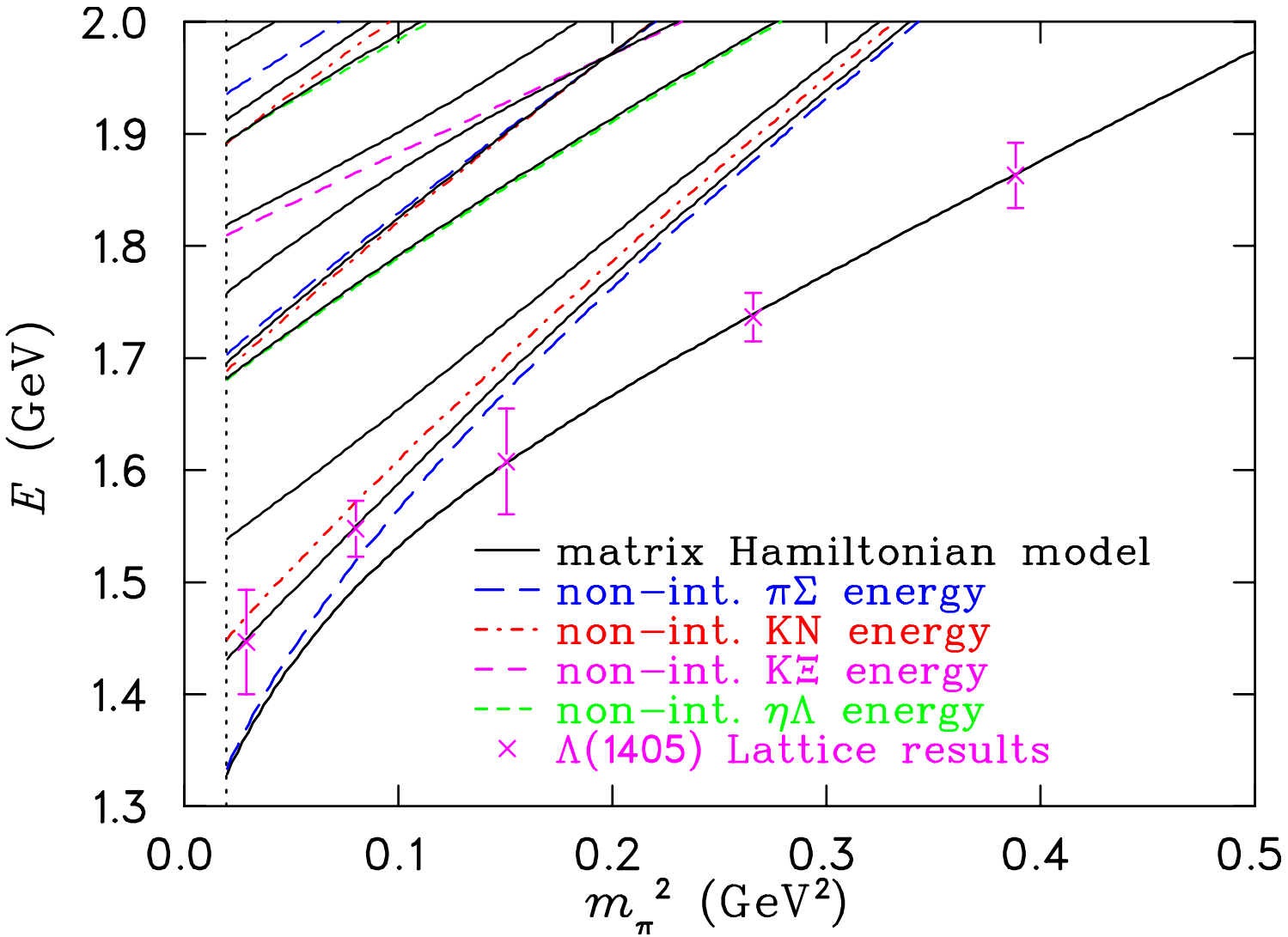

Avoided Level Crossing

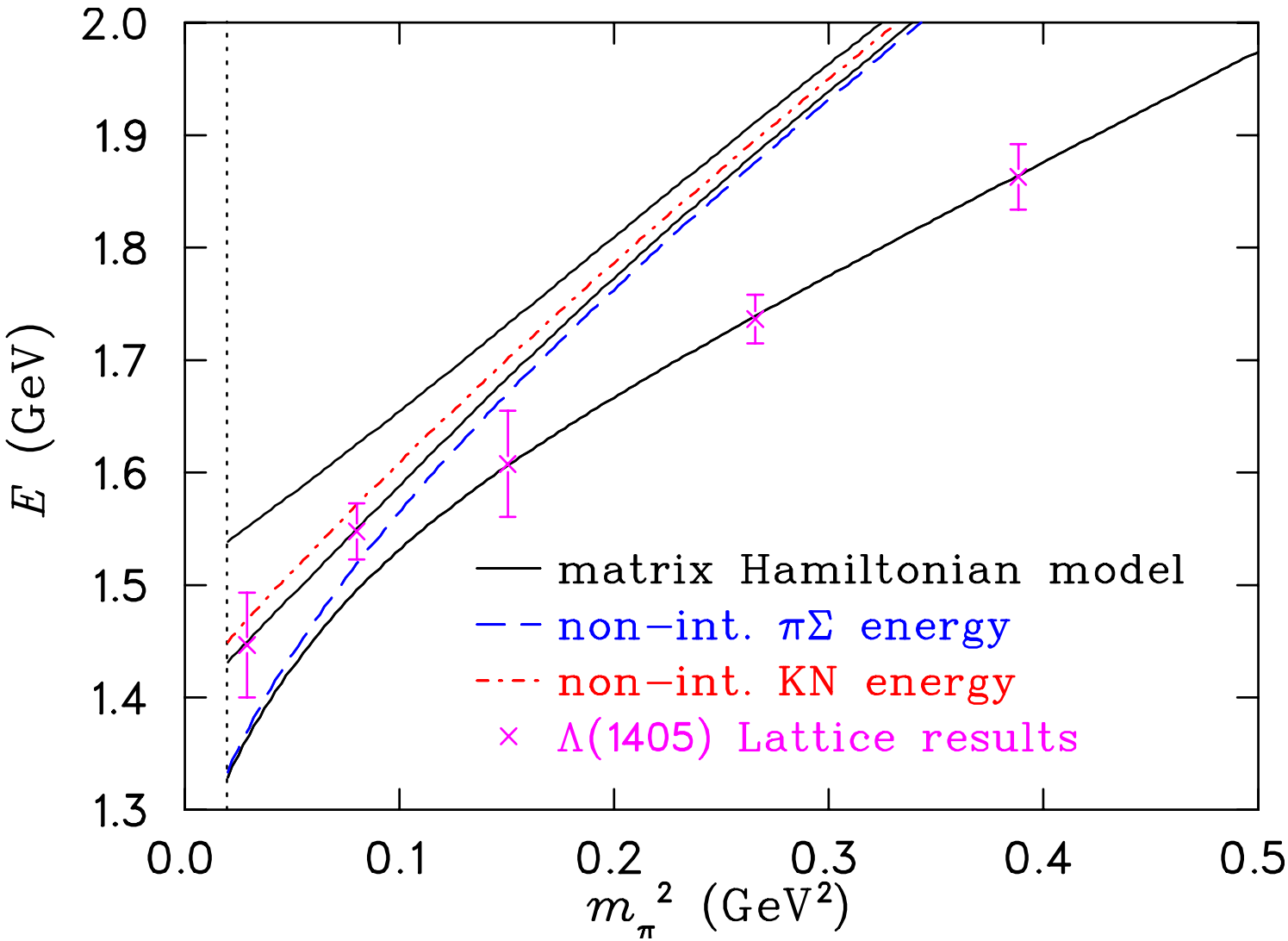

Energy eigenstate, $|E\rangle$, basis $|state\rangle$ composition

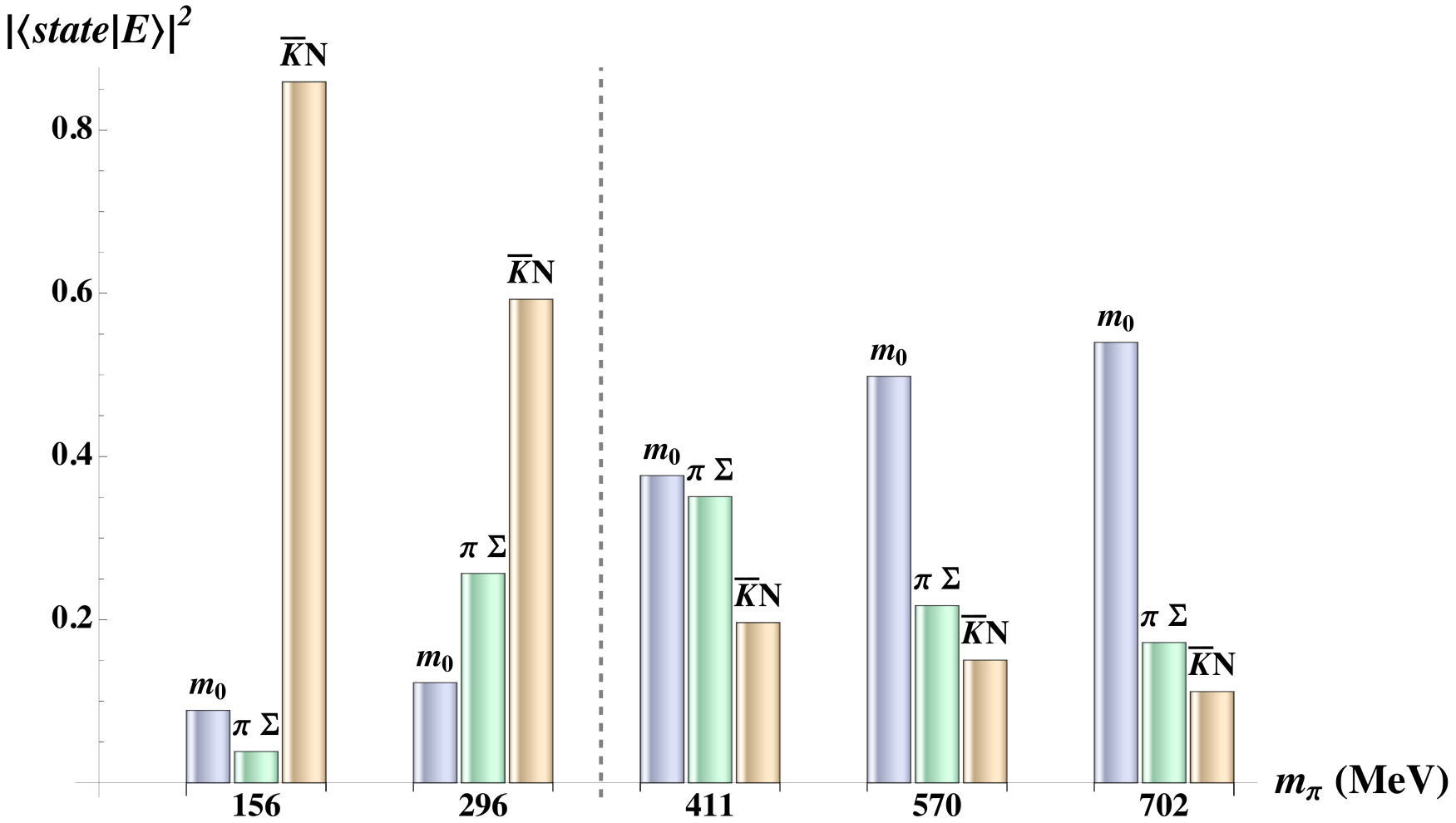

Strange Magnetic Form Factor

- Provides direct insight into the possible dominance of a molecular $\overline{K}N$ bound state.

Strange Magnetic Form Factor

- Provides direct insight into the possible dominance of a molecular $\overline{K}N$ bound state.
- In forming such a molecular state, the $\Lambda(u,d,s)$ valence quark configuration is complemented by
  - A $u,\overline{u}$ pair making a $K^-(s,\overline{u})$ - proton (u,u,d) bound state, or
  - A $d,\overline{d}$ pair making a $\overline{K}^0(s,\overline{d})$ - neutron (d,d,u) bound state.

Strange Magnetic Form Factor

- Provides direct insight into the possible dominance of a molecular $\overline{K}N$ bound state.
- In forming such a molecular state, the $\Lambda(u, d, s)$ valence quark configuration is complemented by
  - A $u, \overline{u}$ pair making a $K^-(s, \overline{u})$ - proton (u, u, d) bound state, or
  - A $d, \overline{d}$ pair making a $\overline{K}^0(s, \overline{d})$ - neutron (d, d, u) bound state.
- In both cases the strange quark is confined within a spin-0 kaon and has no preferred spin orientation.

Strange Magnetic Form Factor

- Provides direct insight into the possible dominance of a molecular $\overline{K}N$ bound state.
- In forming such a molecular state, the $\Lambda(u, d, s)$ valence quark configuration is complemented by
  - A $u, \overline{u}$ pair making a $K^-(s, \overline{u})$ - proton (u, u, d) bound state, or
  - A $d, \overline{d}$ pair making a $\overline{K}^0(s, \overline{d})$ - neutron (d, d, u) bound state.
- In both cases the strange quark is confined within a spin-0 kaon and has no preferred spin orientation.
- To conserve parity, the kaon has zero orbital angular momentum.

Strange Magnetic Form Factor

- Provides direct insight into the possible dominance of a molecular $\overline{K}N$ bound state.
- In forming such a molecular state, the $\Lambda(u, d, s)$ valence quark configuration is complemented by
  - A $u, \overline{u}$ pair making a $K^-(s, \overline{u})$ - proton (u, u, d) bound state, or
  - A $d, \overline{d}$ pair making a $\overline{K}^0(s, \overline{d})$ - neutron (d, d, u) bound state.
- In both cases the strange quark is confined within a spin-0 kaon and has no preferred spin orientation.
- To conserve parity, the kaon has zero orbital angular momentum.
- Thus, the strange quark does not contribute to the magnetic form factor of the $\Lambda(1405)$ when it is a $\overline{K}N$ molecule.

$\mathcal{G}_M$ for the $\Lambda(1405)$ at $Q^2 \sim 0.16\,\mathrm{GeV}^2$

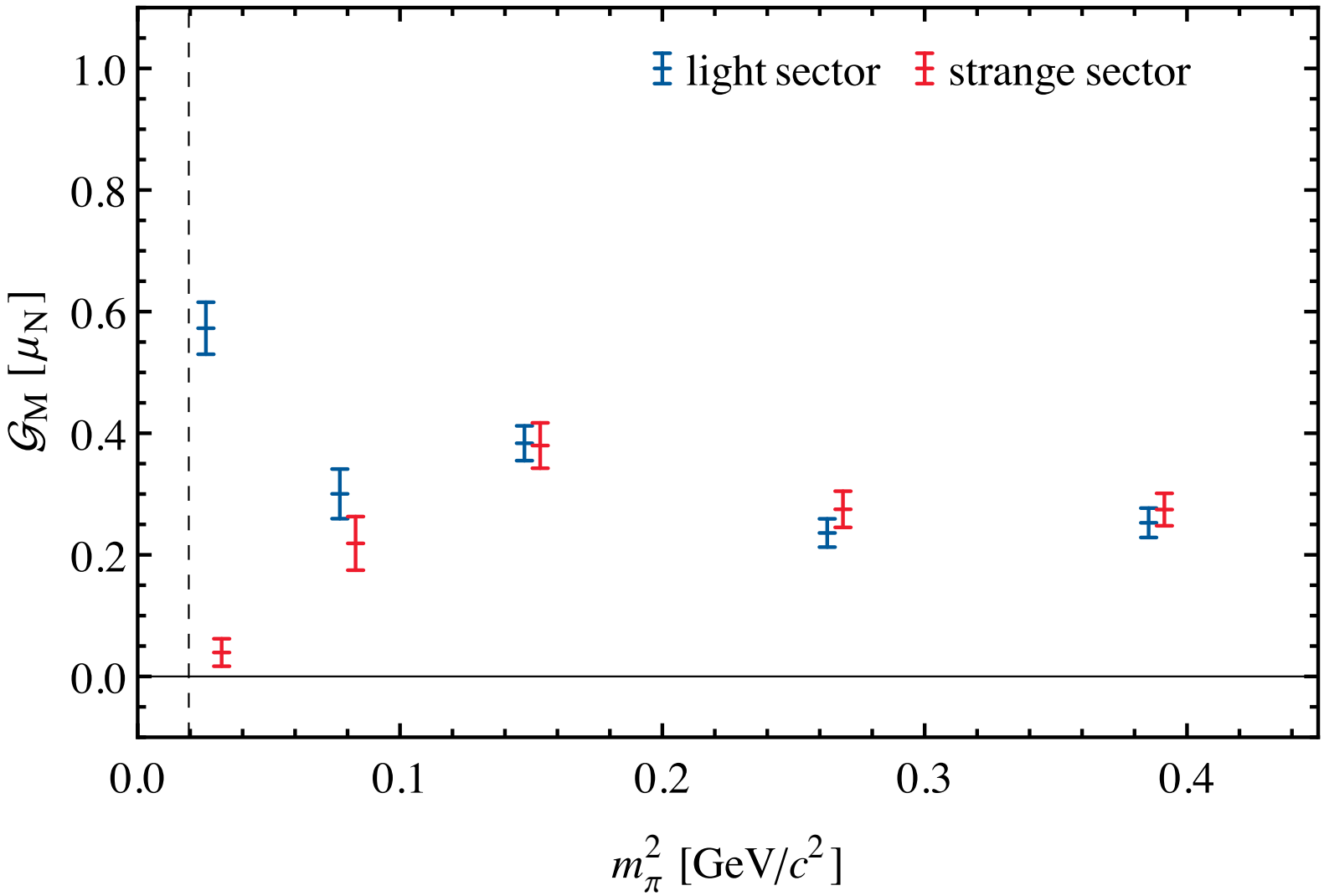

$\mathcal{G}_M$ for the $\Lambda(1405)$ at $Q^2 \sim 0.16\,\mathrm{GeV}^2$

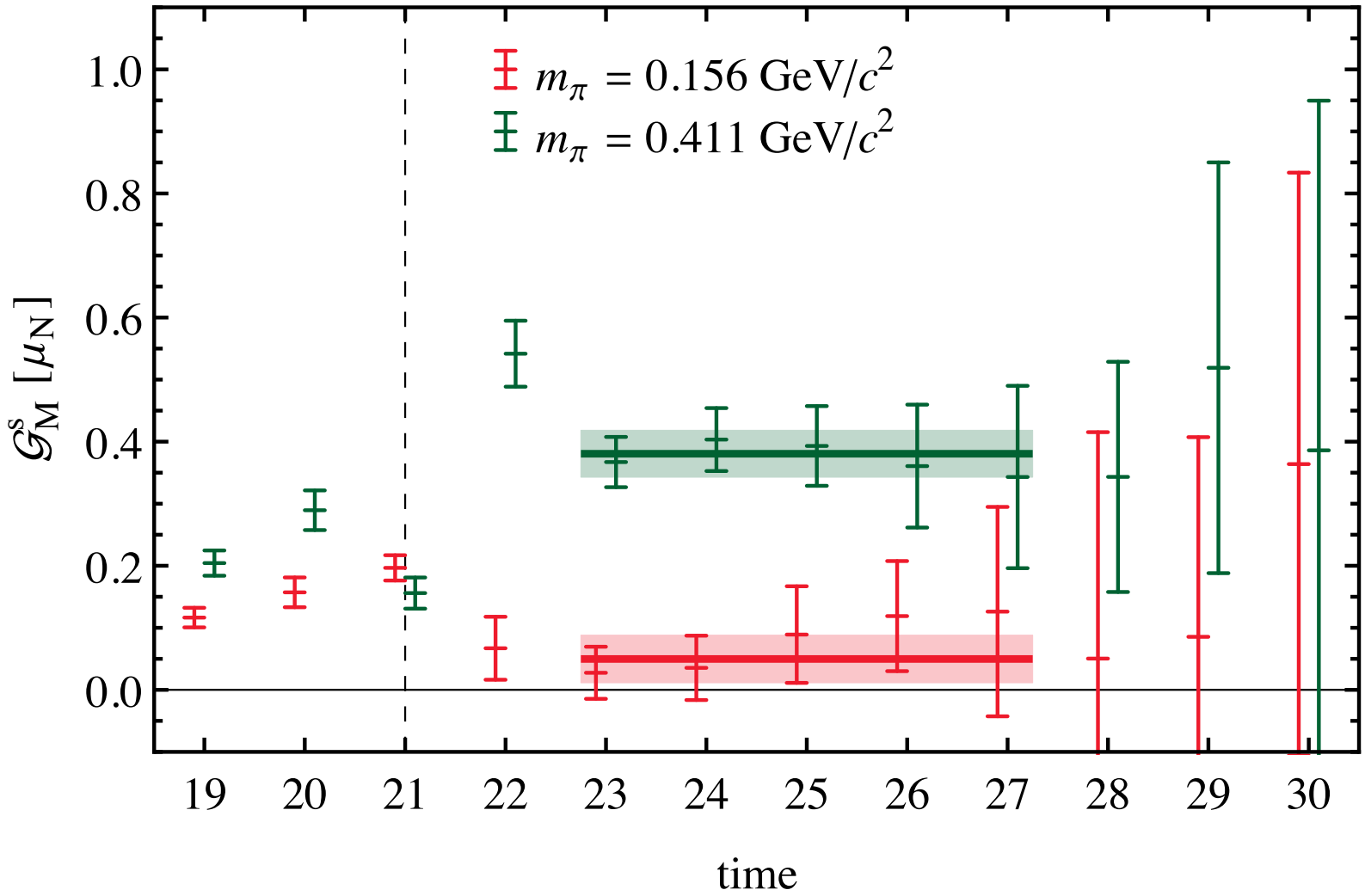

Artistic view of $\Lambda(1405)$ Structure

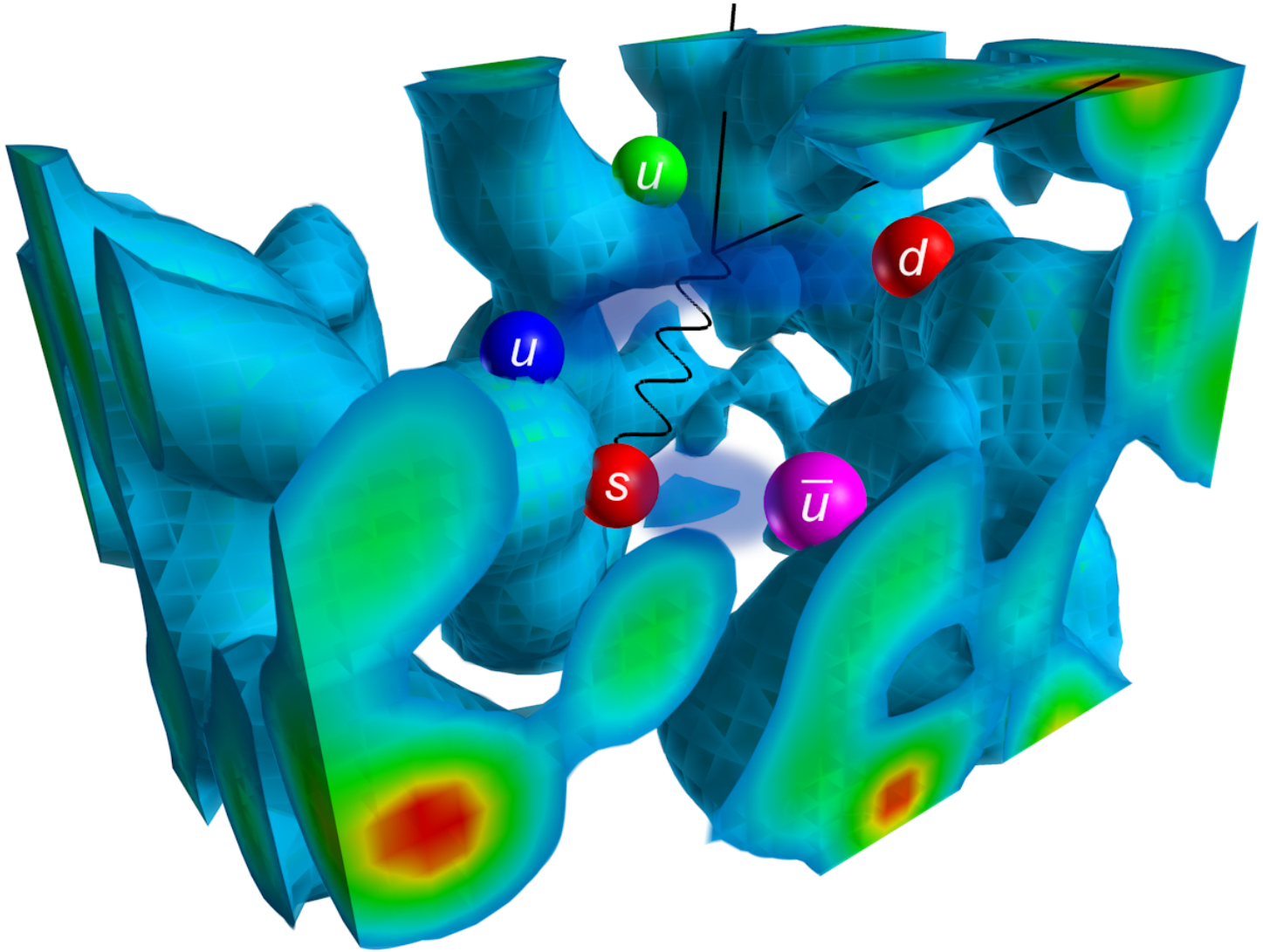

Low-lying negative-parity N^* Spectrum

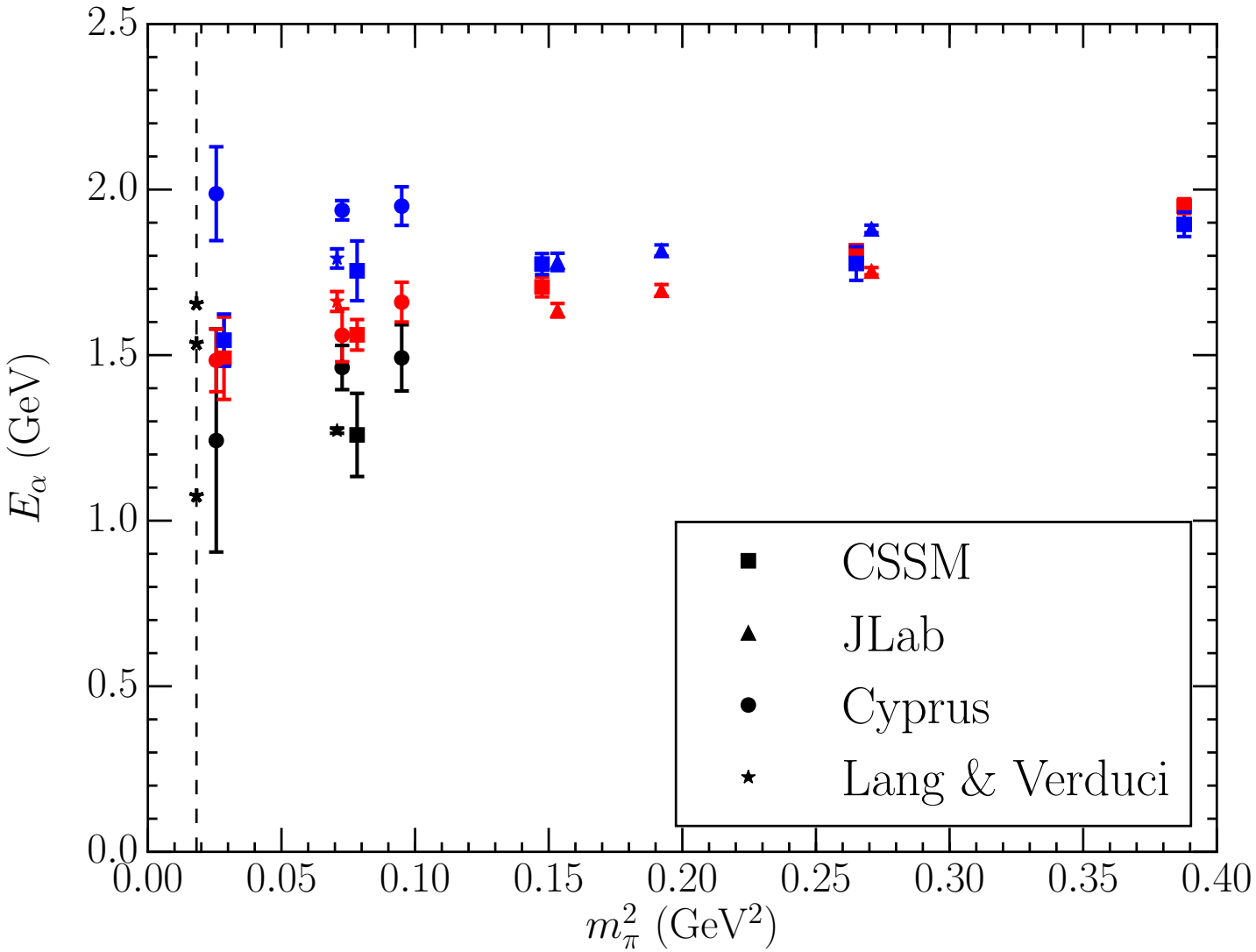

Constrain model parameters to experimental data

- Consider πN and ηN channels, dressing a bare state.
- Fit to phase shift and inelasticity

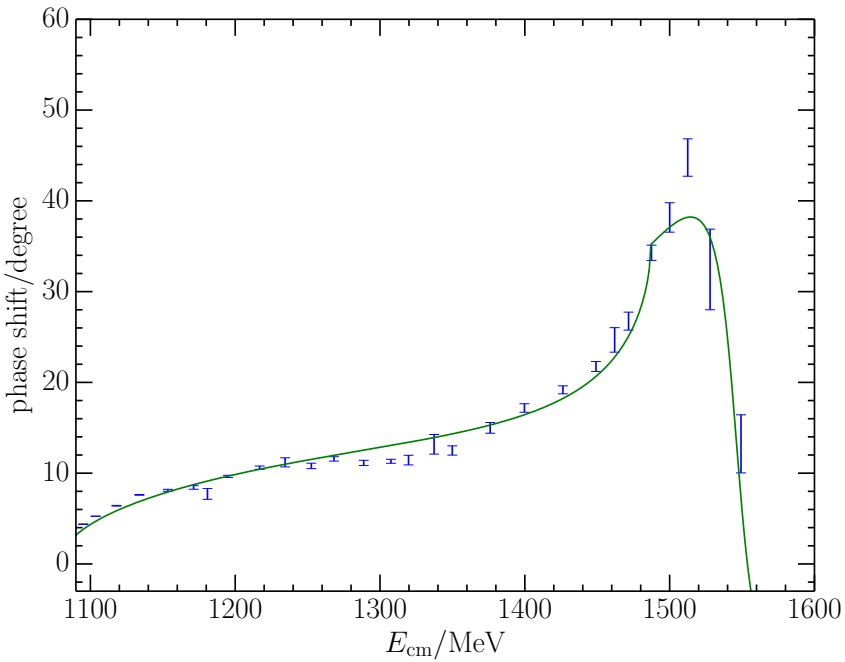

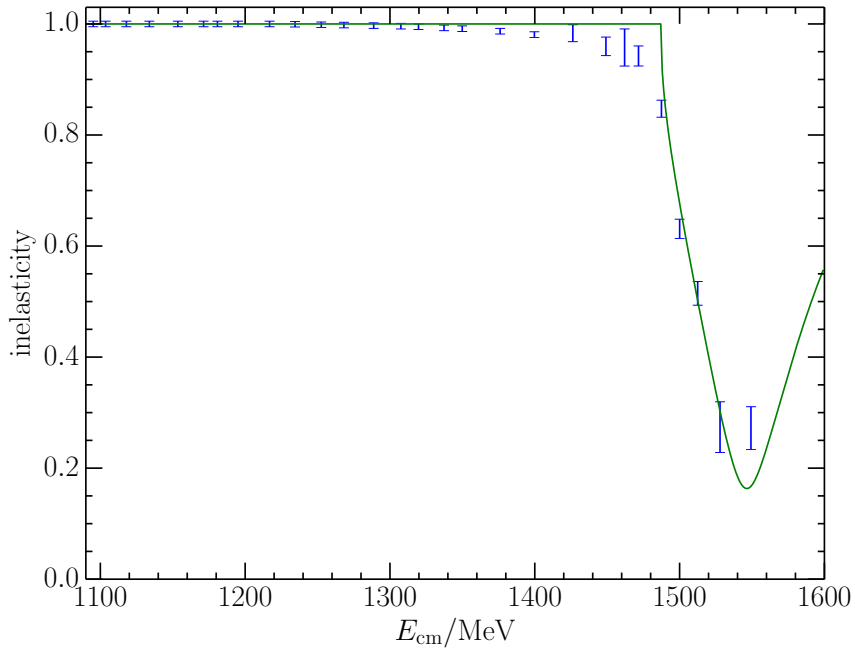

- Fit yields a pole at $1531 \pm 29 - i\,88 \pm 2$ MeV.
- Compare PDG estimate $1510 \pm 20 - i\,85 \pm 40$ MeV.

Hamiltonian Model N^* Spectrum: 2 fm

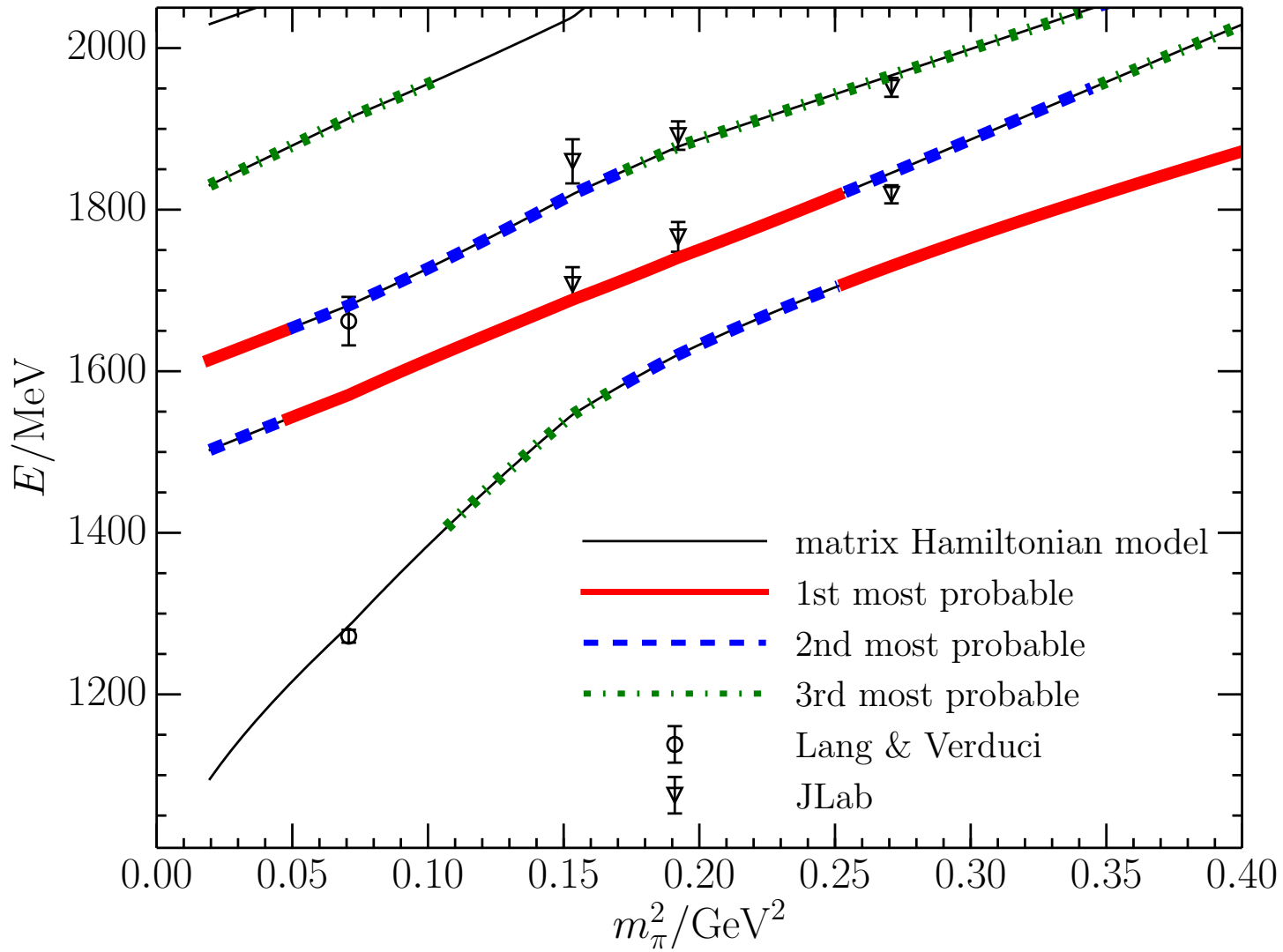

Hamiltonian Model N^* Spectrum: 3 fm

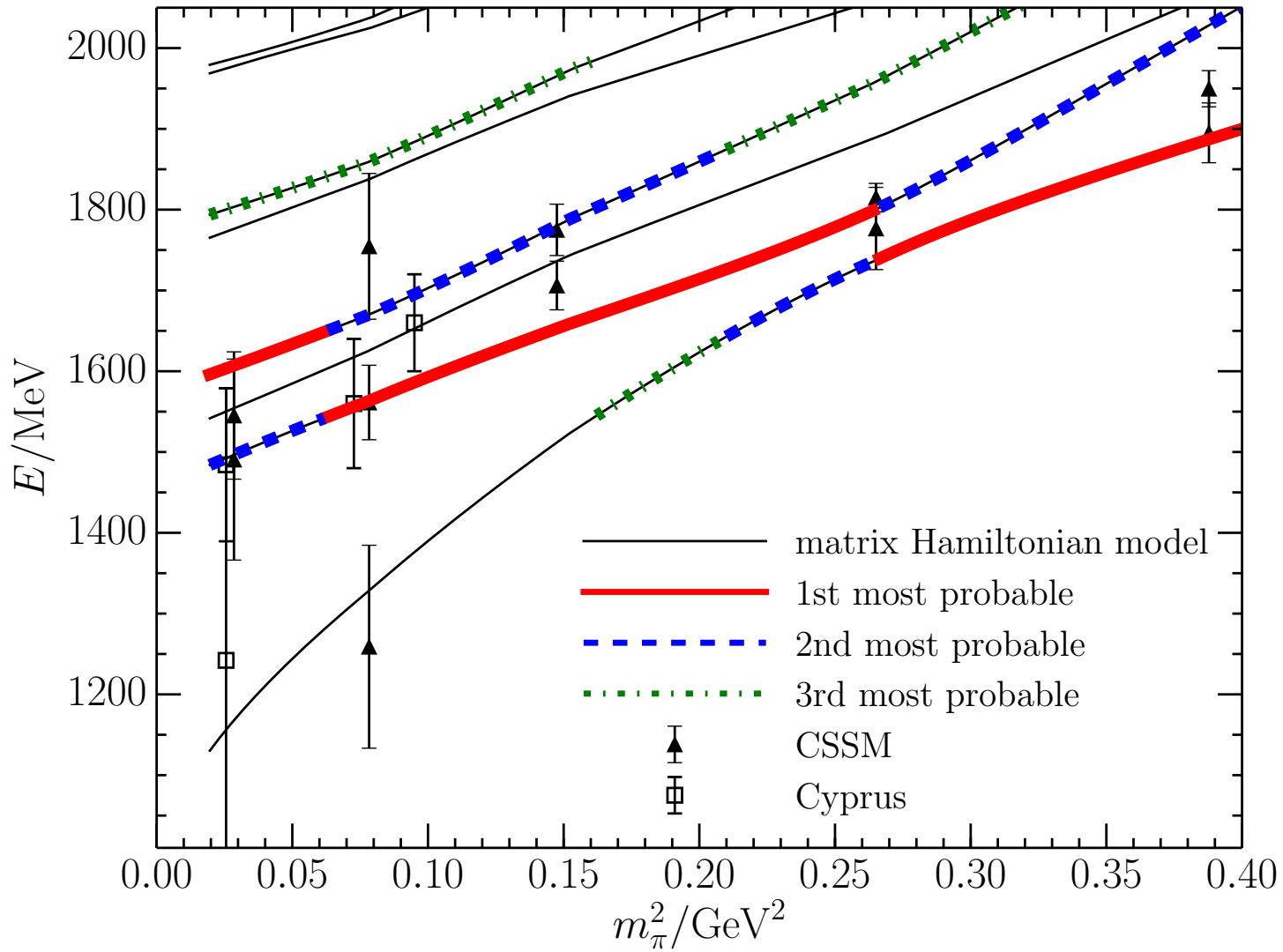

What about the Roper? Lattice results at $L \simeq 3$ fm

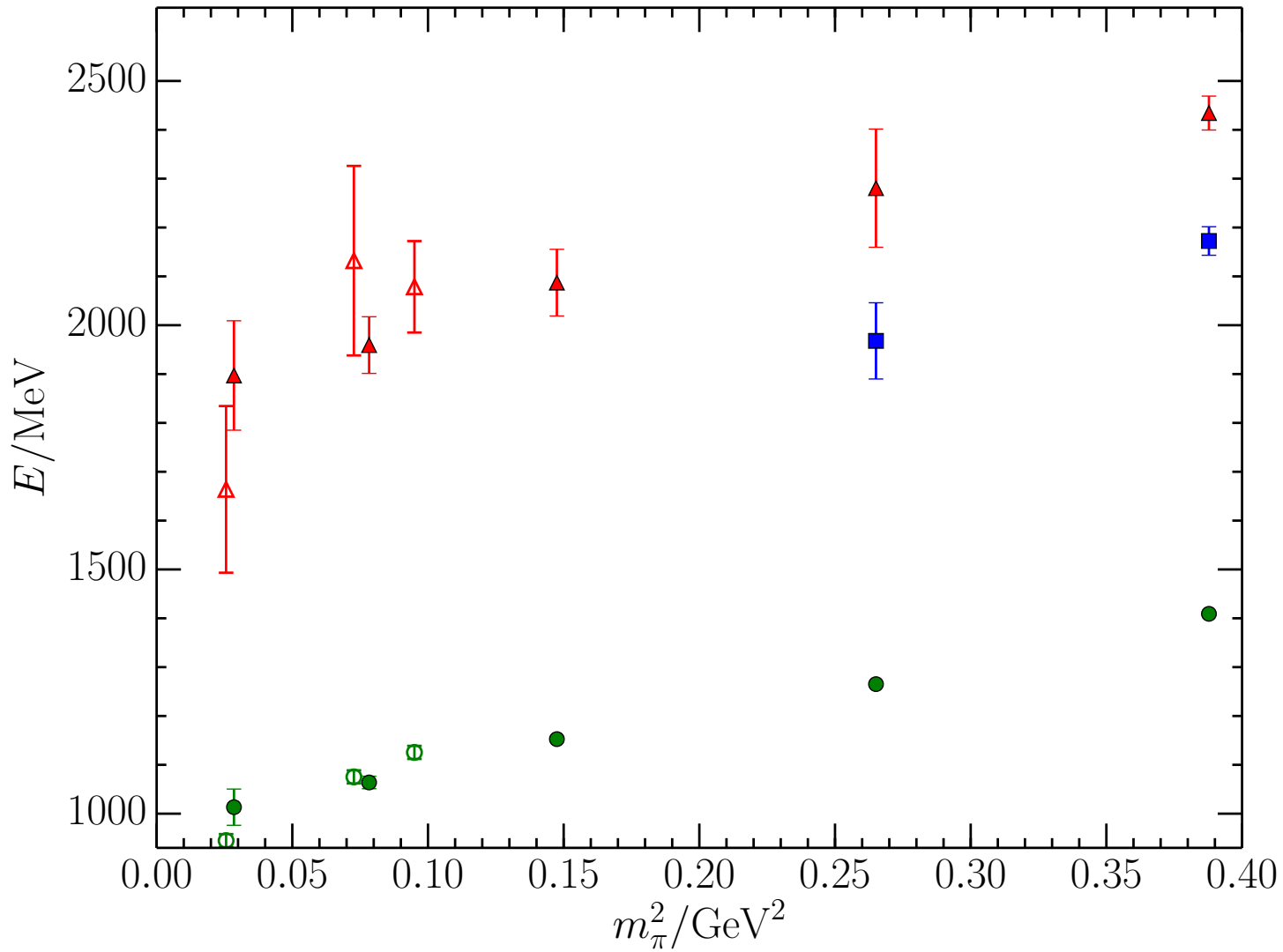

Constrain Roper model parameters to experiment

- Consider πN, $\pi\Delta$ and σN channels, dressing a bare state.
- Fit to phase shift and inelasticity

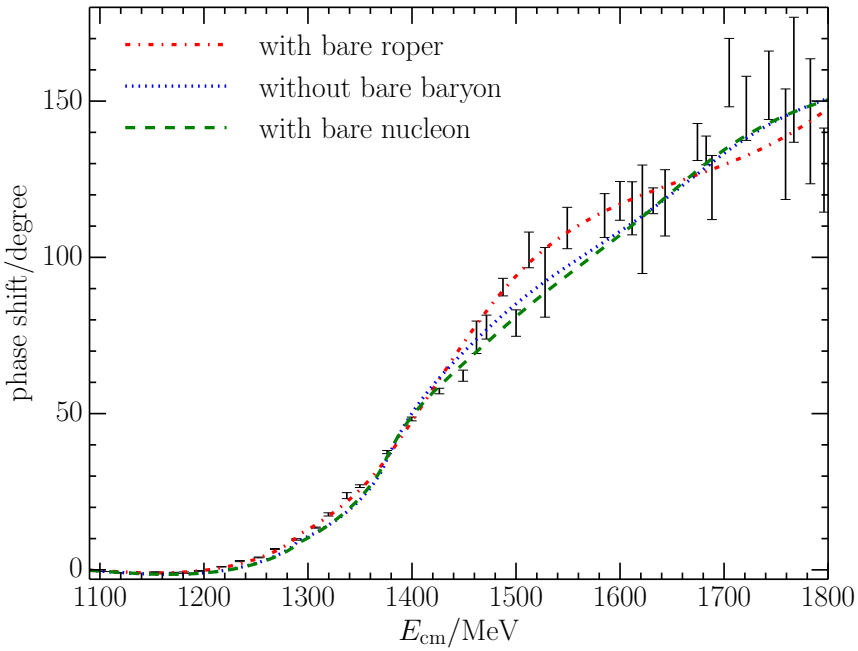

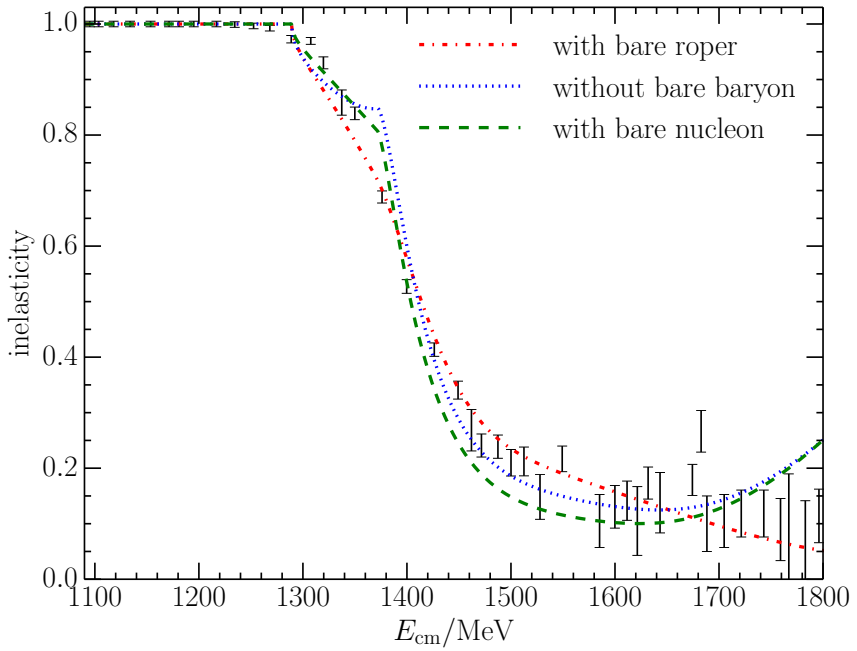

- Fit yields a pole at 1357 $- i\,36$ MeV.
- Compare PDG estimate $1365 \pm 15 - i\,95 \pm 15$ MeV.

Non-interacting meson-baryon channels considered

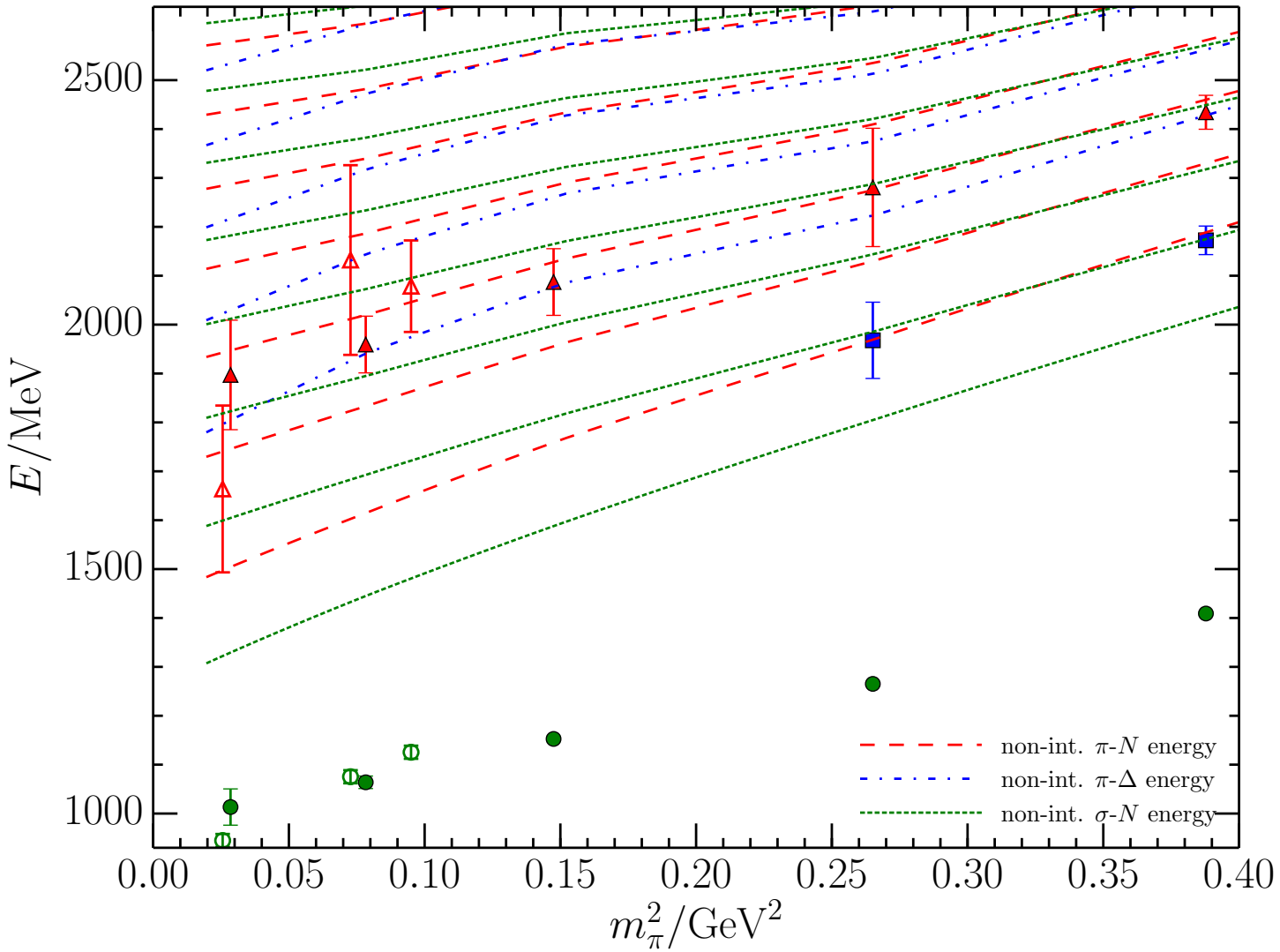

Hamiltonian Model N' Spectrum

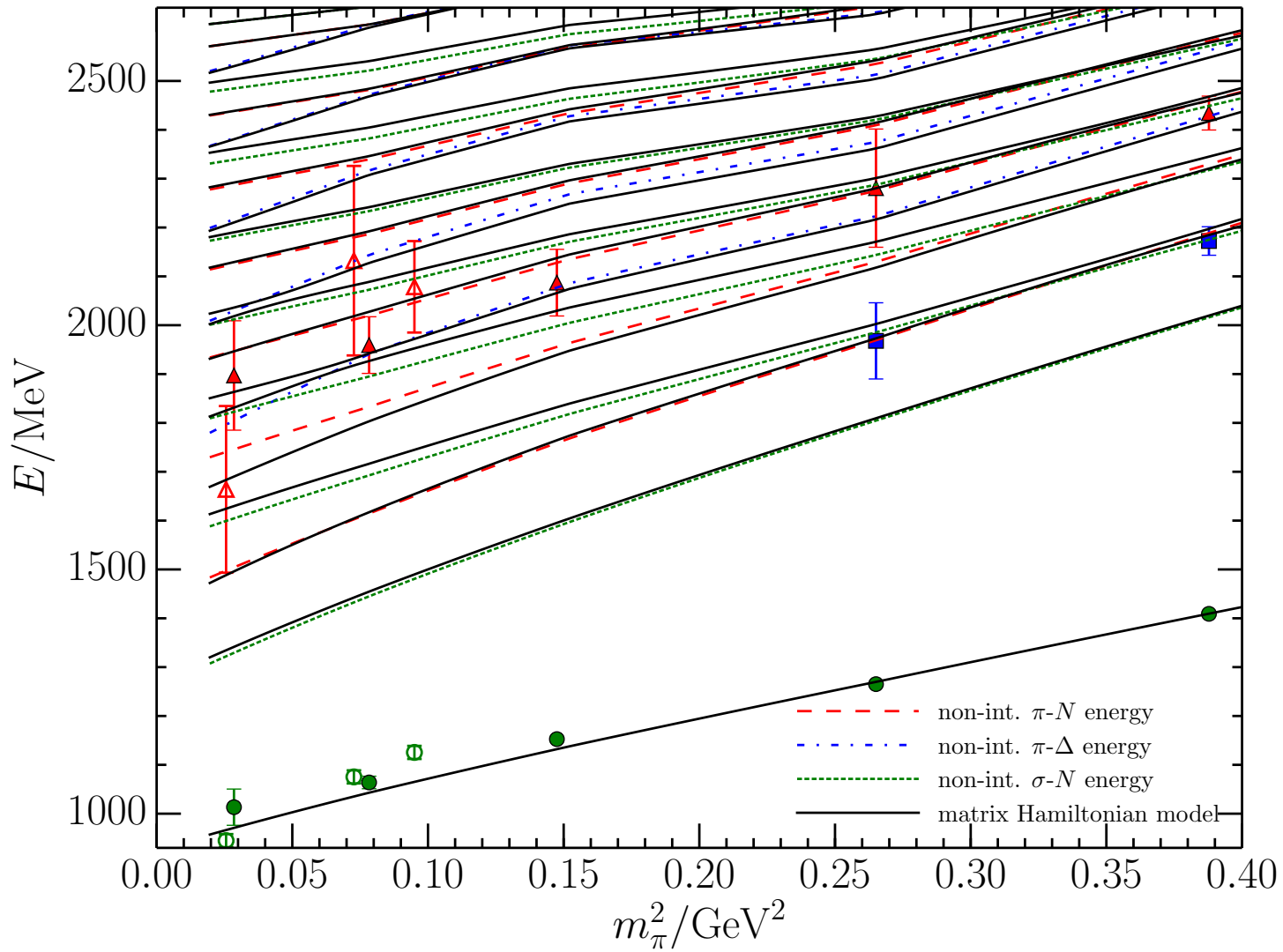

Hamiltonian Model N' Spectrum

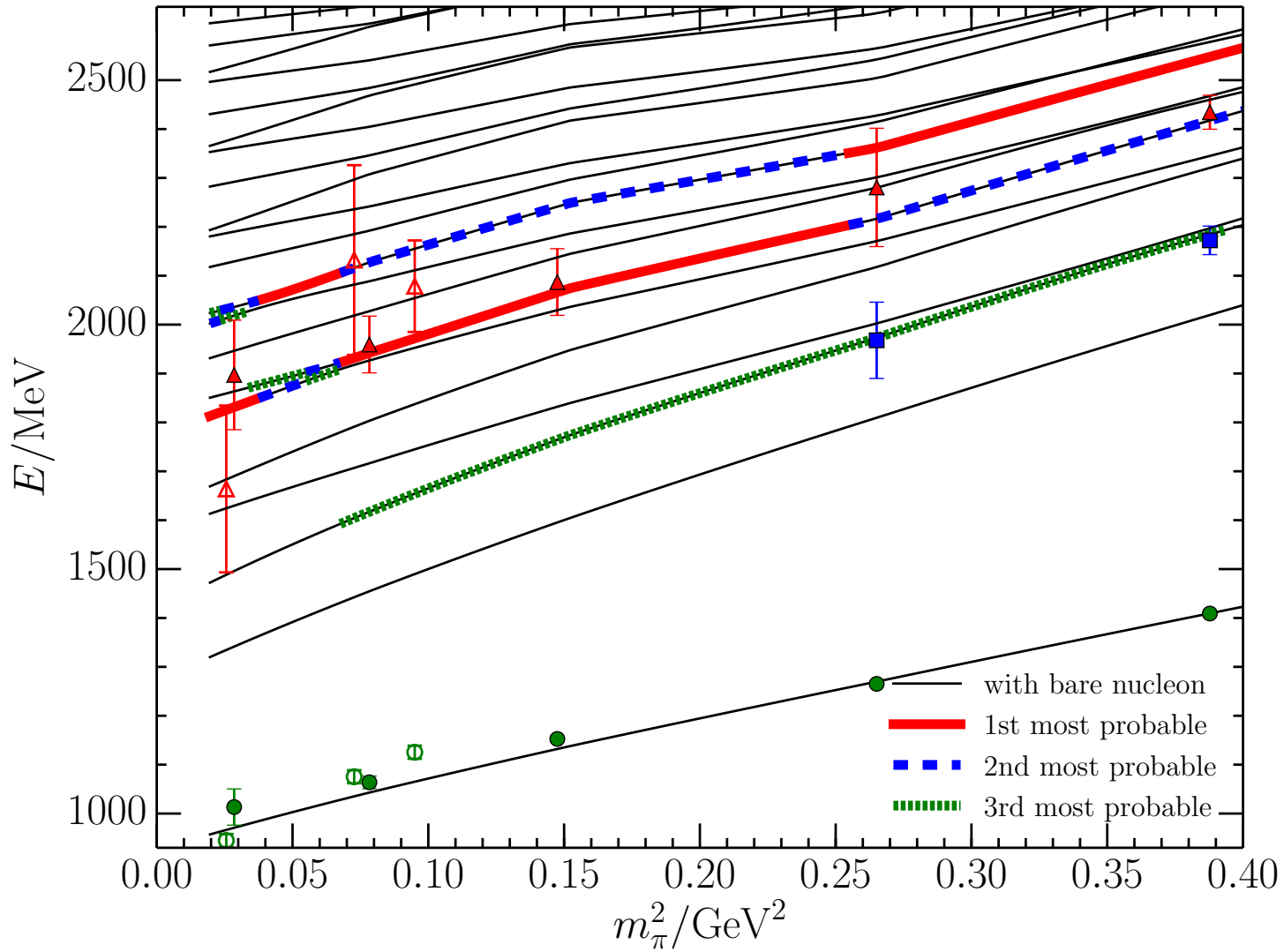

Bare State Strength in the N' Spectrum: 3 fm

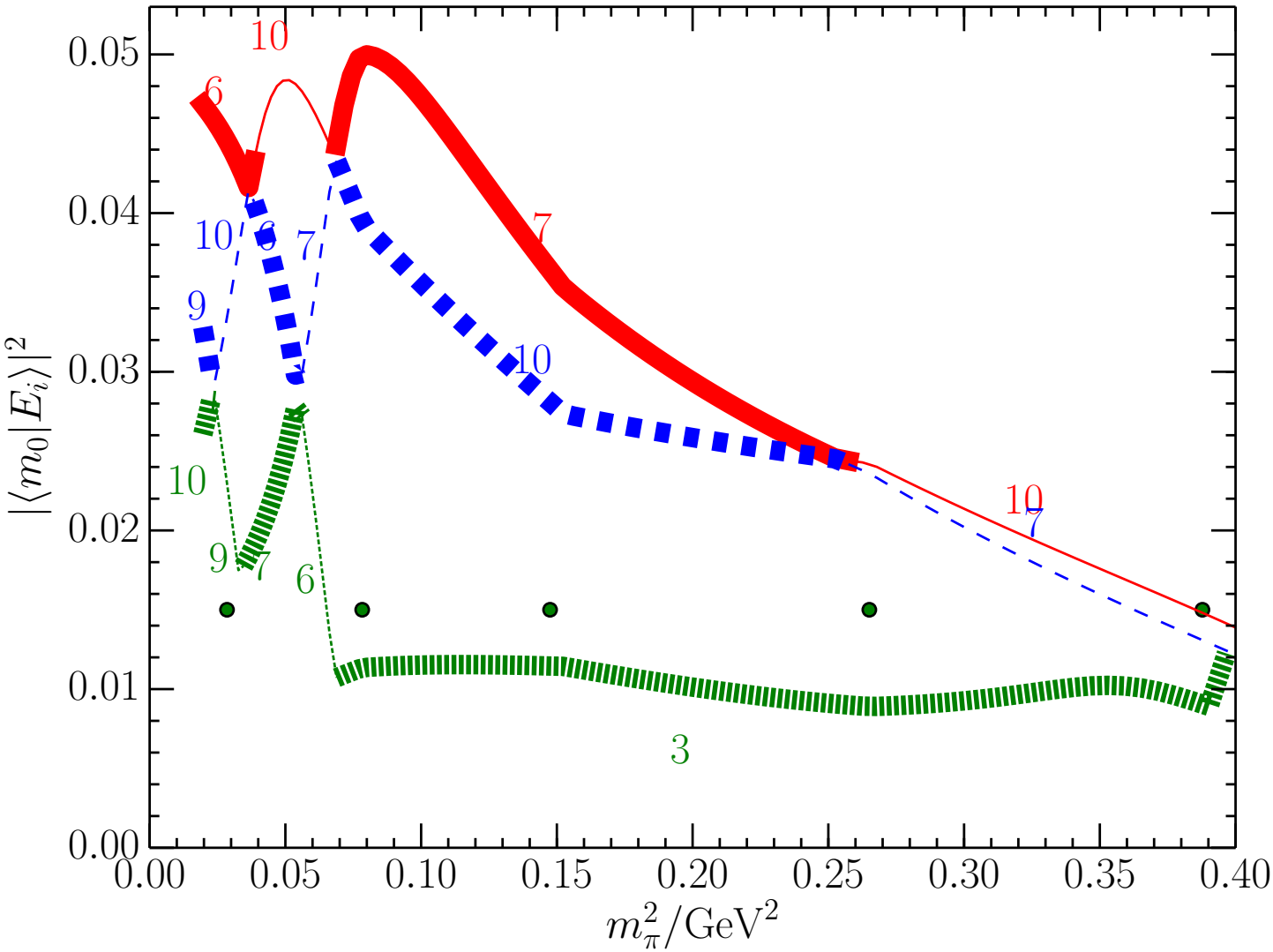

Composition of the ground state: 3 fm

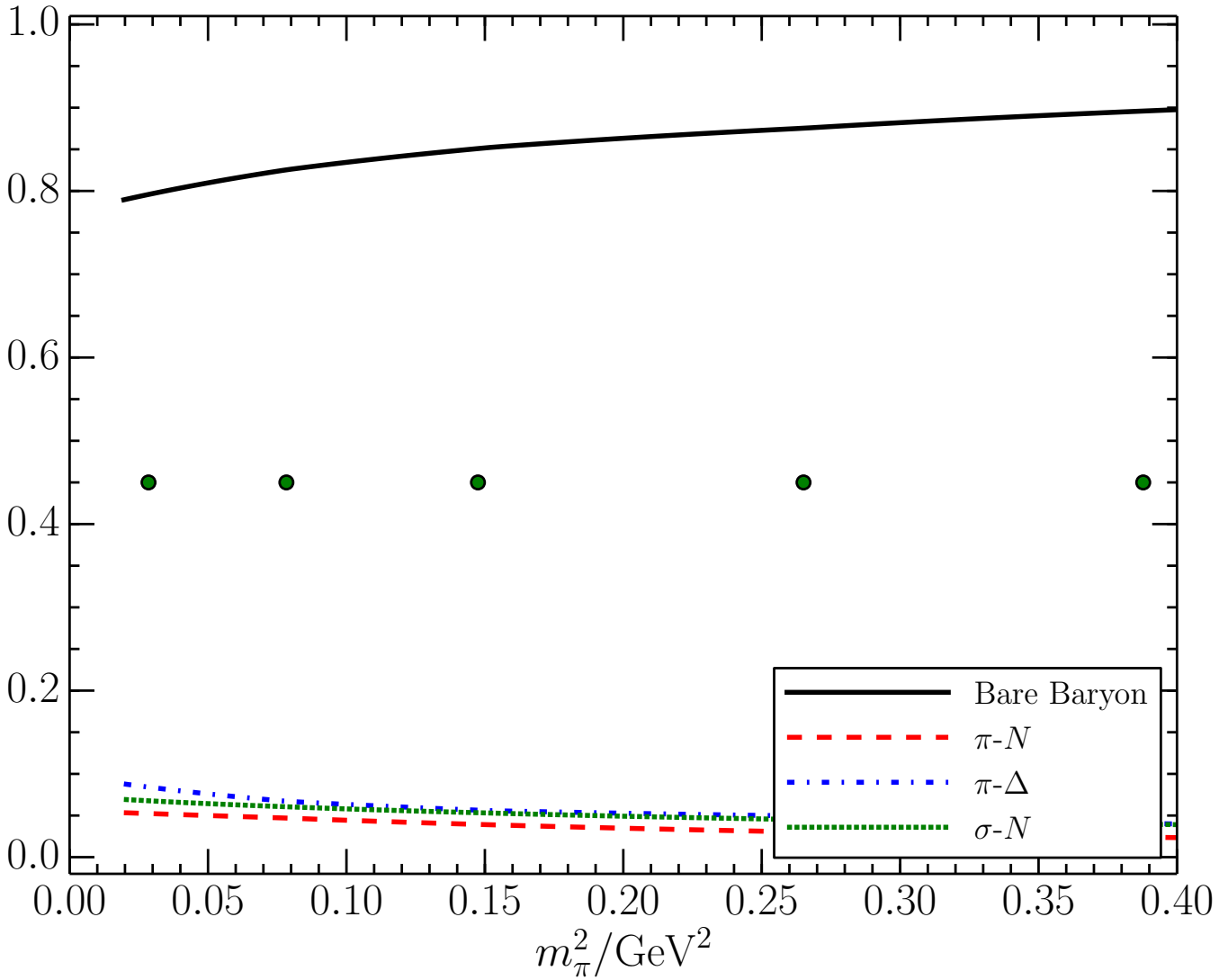

Composition of the 7th state: 3 fm

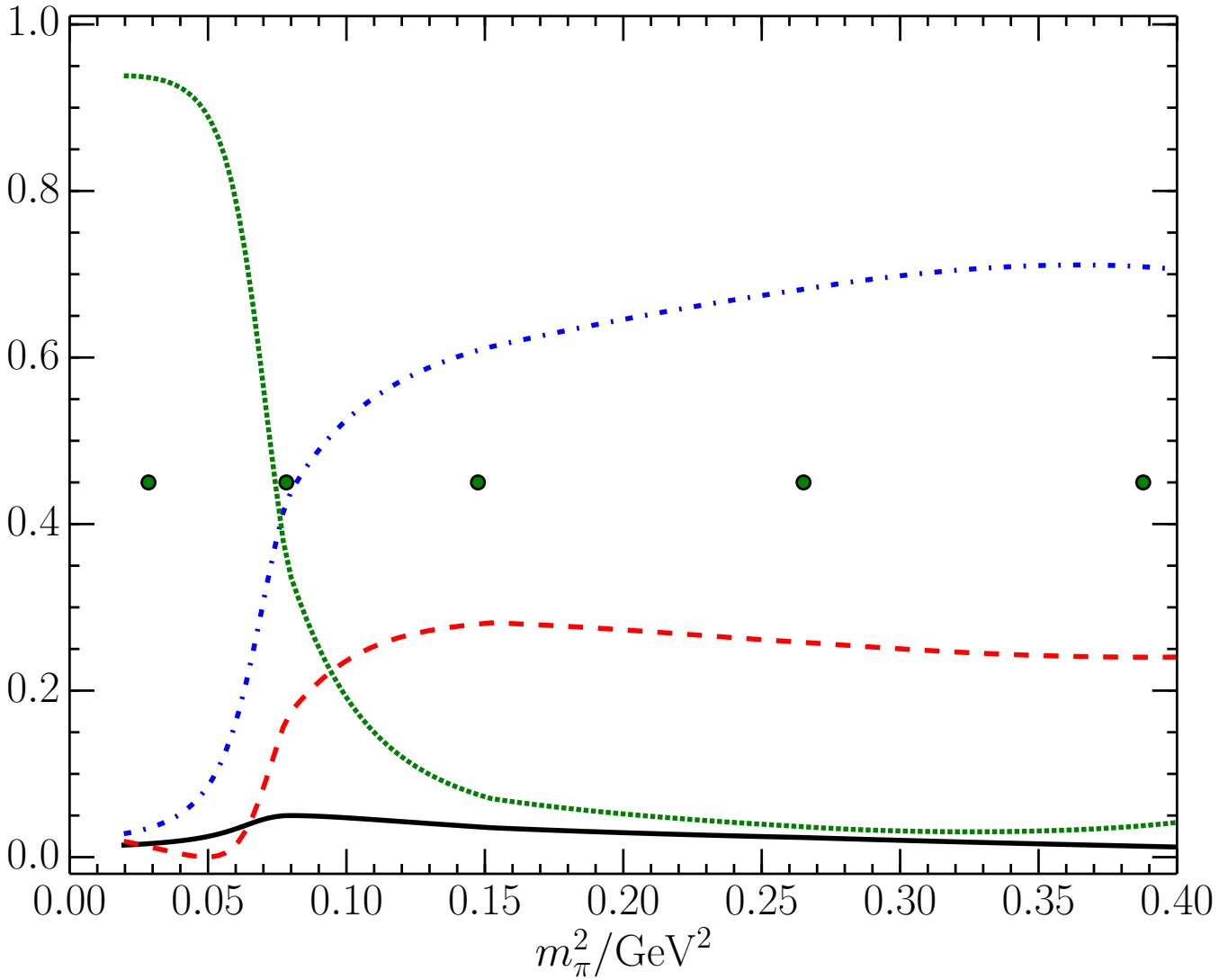

Conclusions

- A survey of the current literature resolves discrepancies among groups exploring the low-lying nucleon spectrum.
  - Results for low-lying nucleon excitations are forming a consensus.

Conclusions

- A survey of the current literature resolves discrepancies among groups exploring the low-lying nucleon spectrum.
  - Results for low-lying nucleon excitations are forming a consensus.
- The negative parity sector appears to be well understood.
  - Hamiltonian Effective Field Theory describes the spectrum well.

Conclusions

- A survey of the current literature resolves discrepancies among groups exploring the low-lying nucleon spectrum.
  - Results for low-lying nucleon excitations are forming a consensus.
- The negative parity sector appears to be well understood.
  - Hamiltonian Effective Field Theory describes the spectrum well.
  - First results for form factors are consistent with model expectations

Conclusions

- A survey of the current literature resolves discrepancies among groups exploring the low-lying nucleon spectrum.
  - Results for low-lying nucleon excitations are forming a consensus.
- The negative parity sector appears to be well understood.
  - Hamiltonian Effective Field Theory describes the spectrum well.
  - First results for form factors are consistent with model expectations
- The structure of the $\Lambda(1405)$ is also understood; it is dominated by a molecular bound state of an anti-kaon and a nucleon.

Conclusions

- A survey of the current literature resolves discrepancies among groups exploring the low-lying nucleon spectrum.
  - Results for low-lying nucleon excitations are forming a consensus.
- The negative parity sector appears to be well understood.
  - Hamiltonian Effective Field Theory describes the spectrum well.
  - First results for form factors are consistent with model expectations
- The structure of the $\Lambda(1405)$ is also understood; it is dominated by a molecular bound state of an anti-kaon and a nucleon.
- Roper of the Constituent Quark Model has been seen on the lattice.
  - Node structure and density is similar to model expectations.

Conclusions

- A survey of the current literature resolves discrepancies among groups exploring the low-lying nucleon spectrum.
  - Results for low-lying nucleon excitations are forming a consensus.
- The negative parity sector appears to be well understood.
  - Hamiltonian Effective Field Theory describes the spectrum well.
  - First results for form factors are consistent with model expectations
- The structure of the $\Lambda(1405)$ is also understood; it is dominated by a molecular bound state of an anti-kaon and a nucleon.
- Roper of the Constituent Quark Model has been seen on the lattice.
  - Node structure and density is similar to model expectations.
- Like the $\Lambda(1405)$, the Roper resonance of Nature is dominated by meson-baryon degrees of freedom with little contribution from a quark-model like core.

Positive Parity Nucleon Spectrum: CSSM

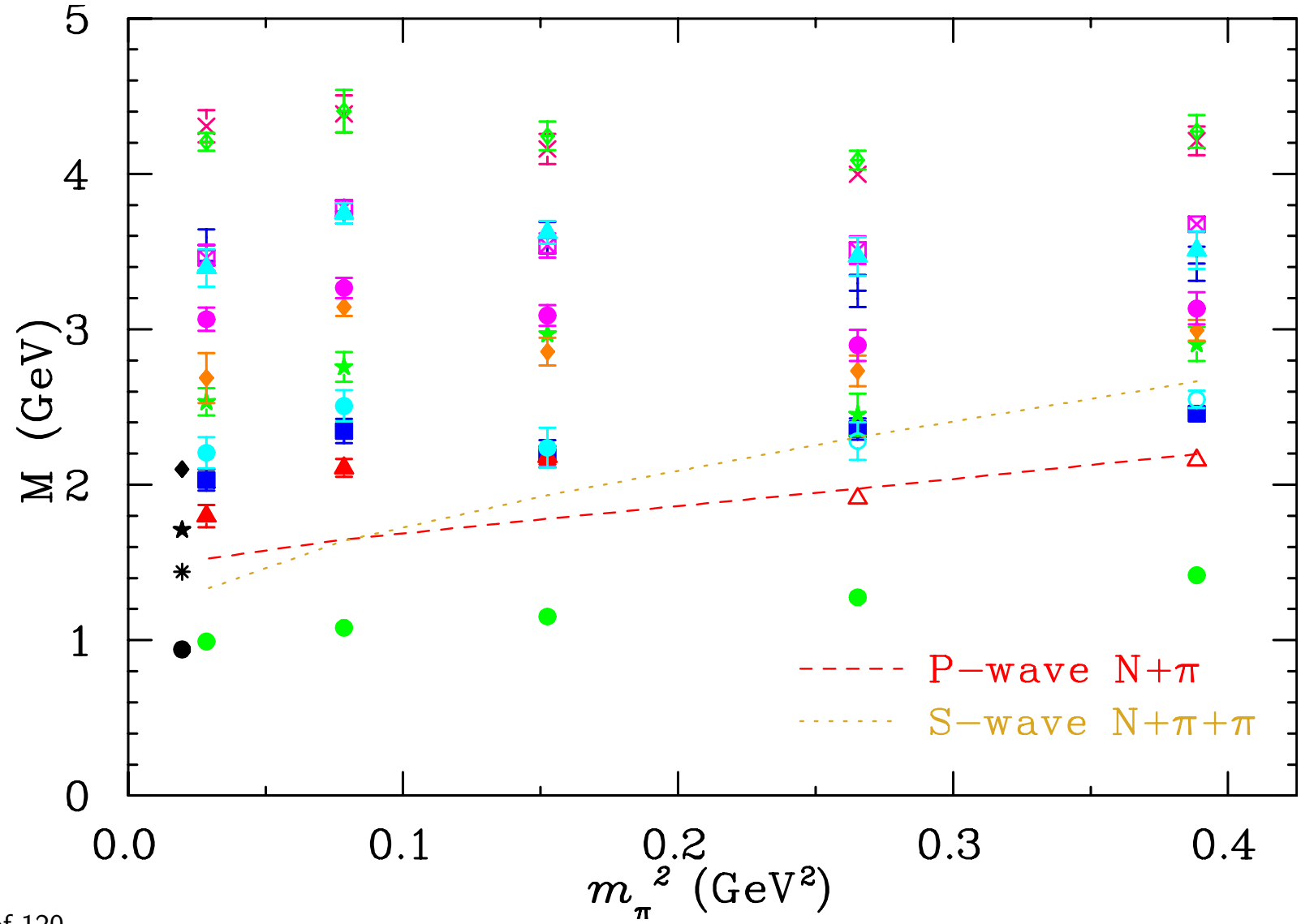

Supplementary Information

The following slides provide additional information which may be of interest.

Operators Used in $\Lambda(1405)$ Analysis

We consider local three-quark operators with the correct quantum numbers for the Λ channel, including

- Flavour-octet operators

$$\chi_1^8 = \frac{1}{\sqrt{6}}\varepsilon^{abc}\left(2(u^a C\gamma_5 d^b)s^c + (u^a C\gamma_5 s^b)d^c - (d^a C\gamma_5 s^b)u^c\right)$$

$$\chi_2^8 = \frac{1}{\sqrt{6}}\varepsilon^{abc}\left(2(u^a C d^b)\gamma_5 s^c + (u^a C s^b)\gamma_5 d^c - (d^a C s^b)\gamma_5 u^c\right)$$

- Flavour-singlet operator

$$\chi^1 = 2\varepsilon^{abc}\left((u^a C\gamma_5 d^b)s^c - (u^a C\gamma_5 s^b)d^c + (d^a C\gamma_5 s^b)u^c\right)$$

Operators Used in $\Lambda(1405)$ Analysis

We also use gauge-invariant Gaussian smearing to increase our operator basis.

- These results use 16 and 100 sweeps.
  - Gives a 6×6 matrix.

Operators Used in $\Lambda(1405)$ Analysis

We also use gauge-invariant Gaussian smearing to increase our operator basis.

- These results use 16 and 100 sweeps.
  - Gives a 6×6 matrix.
- Also considered 35 and 100 sweeps.
  - Results are consistent with larger statistical uncertainties.

Flavour structure of the $\Lambda(1405)$

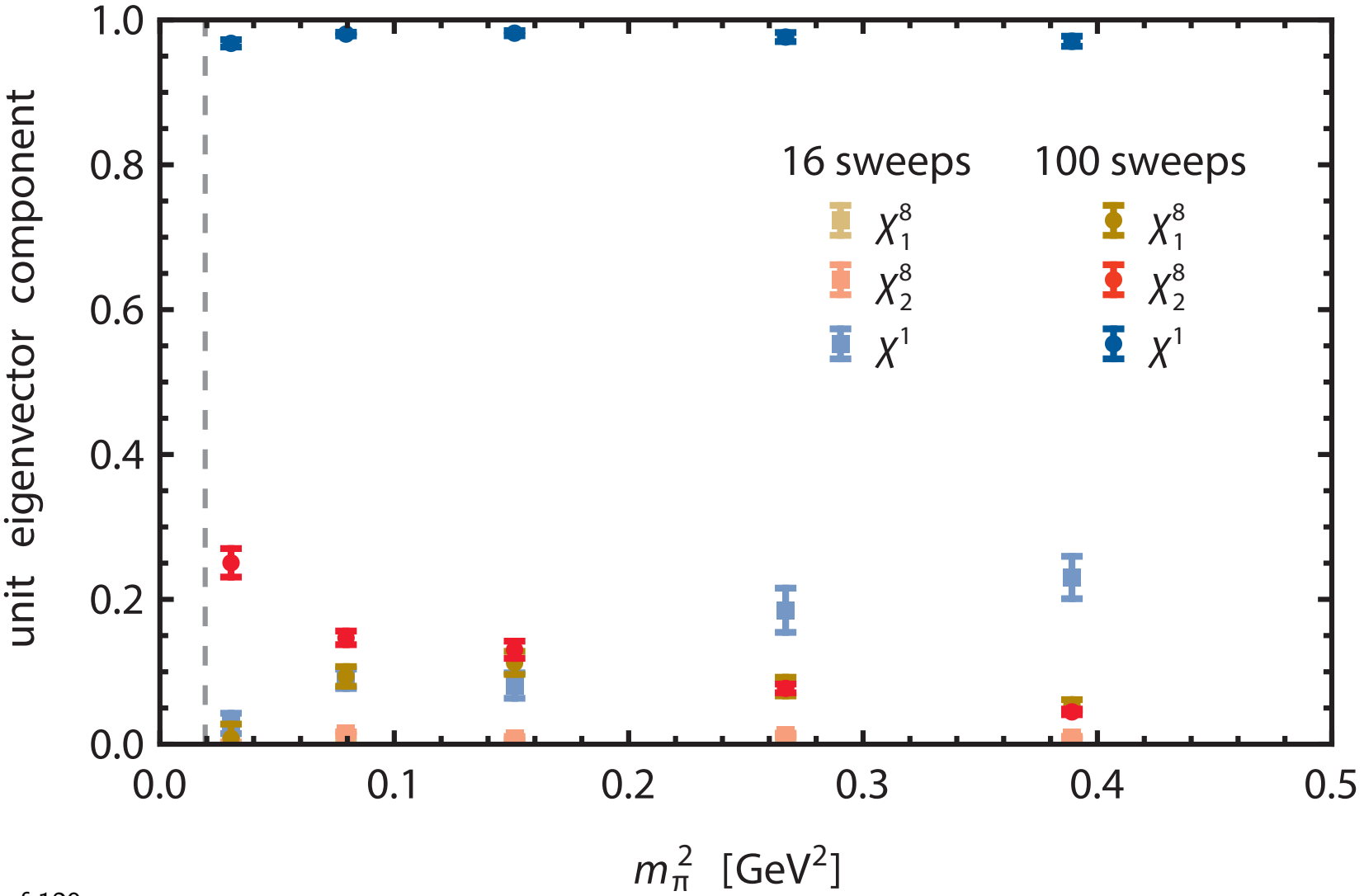

Volume dependence of the odd-parity Λ spectrum

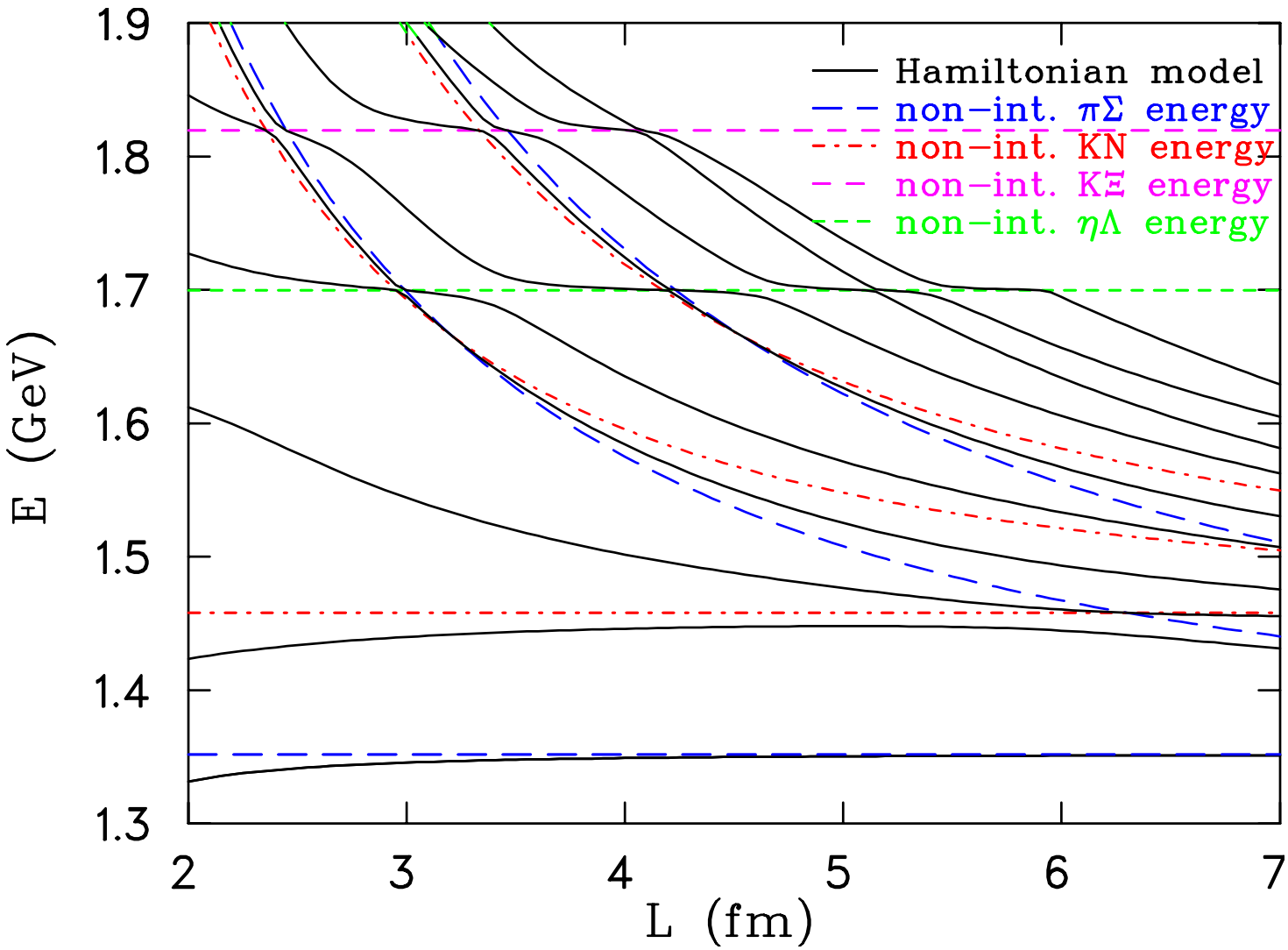

Infinite-volume reconstruction of the $\Lambda(1405)$ energy

- Bootstraps are calculated by altering the value of each lattice data point by a Gaussian-distributed random number, weighted by the uncertainty.

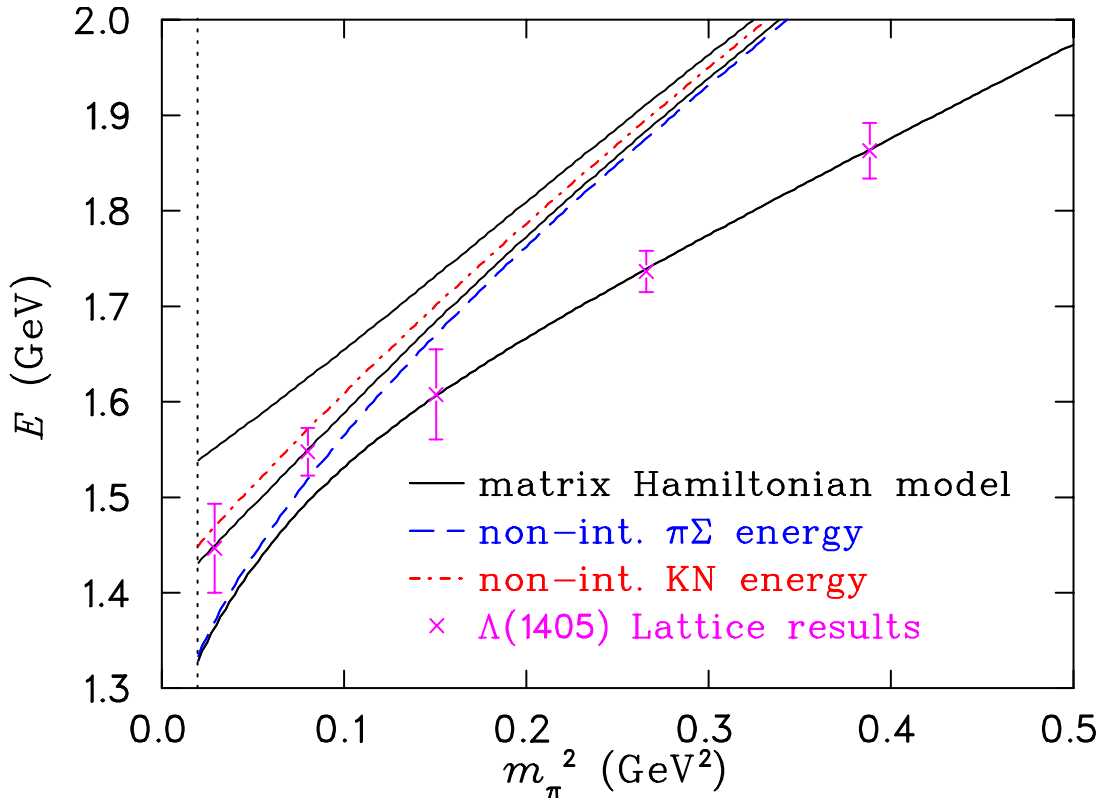

Infinite-volume $\Lambda(1405)$ mass distribution at m_π^{phys}

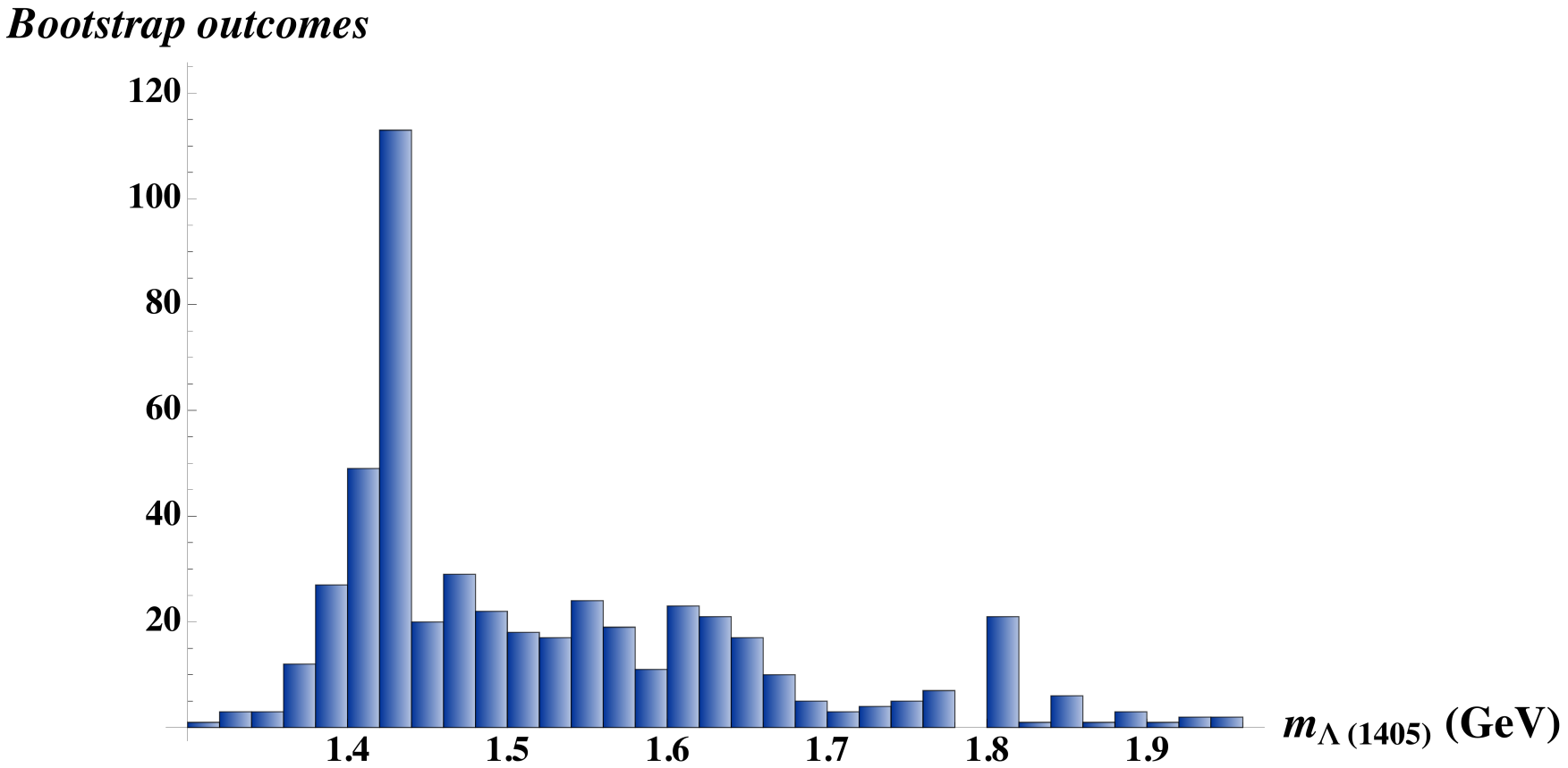

Dispersion Relation Test for the Λ(1405)

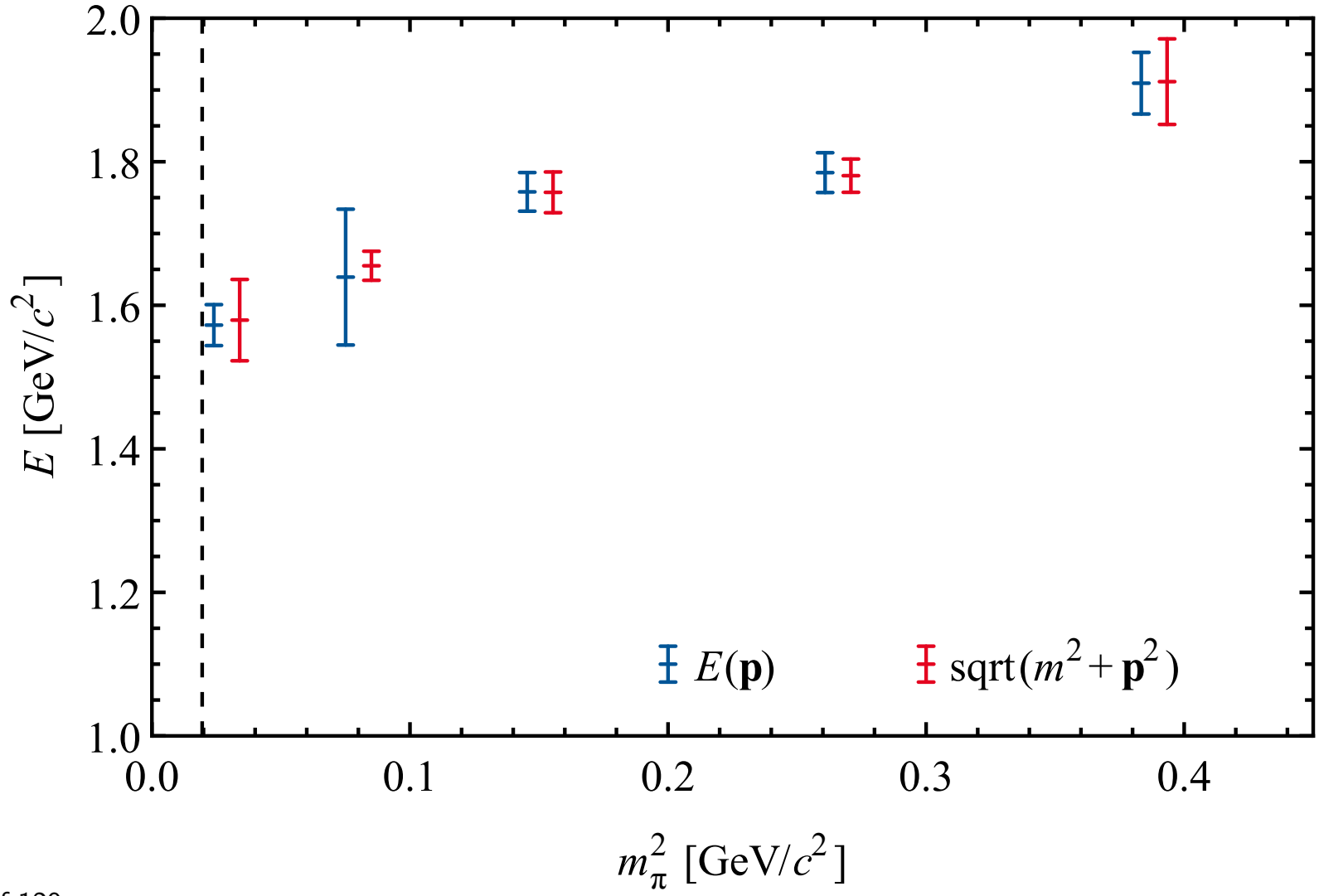

$\mathcal{G}_E$ for the $\Lambda(1405)$

When compared to the ground state, the results for $\mathcal{G}_E$ are consistent with the development of a non-trivial $\overline{K}N$ component at light quark masses.

$\mathcal{G}_E$ for the $\Lambda(1405)$

When compared to the ground state, the results for $\mathcal{G}_E$ are consistent with the development of a non-trivial $\overline{\mathrm{K}}\mathrm{N}$ component at light quark masses.

- Noting that the centre of mass of the $\overline{K}(s,\overline{\ell})\ N(\ell,u,d)$ is nearer the heavier N,
  - The anti–light-quark contribution, $\overline{\ell}$, is distributed further out by the $\overline{\mathrm{K}}$ and leaves an enhanced light-quark form factor.

$\mathcal{G}_E$ for the $\Lambda(1405)$

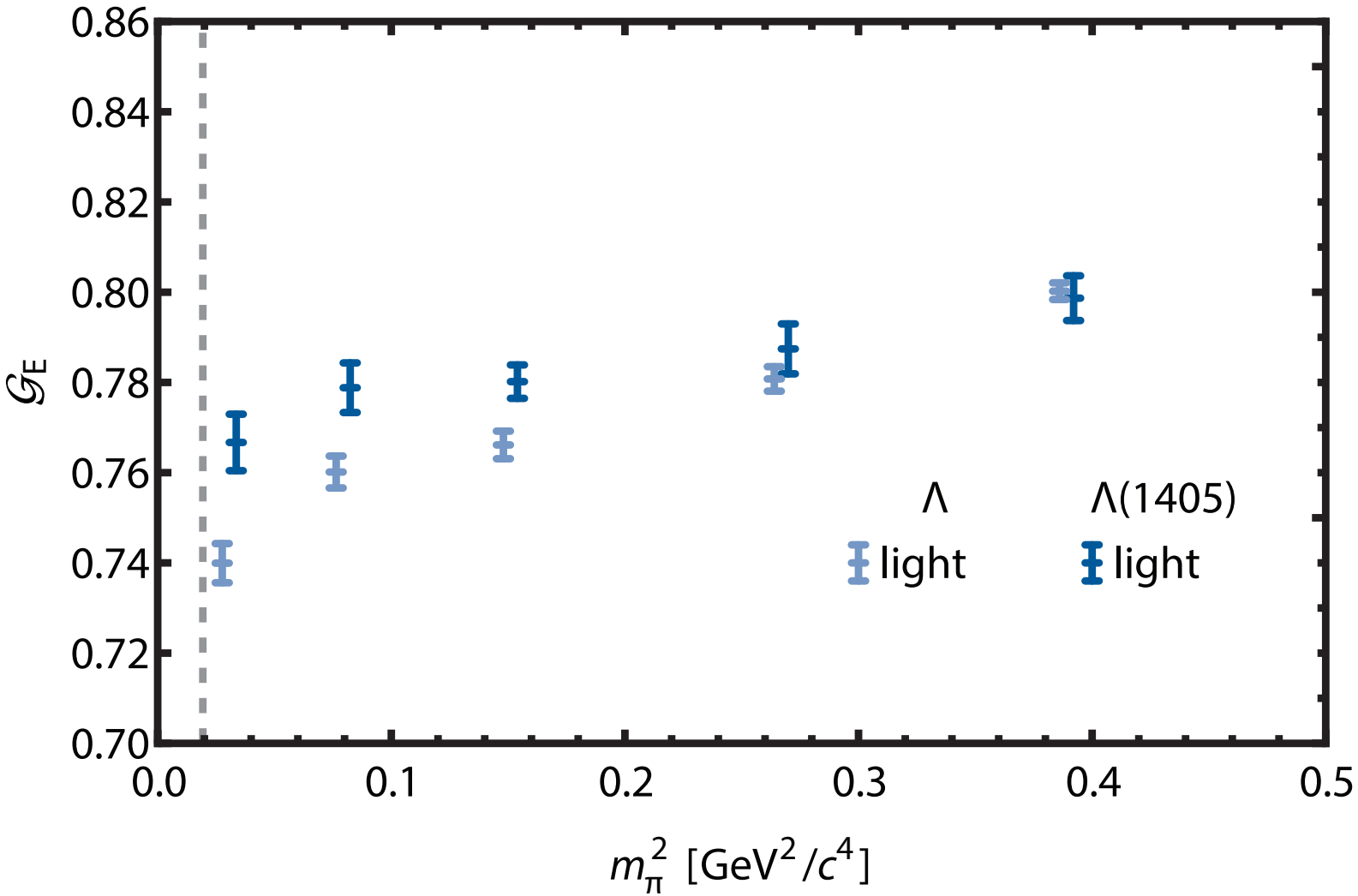

$\mathcal{G}_E$ for the $\Lambda(1405)$

When compared to the ground state, the results for $\mathcal{G}_E$ are consistent with the development of a non-trivial $\overline{\mathrm{K}}\mathrm{N}$ component at light quark masses.

- Noting that the centre of mass of the $\overline{K}(s,\overline{\ell})\ N(\ell,u,d)$ is nearer the heavier N,
  - The anti–light-quark contribution, $\overline{\ell}$, is distributed further out by the $\overline{\mathrm{K}}$ and leaves an enhanced light-quark form factor.
  - The strange quark may be distributed further out by the $\overline{\mathrm{K}}$ and thus have a smaller form factor.

$\mathcal{G}_E$ for the $\Lambda(1405)$

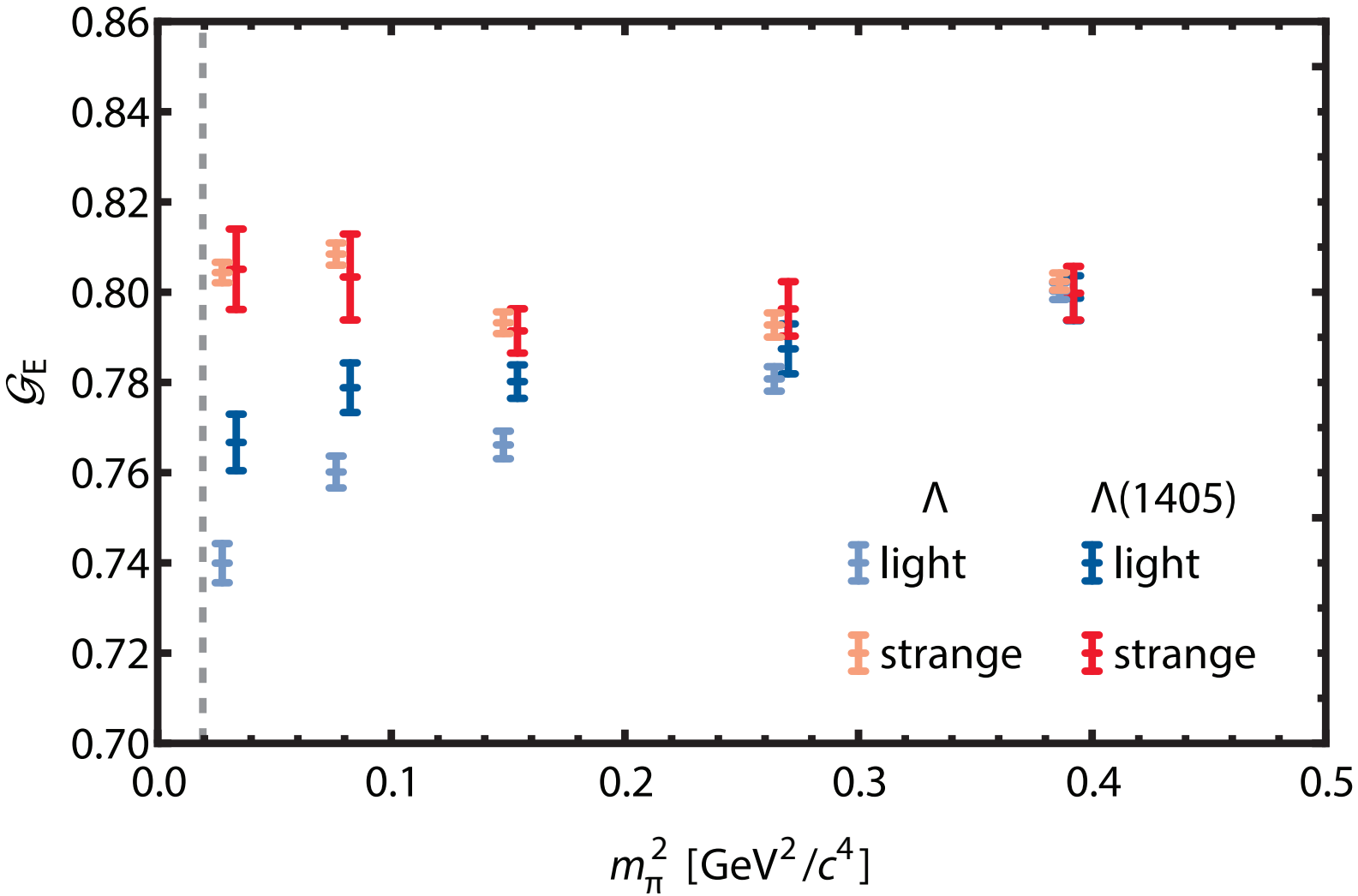

Hamiltonian model, H_I

- The form of the interaction is derived from chiral effective field theory.

$$g_{MB}(k_n) = \left(\frac{\kappa_{MB}}{16\pi^2 f_\pi^2} \frac{C_3(n)}{4\pi} \left(\frac{2\pi}{L}\right)^3 \omega_M(k_n)\, u^2(k_n) \right)^{1/2}.$$

- κ_{MB} denotes the $SU(3)$-flavour singlet couplings

$$\kappa_{\pi\Sigma} = 3\xi_0, \qquad \kappa_{\bar{K}N} = 2\xi_0, \qquad \kappa_{K\Xi} = 2\xi_0, \qquad \kappa_{\eta\Lambda} = \xi_0,$$

with $\xi_0 = 0.75$ reproducing the physical $\Lambda(1405) \to \pi\Sigma$ width.

Hamiltonian model, H_I

- The form of the interaction is derived from chiral effective field theory.

$$g_{MB}(k_n) = \left(\frac{\kappa_{MB}}{16\pi^2 f_\pi^2} \frac{C_3(n)}{4\pi} \left(\frac{2\pi}{L} \right)^3 \omega_M(k_n)\, u^2(k_n) \right)^{1/2}.$$

- κ_{MB} denotes the $SU(3)$-flavour singlet couplings

$$\kappa_{\pi\Sigma} = 3\xi_0, \qquad \kappa_{\bar{K}N} = 2\xi_0, \qquad \kappa_{K\Xi} = 2\xi_0, \qquad \kappa_{\eta\Lambda} = \xi_0,$$

  with $\xi_0 = 0.75$ reproducing the physical $\Lambda(1405) \to \pi\Sigma$ width.
- $C_3(n)$ is a combinatorial factor equal to the number of unique permutations of the momenta indices $\pm n_x$, $\pm n_y$ and $\pm n_z$.

Hamiltonian model, H_I

- The form of the interaction is derived from chiral effective field theory.

$$g_{MB}(k_n) = \left(\frac{\kappa_{MB}}{16\pi^2 f_\pi^2} \frac{C_3(n)}{4\pi} \left(\frac{2\pi}{L} \right)^3 \omega_M(k_n)\, u^2(k_n) \right)^{1/2}.$$

- κ_{MB} denotes the $SU(3)$-flavour singlet couplings

$$\kappa_{\pi\Sigma} = 3\xi_0, \qquad \kappa_{\bar{K}N} = 2\xi_0, \qquad \kappa_{K\Xi} = 2\xi_0, \qquad \kappa_{\eta\Lambda} = \xi_0,$$

  with $\xi_0 = 0.75$ reproducing the physical $\Lambda(1405) \to \pi\Sigma$ width.
- $C_3(n)$ is a combinatorial factor equal to the number of unique permutations of the momenta indices $\pm n_x$, $\pm n_y$ and $\pm n_z$.
- $u(k_n)$ is a dipole regulator, with regularization scale $\Lambda = 0.8$ GeV.

Infinite-volume reconstruction of the Λ(1405) energy

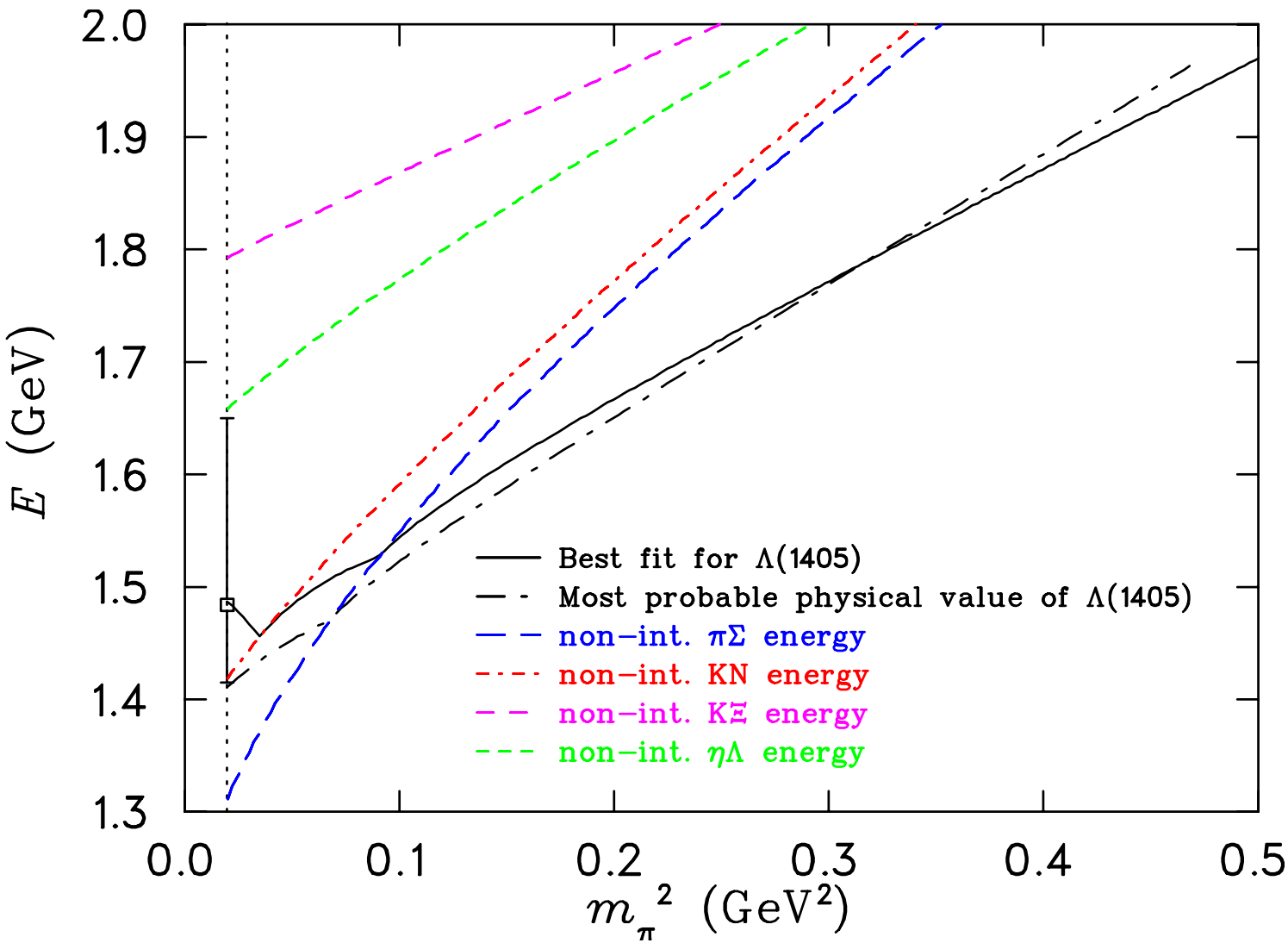

Excited State Form Factors

- The eigenstate-projected three-point correlation function is

$$G_\alpha^\mu(\mathbf{p}', \mathbf{p}; t_2, t_1) = \sum_{\mathbf{x}_1, \mathbf{x}_2} \mathrm{e}^{-\mathrm{i}\,\mathbf{p}'\cdot\mathbf{x}_2} \mathrm{e}^{\mathrm{i}(\mathbf{p}'-\mathbf{p})\cdot\mathbf{x}_1} \times$$
$$\times \langle\Omega| v_i^\alpha(\mathbf{p}')\, \chi_i(x_2)\, j^\mu(x_1)\, \overline{\chi}_j(0)\, u_i^\alpha(\mathbf{p})|\Omega\rangle$$
$$= \mathbf{v}^{\alpha\mathsf{T}}(\mathbf{p}')\, G_{ij}^\mu(\mathbf{p}', \mathbf{p}; t_2, t_1)\, \mathbf{u}^\alpha(\mathbf{p})$$

where

$$G_{ij}^\mu(\mathbf{p}', \mathbf{p}; t_2, t_1) = \sum_{\mathbf{x}_1, \mathbf{x}_2} \mathrm{e}^{-\mathrm{i}\,\mathbf{p}'\cdot\mathbf{x}_2} \mathrm{e}^{\mathrm{i}(\mathbf{p}'-\mathbf{p})\cdot\mathbf{x}_1} \langle\Omega|\chi_i(x_2)\, j^\mu(x_1)\, \overline{\chi}_j(0)|\Omega\rangle$$

is the matrix constructed from the three-point correlation functions of the original operators $\{\chi_i\}$.

Extracting Form Factors from Lattice QCD

- To eliminate the time dependence of the three-point correlation function, we construct the ratio

$$R_\alpha^\mu(\mathbf{p}', \mathbf{p}; t_2, t_1) = \left(\frac{G_\alpha^\mu(\mathbf{p}', \mathbf{p}; t_2, t_1)\, G_\alpha^\mu(\mathbf{p}, \mathbf{p}'; t_2, t_1)}{G_\alpha(\mathbf{p}'; t_2)\, G_\alpha(\mathbf{p}; t_2)} \right)^{1/2}$$

Extracting Form Factors from Lattice QCD

- To eliminate the time dependence of the three-point correlation function, we construct the ratio

$$R_\alpha^\mu(\mathbf{p}', \mathbf{p}; t_2, t_1) = \left(\frac{G_\alpha^\mu(\mathbf{p}', \mathbf{p}; t_2, t_1)\, G_\alpha^\mu(\mathbf{p}, \mathbf{p}'; t_2, t_1)}{G_\alpha(\mathbf{p}'; t_2)\, G_\alpha(\mathbf{p}; t_2)} \right)^{1/2}$$

- To further simply things, we define the reduced ratio

$$\overline{R}_\alpha^\mu = \left(\frac{2E_\alpha(\mathbf{p})}{E_\alpha(\mathbf{p}) + m_\alpha} \right)^{1/2} \left(\frac{2E_\alpha(\mathbf{p}')}{E_\alpha(\mathbf{p}') + m_\alpha} \right)^{1/2} R_\alpha^\mu$$

Current Matrix Element for Spin-1/2 Baryons

The current matrix element for spin-1/2 baryons has the form

$$\langle p', s'|j^{\mu}|p, s\rangle = \left(\frac{m_{\alpha}^2}{E_{\alpha}(\mathbf{p})E_{\alpha}(\mathbf{p}')}\right)^{1/2} \times \\ \times \overline{u}(\mathbf{p}')\left(F_1(q^2)\,\gamma^{\mu} + \mathrm{i}\,F_2(q^2)\,\sigma^{\mu\nu}\frac{q^{\nu}}{2m_{\alpha}}\right)u(\mathbf{p})$$

Current Matrix Element for Spin-1/2 Baryons

The current matrix element for spin-1/2 baryons has the form

$$\langle p', s' | j^\mu | p, s \rangle = \left(\frac{m_\alpha^2}{E_\alpha(\mathbf{p}) E_\alpha(\mathbf{p}')} \right)^{1/2} \times \bar{u}(\mathbf{p}') \left(F_1(q^2)\, \gamma^\mu + \mathrm{i}\, F_2(q^2)\, \sigma^{\mu\nu} \frac{q^\nu}{2m_\alpha} \right) u(\mathbf{p})$$

- The Dirac and Pauli form factors are related to the Sachs form factors through

$$\mathcal{G}_\mathrm{E}(q^2) = F_1(q^2) - \frac{q^2}{(2m^\alpha)^2} F_2(q^2)$$
$$\mathcal{G}_\mathrm{M}(q^2) = F_1(q^2) + F_2(q^2)$$

Sachs Form Factors for Spin-1/2 Baryons

- A suitable choice of momentum ($\mathbf{q} = (q, 0, 0)$) and the (implicit) Dirac matrices allows us to directly access the Sachs form factors:
  - for $\mathcal{G}_\mathrm{E}$: using $\Gamma_4^\pm$ for both two- and three-point,

$$\mathcal{G}_\mathrm{E}^\alpha(q^2) = \overline{R}_\alpha^4(\mathbf{q}, \mathbf{0}; t_2, t_1)$$

  - for $\mathcal{G}_\mathrm{M}$: using $\Gamma_4^\pm$ for two-point and $\Gamma_j^\pm$ for three-point,

$$|\varepsilon_{ijk}\, q^i|\, \mathcal{G}_\mathrm{M}^\alpha(q^2) = (E_\alpha(\mathbf{q}) + m_\alpha)\, \overline{R}_\alpha^k(\mathbf{q}, \mathbf{0}; t_2, t_1)$$

  - where for positive parity states,

$$\Gamma_j^+ = \frac{1}{2}\begin{bmatrix}\sigma_j & 0\\ 0 & 0\end{bmatrix} \qquad \Gamma_4^+ = \frac{1}{2}\begin{bmatrix}\mathbb{I} & 0\\ 0 & 0\end{bmatrix}$$

    and for negative parity states,

$$\Gamma_j^- = -\gamma_5\Gamma_j^+\gamma_5 = -\frac{1}{2}\begin{bmatrix}0 & 0\\ 0 & \sigma_j\end{bmatrix} \qquad \Gamma_4^- = -\gamma_5\Gamma_4^+\gamma_5 = -\frac{1}{2}\begin{bmatrix}0 & 0\\ 0 & \mathbb{I}\end{bmatrix}$$

Scattering State Contamination in Projected Correlator: CSSM

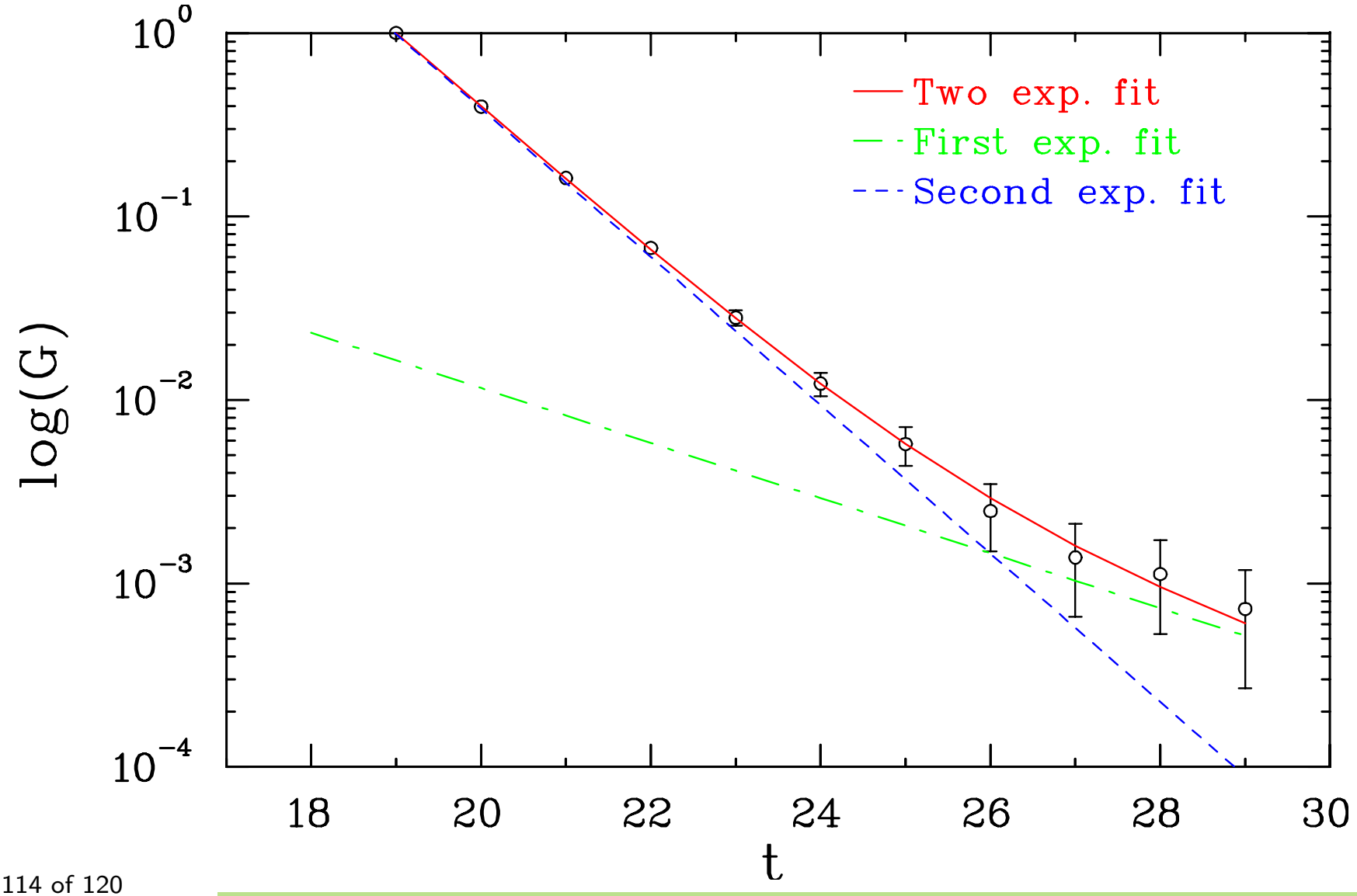

Negative Parity Nucleon: Five-quark Operators:

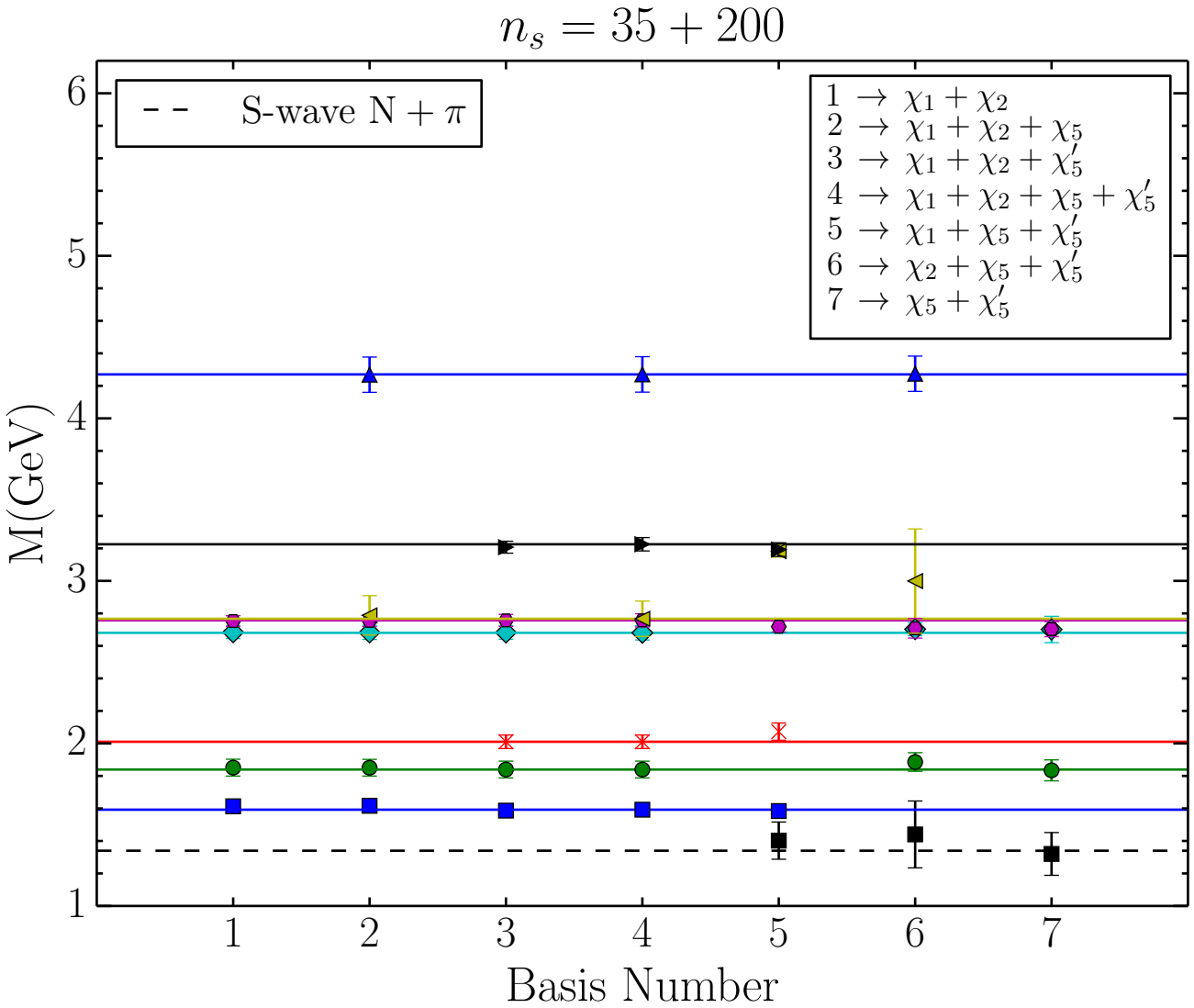

Negative Parity Nucleon Scattering Thresholds

- "Searching for low-lying multi-particle thresholds in lattice spectroscopy,"
  M. S. Mahbub, *et al.* [CSSM],
  Annals Phys. **342**, 270 (2014)
  arXiv:1310.6803 [hep-lat]

- "Lattice baryon spectroscopy with multi-particle interpolators,"
  Adrian Kiratidis, Waseem Kamleh, Derek Leinweber, Benjamin Owen [CSSM]
  Phys. Rev. D **91**, 094509 (2015)
  arXiv:1501.07667 [hep-lat].

Negative Parity Nucleon Spectrum: Lang and Verduci

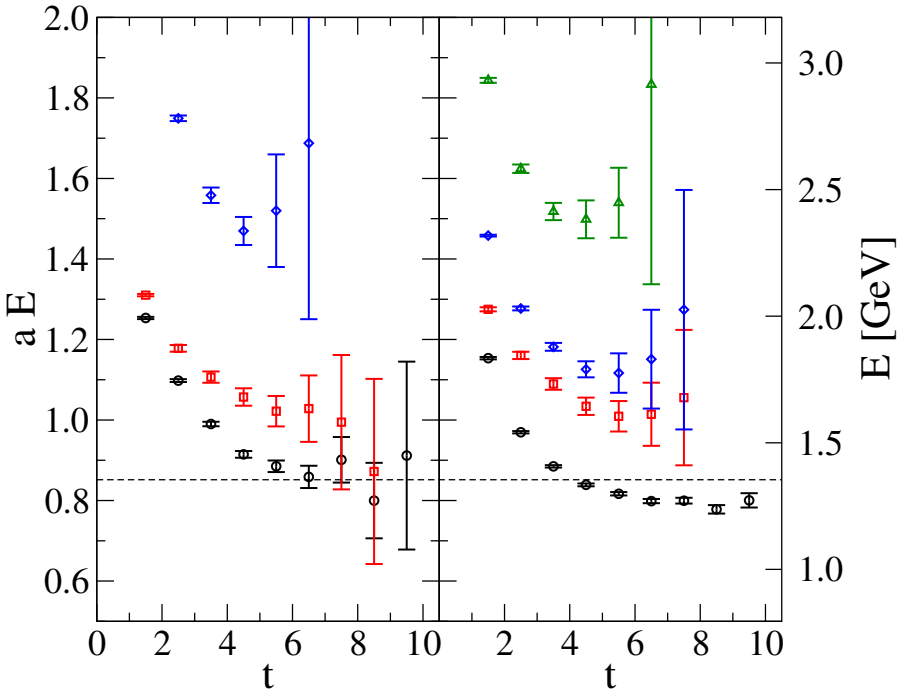

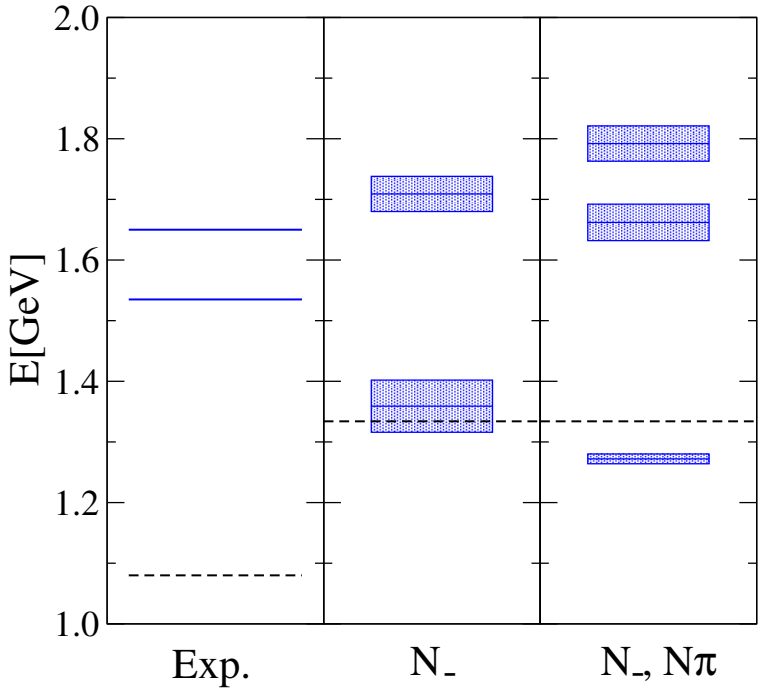

Negative Parity Nucleon Spectrum: Lang and Verduci

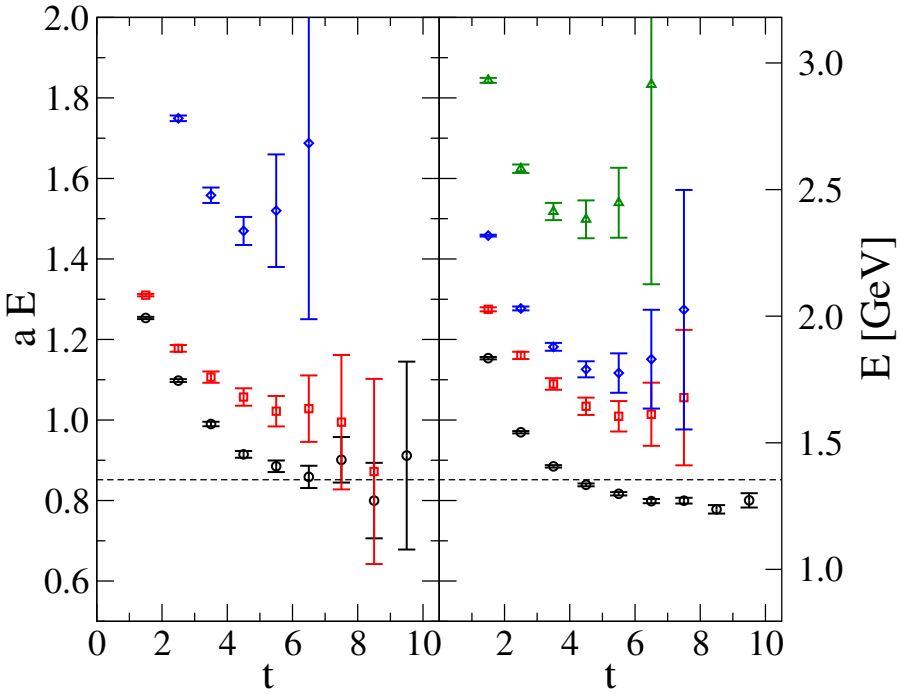

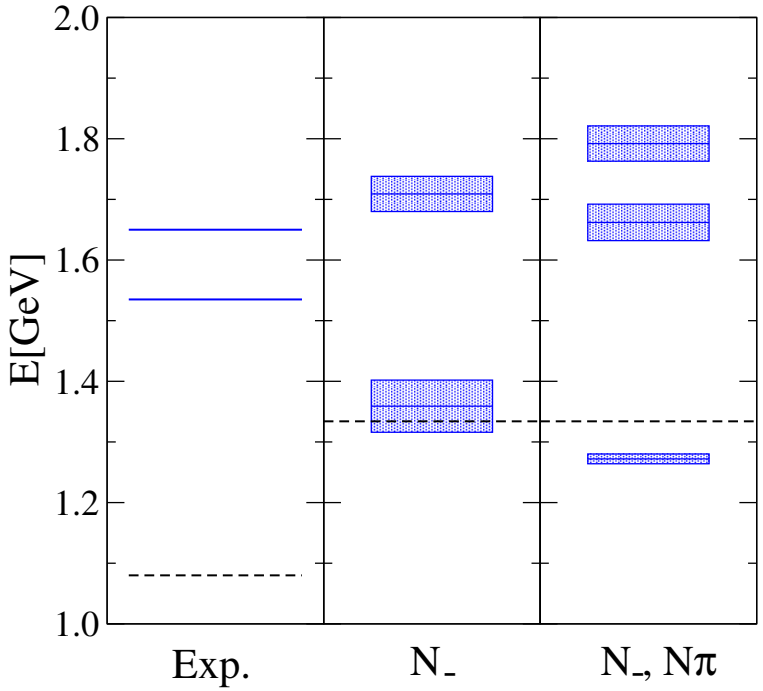

- Small correlation matrix: $\chi_1 + \chi_2 \times 2$ smearings $= 4 \times 4$

Negative Parity Nucleon Spectrum: Lang and Verduci

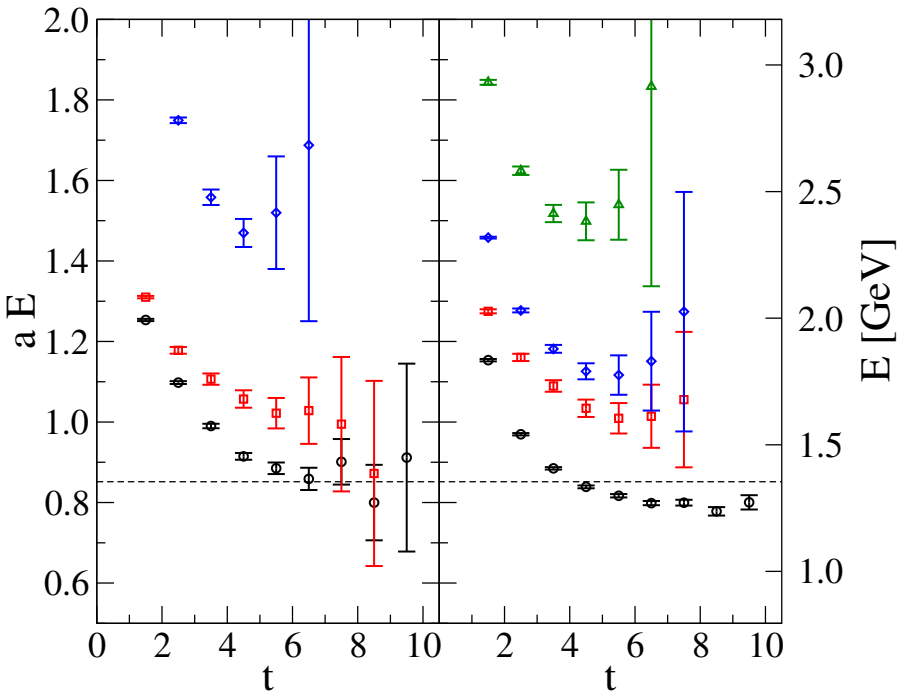

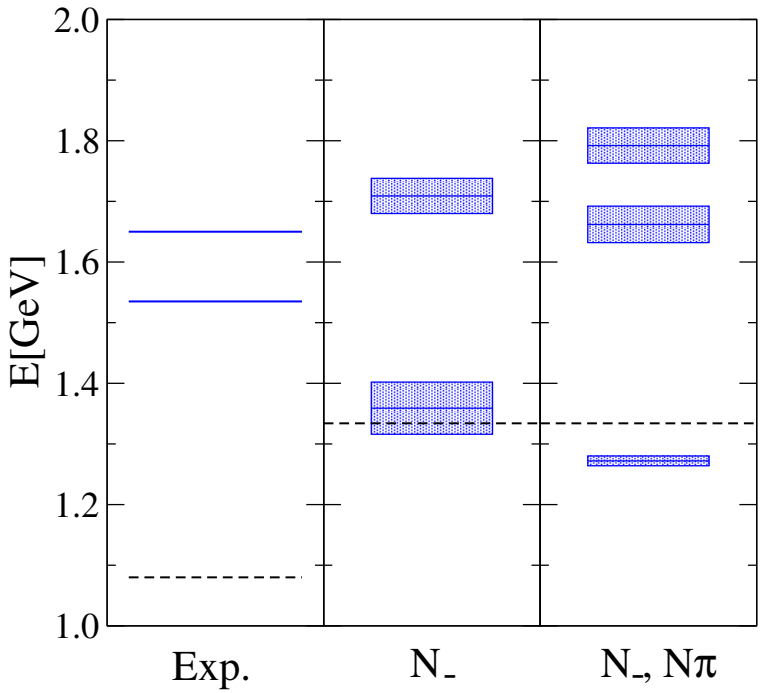

- Small correlation matrix: $\chi_1 + \chi_2 \times 2$ smearings $= 4 \times 4$
- Did not construct projected correlators.
- Limited Euclidean time evolution prior to ill conditioning.

Negative Parity Nucleon Spectrum: Lang and Verduci

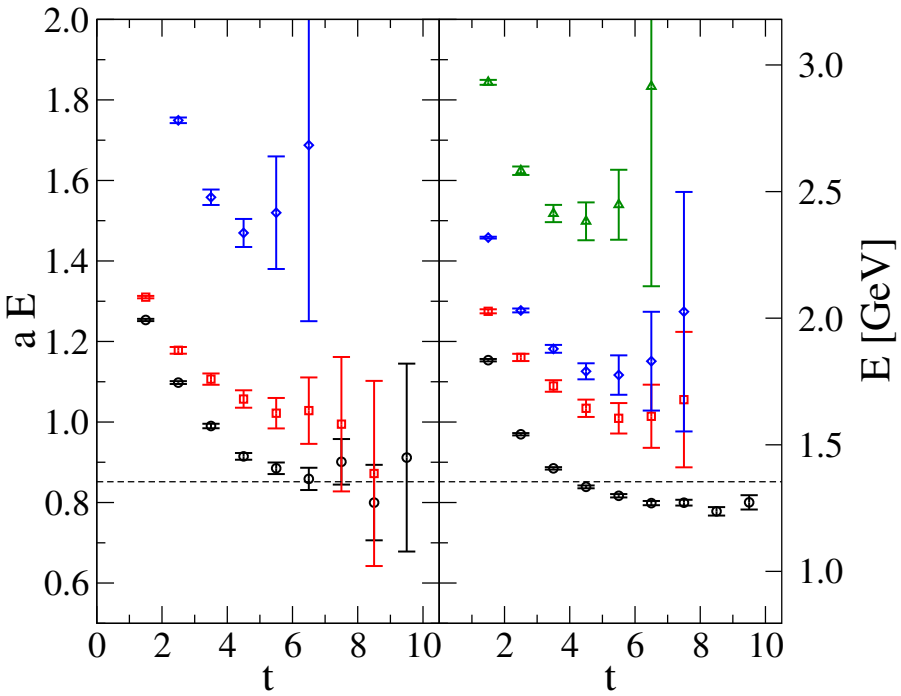

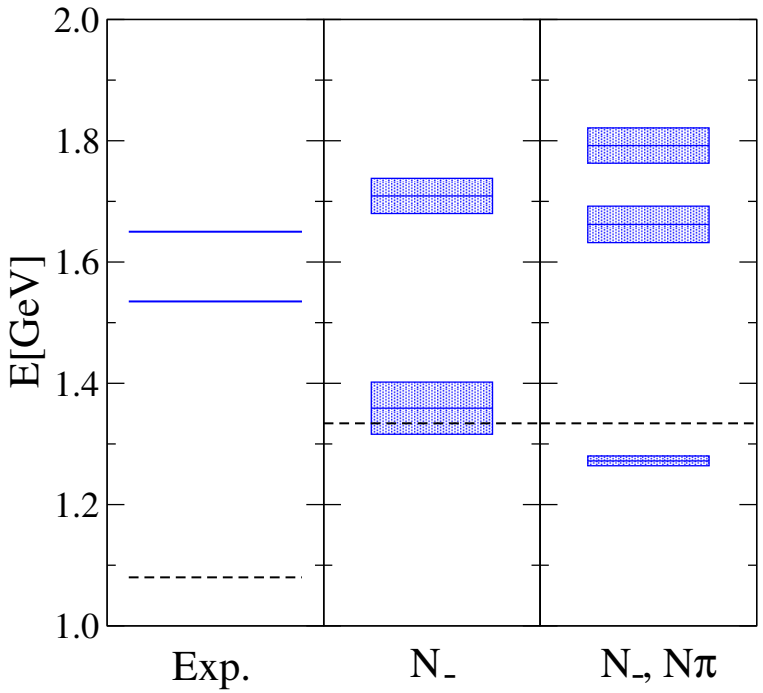

- Small correlation matrix: $\chi_1 + \chi_2 \times 2$ smearings $= 4 \times 4$
- Did not construct projected correlators.
- Limited Euclidean time evolution prior to ill conditioning.
- Adding $N\pi$ sufficient but not necessary. *cf.* Cyprus Results...

Common Proton Interpolating Fields

- Many groups (BGR, Cyprus, χQCD, CSSM) consider the following local interpolating fields

$$\chi_1(x) = \epsilon^{abc}(u^{Ta}(x)\, C\gamma_5\, d^b(x))\, u^c(x)\,,$$

$$\chi_2(x) = \epsilon^{abc}(u^{Ta}(x)\, C\, d^b(x))\, \gamma_5\, u^c(x)\,.$$

d-quark density in 1st excited state of proton: Lower Dirac Component

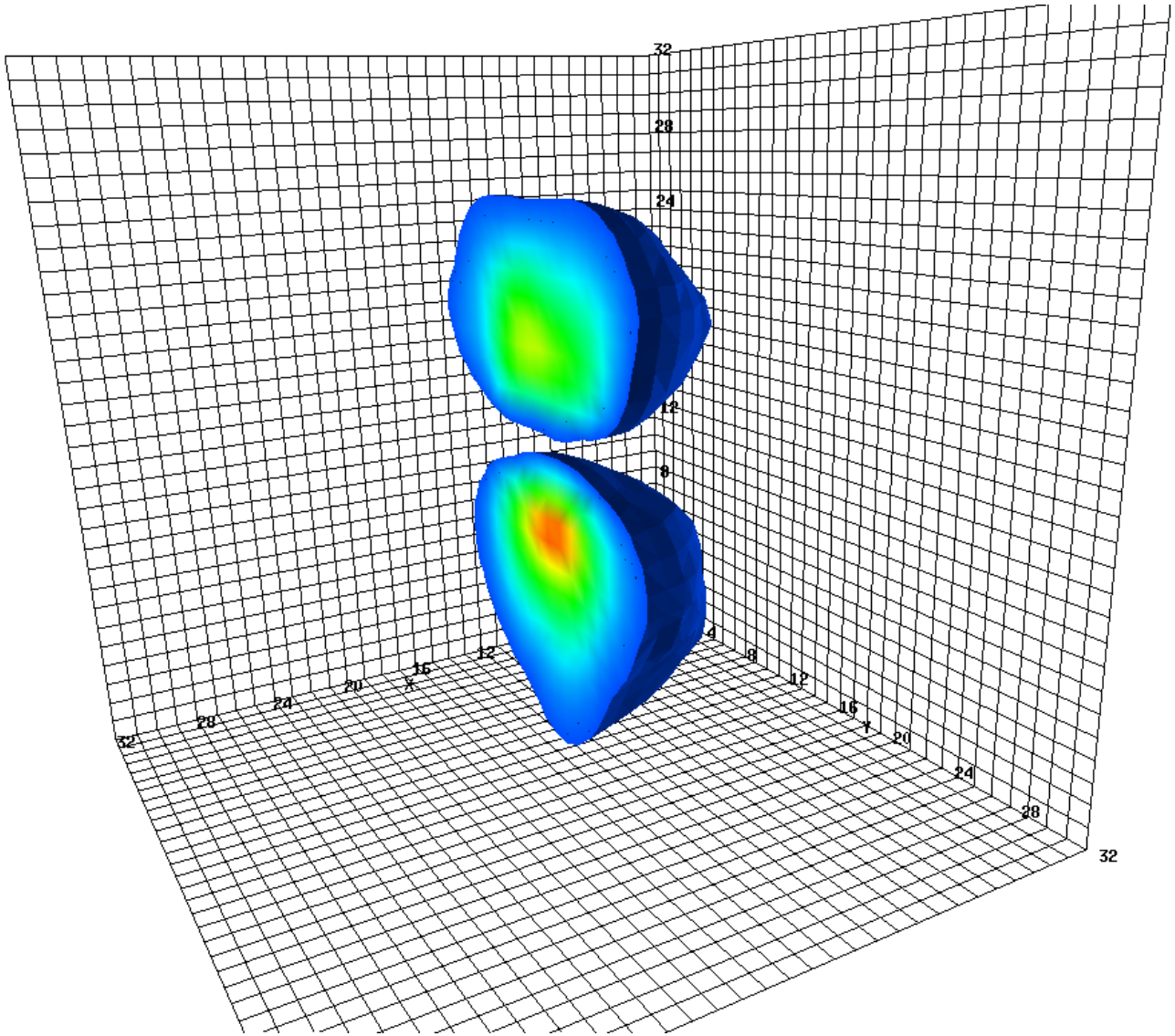

Hybrid Baryons: Hadron Spectrum Collaboration